Structural development of a major late Cenozoic basin and transpressional belt in central Iran: The Central Basin in the Qom-Saveh area

Chris K. Morley
PTTEP (PTT Exploration and Production), Office Building, 555 Vibhavadi Rangsit Road, Chatuchak, Bangkok 10900, Thailand

Booncherd Kongwung
PTTEP (PTT Exploration and Production), Tehran Branch Office, Unit 5 & 6, 5th Floor Sayeh Tower, Vali-e-Asr Avenue, 19677 13671 Tehran, Iran

Ali A. Julapour
Mohsen Abdolghafourian
Mahmoud Hajian
National Iranian Oil Company (NIOC) Exploration Directorate, 1st Dead-end, Seoul St., NE Sheikh Bahaei Sq., P.O. Box 19395-6669 Tehran, Iran

Douglas Waples
Consultant, PTTEP (PTT Exploration and Production), 555 Vibhavadi Rangsit Road, Chatuchak, Bangkok 10900, Thailand

John Warren*
Shell Chair in Carbonate Studies, Sultan Qaboos University, P.O. Box 17, Postal Code Al-Khodh-123, Muscat, Sultanate of Oman

Heiko Otterdoom
PTTEP (PTT Exploration and Production), Tehran Branch Office, Unit 5 & 6, 5th Floor Sayeh Tower, Vali-e-Asr Avenue, 19677 13671 Tehran, Iran

Kittipong Srisuriyon
PTTEP (PTT Exploration and Production), Office Building, 555 Vibhavadi Rangsit Road, Chatuchak, Bangkok 10900, Thailand

Hassan Kazemi
PTTEP (PTT Exploration and Production), Tehran Branch Office, Unit 5 & 6, 5th Floor Sayeh Tower, Vali-e-Asr Avenue, 19677 13671 Tehran, Iran

ABSTRACT

The Central Basin of the Iran Plateau is between the geologically better-known regions of the Zagros and Alborz Mountains. Hydrocarbon exploration in the Central Basin has revealed the details of the late Eocene–Holocene evolution of the basin based on seismic reflection data, geological field work, basin modeling, and satellite interpretation. The multistage basin history commenced with broad sag-type subsidence and isolated normal faults during Oligocene–early Miocene time. It evolved to an extensional or transtensional basin in the early-middle Miocene, with as much as 4–5 km of Upper Red Formation section being deposited in some parts of the basin during this stage. The upper part of the Upper Red Formation is associated with a change to transpressional deformation, with the development of thrusts and folds. This latest (probably middle and/or late Miocene–Holocene) deformation is transpressional, and includes a mixture of basement-involved strike-slip and thrust faults and thin-skinned folding and thrusting detached on Oligocene evaporites. Local detachment levels higher in the stratigraphy also exist. Subsidence in mini-foredeep basins and strike-slip fault bounded basins occurred during this stage, and several kilometers of Upper Red Formation were deposited in the main depocenters. Northwest-southeast– to north-northwest–south-southeast–striking dextral strike-slip to compressional faults dominate the area, with subordinate east-west and north-south fault orientations also present. These different fault sets combine in places to form major strike-slip duplex geometries. The Eocene volcanic belt (Urumieh-Dokhtar zone) along the southern margin of the basin forms a chain of massifs as much as 3 km high, the outcrops of which were exhumed by movement along major thrusts from 5–6 km depth between the middle Miocene and present day. The Central Basin–Urumieh-Dokhtar zone forms a

*Present address: Petroleum Geoscience, Department of Geology, Chulalongkorn University, Phatumphan, Bangkok 10330, Thailand

Geosphere; August 2009; v. 5; no. 4; p. 325–362; doi: 10.1130/GES00223.1; 31 figures.

For permission to copy, contact editing@geosociety.org
© 2009 Geological Society of America

Downloaded from http://pubs.geoscienceworld.org/gsa/geosphere/article-pdf/5/4/325/3337666/i1553-040X-5-4-325.pdf
by guest

distinctive transpressional belt that underwent a minimum of 38 km shortening between the late Miocene and Holocene. The Central Basin and the Zagros and Alborz Mountains all indicate that the onset of widespread crustal shortening in Iran occurred late (latest early Miocene or later), relative to the initial collision of the Arabia Peninsula with Eurasia during the late Eocene or early Oligocene. Uplift of the Central Basin surface from approximately sea level to 900–1000 m occurred during the middle or late Miocene, after deposition of the marine Qom Formation.

INTRODUCTION

Iran is one of the world's best examples of a youthful stage of continent-continent collision. The collision between Arabia and Eurasia appears to have commenced during the late Eocene–early Oligocene (Agard et al., 2005; Vincent et al., 2005, 2007; Allen and Armstrong, 2008; Horton et al., 2008). However, the most conspicuous manifestations of the collision, the Zagros and Alborz Mountains, have undergone their most significant deformation during the middle Miocene–Holocene (see review in Allen et al., 2004), and earlier deformation is largely confined to a much narrower belt between the Sanadaj-Sirjan zone and High Zagros (Agard et al., 2005; Fakhari et al., 2008). A better understanding of the orogenic belt requires defining and dating the geological events associated with (1) the poorly known early stages of collision (Oligocene–early Miocene), and (2) Miocene–Holocene deformation in the Iran Plateau, which is between the more intensively studied Alborz and Zagros Mountains (Fig. 1). In this regard, the Oligocene–Pliocene sedimentary rocks of the Central Basin of the Iran Plateau are particularly important.

The Central Basin is deficient in published modern studies, despite important contributions by Jackson et al. (1990), Walker and Jackson (2004), Allen et al. (2004), Talbot and Aftabi (2004), and Letouzey and Rudkiewicz (2005). Excellent older descriptions of the Central Basin structure and stratigraphy were given by Huber (1951), Sonder (1951, 1954, 1956), Gansser (1955a, 1957), Furrer and Sonder (1955), and in 1:100,000-scale map sheets (Geological Survey of Iran, Geological Maps of Iran, Aran, Farmahin, Qom, Saveh, Tafresh). Recent exploration for hydrocarbons in the Oligocene–Pliocene sedimentary rocks of the Central Basin has resulted in new data and descriptions of the structure of the plateau.

The aim of this paper is to describe the structural styles and evidence for timing of

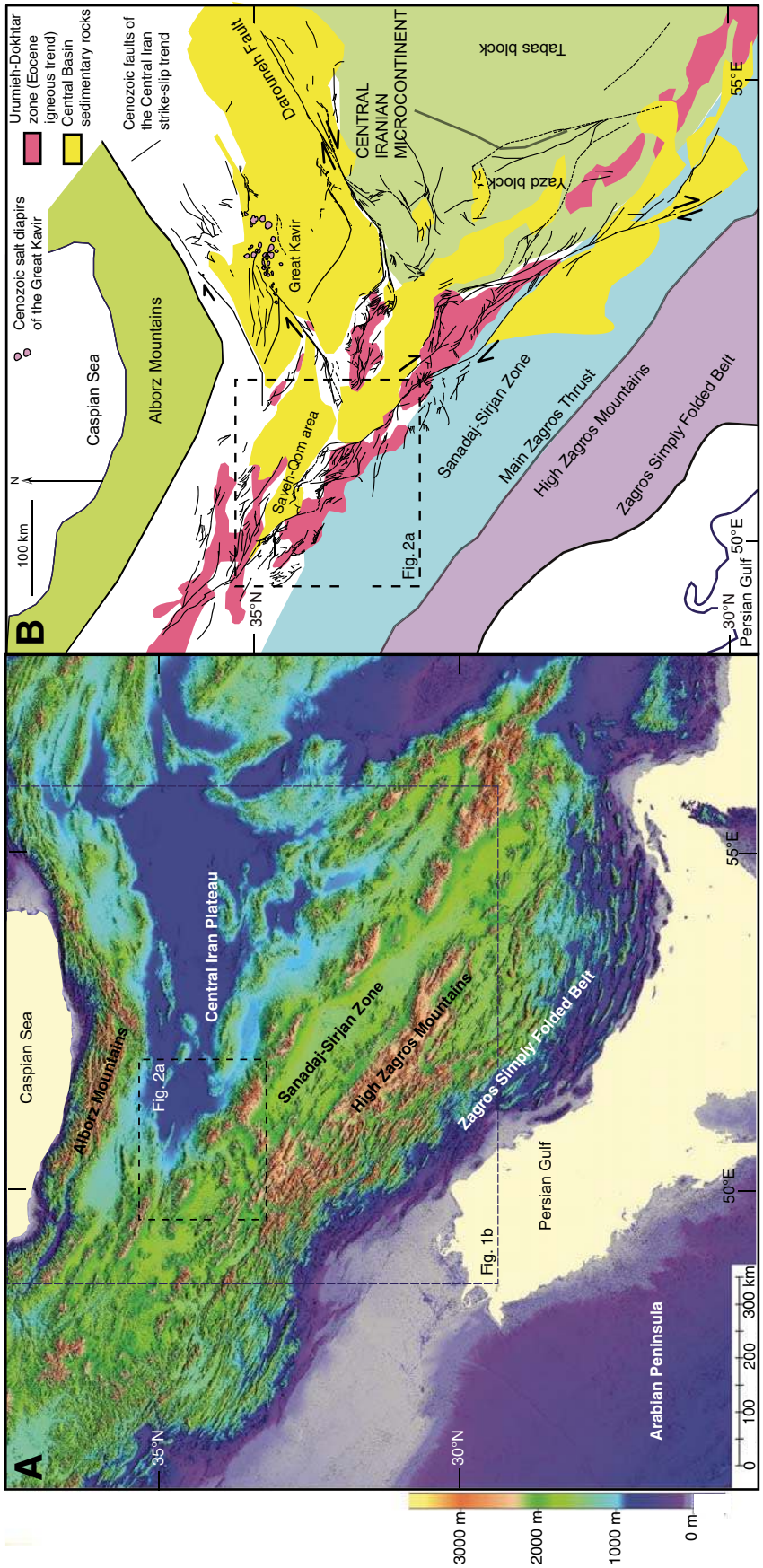

Figure 1. Regional geological setting. (A) Regional topographic map. (B) Tectonic map of Iran showing the main tectonic provinces and the main Cenozoic fault trends associated with central Iran.

Downloaded from http://pubs.geoscienceworld.org/gsa/geosphere/article-pdf/5/4/325/3337666/i1553-040X-5-4-325.pdf
by guest

deformation in a part of the Central Basin referred to here as the Saveh-Qom area. The PTT Exploration and Production Public Company Limited (PTTEP) and the National Iranian Oil Company (NIOC) have together been exploring for hydrocarbons in the Saveh-Qom area, which is ~100 km south of Tehran (Fig. 1). The data presented here are based on new two-dimensional (2D) seismic reflection data, reprocessing and reinterpretation of older vintage 2D seismic reflection data, field work, and satellite image interpretation conducted between 2005 and 2007. Figure 2B shows the location of the 2D seismic lines with respect to the outcrop geology.

This paper describes the polyphase history of the Central Basin and its varying structural styles through time. The final and dominant style is strong dextral transpressional deformation that occurred toward the end of basin development during the Neogene. This latest deformation lifted parts of the basin as substantial massifs to as much as ~3000 m high, and left remnant parts of the basin behind, forming flat-lying plains at elevations between 850 and 1000 m (Fig. 1). The massifs, which predominantly expose Eocene volcanics, are referred to as the Urumieh-Dokhtar zone. The Central Basin and Urumieh-Dokhtar zone contain very extensive outcrops in hilly to mountainous terrane. Consequently, large-scale folds, thrusts, strike-slip faults, and halokinetic features within the basin sediments and underlying Eocene volcanics can be clearly identified in outcrop and on satellite images. Immediately adjacent to the excellent exposures are large, flat remnant basins that are covered by 2D seismic data (Fig. 2). The combination of surface and subsurface data makes the Central Basin a spectacular and well-documented example of transpressional deformation, yet the basin is little known outside Iran.

GEOLOGICAL BACKGROUND

The broad tectonic divisions of Iran compose the Eurasian plate in the northeast half of the country and the Arabian plate in the southwest half, separated by the central Iran Zagros suture zone (Fig. 1B). During the Cretaceous, the Arabian plate moved northward and converged with Eurasia. According to Stampfli and Borel

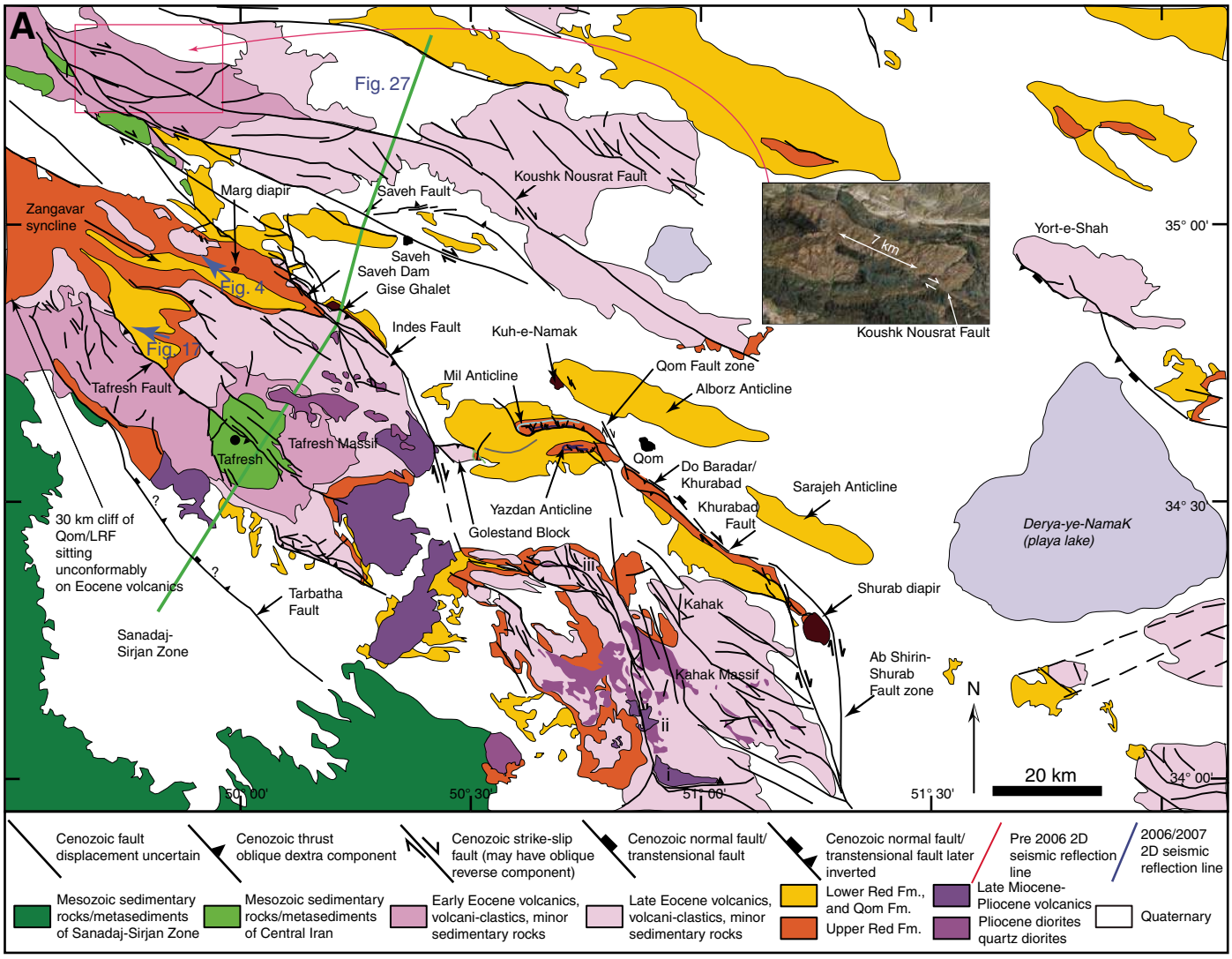

Figure 2 (*continued on next page*). Regional geology of central Iran based on geological maps and satellite interpretation. (A) Regional setting, with key locations referred to in the text labeled. LRF—Lower Red Formation.

Downloaded from http://pubs.geoscienceworld.org/gsa/geosphere/article-pdf/5/4/325/3337666/i1553-040X-5-4-325.pdf
by guest

(2002), this convergence resulted in subduction of the Neo-Tethys ocean in an intraoceanic plate setting beneath oceanic crust of the Semail (backarc) ocean. In Iran Cretaceous ophiolites, such as the Neyriz and Nain-Baft ophiolites, are found within the crush zone (e.g., Delaloye and Desmons, 1980; Berberian and King, 1981; Lanphere and Pamic, 1983; Ghazi and Hassanipak, 1999; Agard et al.; 2005); they are dismembered remnants of an extensive ophiolite suite that was obducted onto the Arabian margin during the Late Cretaceous (e.g., Searle and Cox 1999; Agard et al., 2005). Stampfli and Borel (2002) attributed these ophiolites to obduction of the Semail backarc crust. Following obduction, the remaining oceanic crust was subducted northward beneath the Eurasian margin and gave rise to the extensive Eocene volcanism of central Iran (Berberian and King, 1981; Bina et al., 1986; Stampfli and Borel, 2002; Agard et al., 2005). Eocene volcanism is very widespread in central and northern Iran, and appears to represent both volcanic arc and backarc volcanism (e.g., Vincent et al., 2005). The suture zone is along the southwestern margin of the Sanadaj-Sirjan zone (Main Zagros thrust, Fig. 1B). The timing of collision has been controversial: models for the timing of collision range between the latest Eocene and/or early Oligocene (Sengor et al., 1993; Agard et al., 2005), to the middle or even late Miocene (Axen et al., 2001; McQuarrie et al., 2003; Guest et al., 2006a). However, recently the issue of timing has been resolved in favor of a late Eocene collision (e.g., Agard et al., 2005; Vincent et al., 2005, 2007; Allen and Armstrong, 2008; Horton et al., 2008; Fakhari et al., 2008).

The main area of the Central Basin is north of the Urumieh-Dokhtar zone, ~300 km long in a northwest-southeast direction and 150 km wide (northeast-southwest), and is characterized by flat-lying topography with occasional low hills (Fig. 1). The basin was considerably more extensive in the past, as indicated by remnant Oligocene–Pliocene outcrops south of the Urumieh-Dokhtar zone, within the Urumieh-Dokhtar zone (Fig. 1B), and in the southern foothills of the Alborz Mountains (Ballato et al., 2008). The Urumieh-Dokhtar zone abuts the Sanadaj-Sirjan zone, which is a structurally complex region predominantly composed of

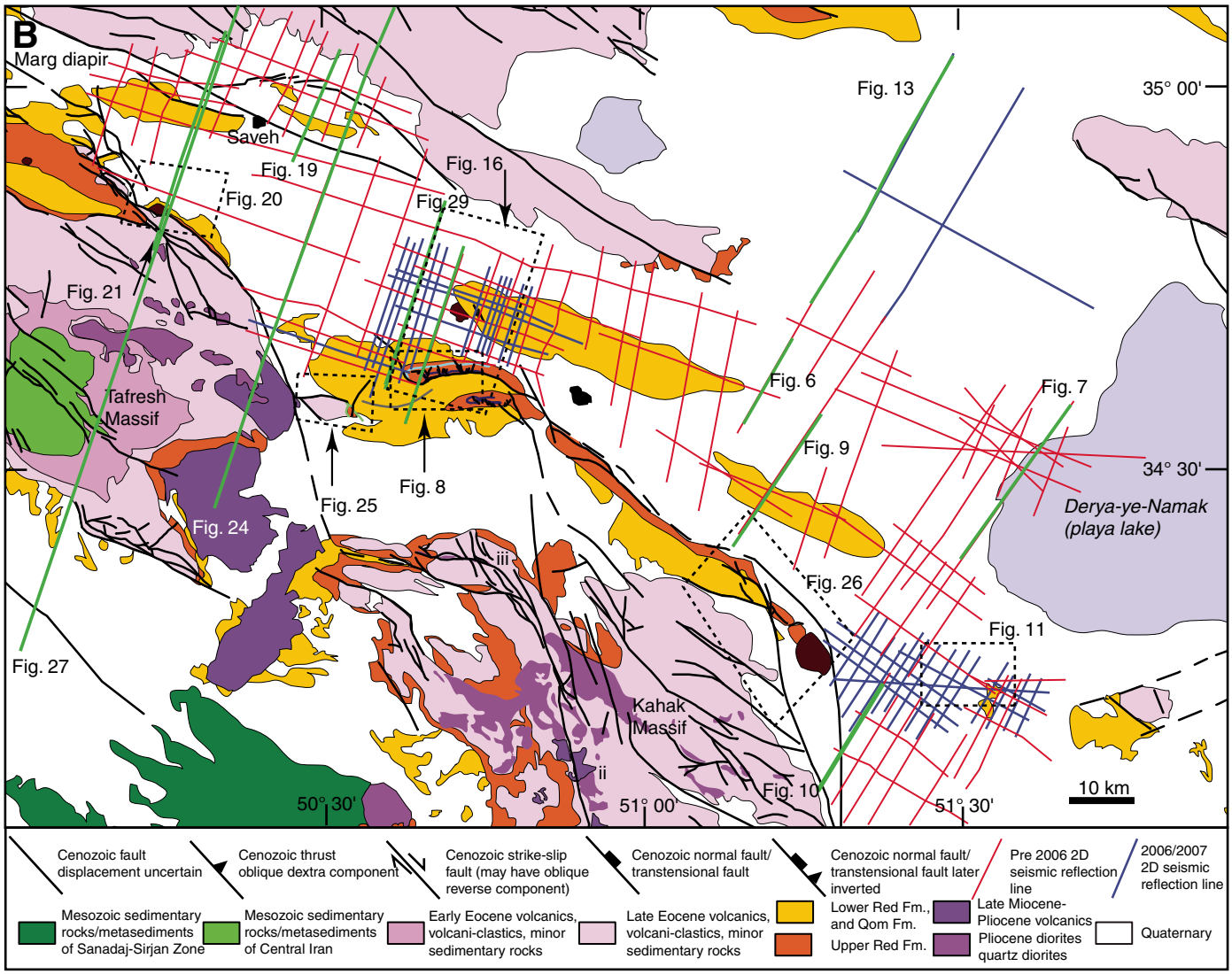

Figure 2 (*continued*). (B) Map focused on the main study area showing the location of seismic lines used in the study (red lines—pre-2006 seismic data, blue lines—2006–2007 data, green lines—location of sections illustrated in this paper); locations of other figures are also given.

Downloaded from http://pubs.geoscienceworld.org/gsa/geosphere/article-pdf/5/4/325/3337666/i1553-040X-5-4-325.pdf
by guest

Mesozoic phyllites and metavolcanics located at the leading edge of the Eurasian plate (Stocklin, 1968; Agard et al., 2005). The Central Basin is limited to the north by the Alborz Mountains, and to the east by the Central Iran microplate (Jackson et al., 1990; Fig. 1B). Along these margins there are well-developed strike-slip fault systems and thrusts (Hessami et al., 2003; Fig. 1B). Some faults are active today; with earthquake focal mechanisms showing dextral motion on northwest-southeast–oriented faults and sinistral motion on northeast-southwest–trending faults (Walker and Jackson, 2004). This fault activity fits with global positioning system (GPS) data that show approximately northward convergence of Arabia with Eurasia (Vernant et al., 2004). The GPS data indicate that there is little detectable internal deformation of the Iran Plateau at present (shortening at rates of 2 mm/a^{-1} or less); instead, shortening is currently focused on the Zagros (6.5 ± 2 mm/a^{-1}) and Alborz Mountains (8 ± 2 mm/a^{-1}; Vernant et al., 2004).

Central Basin Stratigraphy

The Central Basin deposits overlie ~3 km thickness of Eocene arc volcanics and volcaniclastics with subordinate marine carbonates and evaporites (Berberian and King, 1981; Bina et al., 1986). The Eocene sequence unconformably overlies Cretaceous and Jurassic sedimentary and metasedimentary rocks. The Eocene succession commences with a basal conglomerate and coarse clastics, followed by a predominantly calc-alkaline volcanic series that dominates the Eocene stratigraphy (Stocklin, 1968). Interbedded with the volcanics and volcaniclastics are limestones (some nummulitic) and evaporites, indicating that the volcanism occurred close to sea level. The Eocene section was deformed, uplifted, and eroded prior to deposition of the Oligocene–Miocene sedimentary rocks of the Central Basin (Huber, 1952; Gansser, 1955b). Three main stratigraphic units are present in the Central Basin: the Lower Red Formation (Oligocene), the Qom Formation (late Oligocene–early Miocene), and the Upper Red Formation (early Miocene–early Pliocene?; Fig. 3; Gansser, 1955a; Furrer and Sonder, 1955; Abaie et al., 1964).

The Central Basin is composed of two main subbasins, a northwest-southeast–trending arm including the Saveh-Qom area discussed here, and a northeast-southwest–trending arm that underlies the Great Kavir desert. In the Great Kavir, outcrops of the Central Basin form extensive, flat-lying rock pavements that exhibit spectacular examples of salt diapirs punched through folded Miocene sedimentary units (Gansser, 1955a; Jackson et al., 1990; Fig. 1B). These outcrops led to the recognition of the salt canopy structural style (Jackson et al., 1990). A ~1–2-km-thick lower salt, of Eocene–Oligocene age, and a younger Miocene salt as thick as 1.5 km are present (Jackson et al., 1990). The Miocene section is predominantly composed of evaporitic marls, siltstones, and fine-grained sandstones. The Great Kavir, while displaying spectacular outcrops, does not have the well information or seismic data coverage that is found in the Saveh-Qom area. The following summary of the Central Basin stratigraphy is based on outcrops and well data in the Saveh-Qom area.

The Lower Red Formation is typically 300–1000 m thick and varies in lithology laterally and vertically; it includes shales, siltstones, marls with gypsum, sandstones, conglomerates, and evaporites (Gansser, 1955a). The coarse clastics show a large component of Eocene volcanic-derived clasts. Basaltic-andesitic lava flows and pyroclastic deposits also occur in places (Furrer and Sonder, 1955). The occasional presence of marine fossils indicates episodic marine incursions into the basin. Near the base of the Lower Red Formation is a halite-dominated evaporite sequence commonly several hundred meters thick. The evaporites are extensively distributed, occurring both in outcrops in the Tafresh Massif and within the basinal area. Some localities display a low-angle angular unconformity between the Lower Red Formation and the Qom Formation (Fig. 4B), which has been attributed to uplift and erosion associated with local orogenic movements (Gansser, 1955a). This deformation appears to be minor and may at least in part be attributed to local, early halokinesis of the Lower Red Formation evaporites. It is usually difficult to identify any clear angular unconformity between the Lower Red and Qom Formations in seismic reflection data.

The Qom Formation is a late Oligocene–early Miocene shelfal–upper slope marine carbonate–dominated unit (Furrer and Sonder, 1955; Gansser, 1955a; Schuster and Wielandt, 1999). Reuter et al. (2007) assigned a late Rupelian to mid-Burdigalian age for the Qom

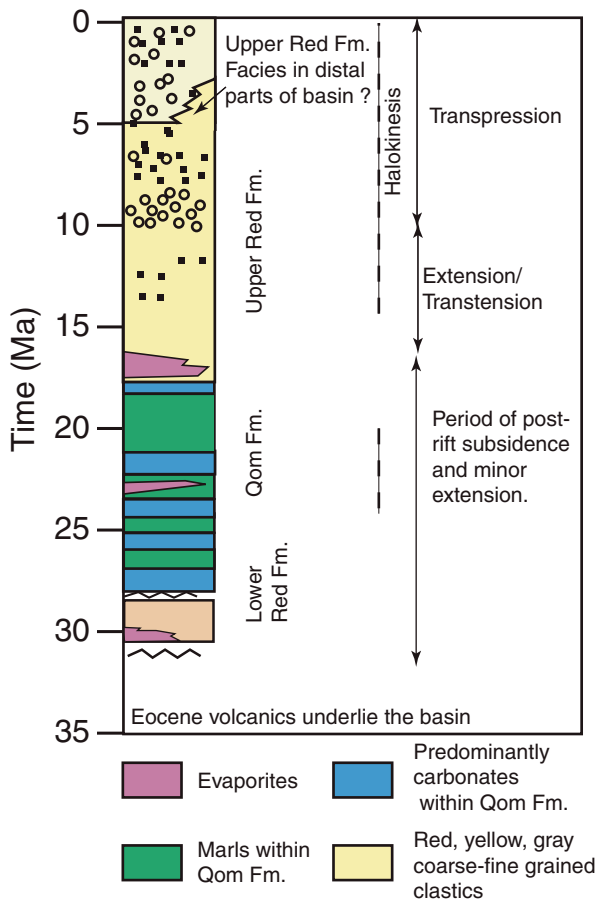

Figure 3. Simplified stratigraphic column for the Central Basin sedimentary rocks.

Downloaded from http://pubs.geoscienceworld.org/gsa/geosphere/article-pdf/5/4/325/3337666/i1553-040X-5-4-325.pdf
by guest

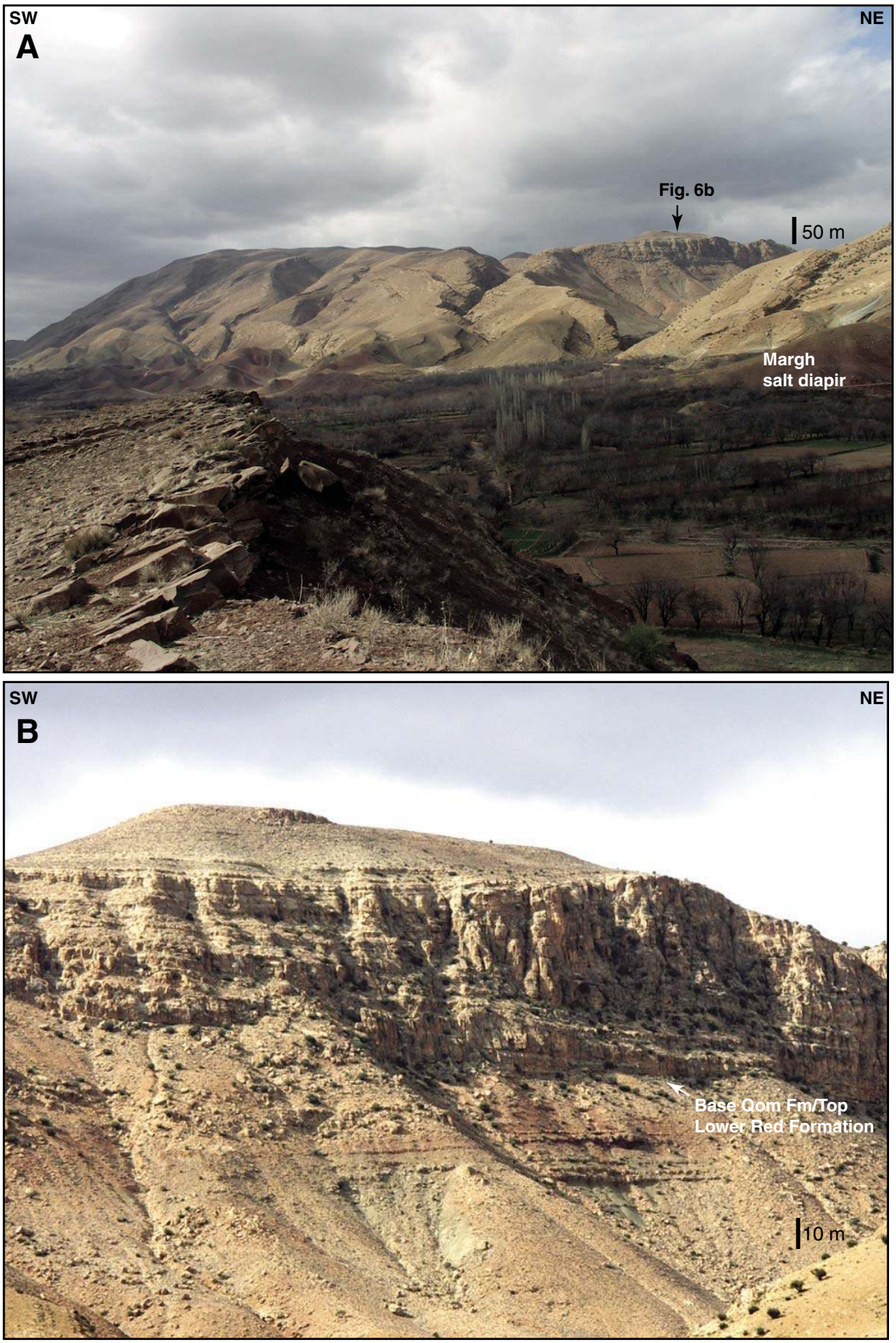

Figure 4. Photos show typical geology of the large-scale folds in Central Basin sedimentary rocks. (A) Photograph of a basement-involved fold in the Tafresh massif. (B) Close-up of the fold crest showing a low-angle angular unconformity between the Qom Formation and the Lower Red Formation. See Figure 2A for location.

Downloaded from http://pubs.geoscienceworld.org/gsa/geosphere/article-pdf/5/4/325/3337666/i1553-040X-5-4-325.pdf
by guest

Formation. It is approximately time equivalent to the Asmari Limestone of the Zagros Mountains, and together the two formations record the Terminal Tethyan Event, when the Tethyan Seaway was closed due to uplift associated with collision of the Arabian and Eurasian plates (e.g., Reuter et al., 2007). The Qom Formation marks an isolated branch of the Tethyan Seaway that was north of the main ocean (Harzhauser and Piller, 2007). In the Saveh-Qom area, the Qom Formation is as much as ~ 1 km thick and composed of marls, carbonates, sandy limestones, and bituminous shales, with occasional anhydrite layers (Gansser, 1955a, 1957; Furrer and Sonder, 1955; Reuter et al., 2007). The most prominent evaporite layer within the Qom Formation is the ~10-m-thick D member anhydrite. The Qom Formation is the main reservoir and source rock for hydrocarbons (Abaie et al., 1964). The carbonates of the Qom Formation are most commonly representative of outer shelf–upper slope deposition on a ramp-type setting, with bryozoan assemblages dominating over corals. In the Saveh-Qom area four main shallowing episodes occur within the Qom Formation (Reuter et al., 2007), and some local highs are present, characterized by erosional unconformities, conglomerates, oolitic limestones, and shallow-marine fossils. Some of these highs appear to be related to normal faults or early movement on Lower Red Formation salt pillows and diapirs.

The Upper Red Formation is generally a clastic-dominated unit as much as 7 km thick, composed of marls, siltstones, sandstones, and conglomerates. At the base of the formation is an evaporite unit that in places exceeds 400 m in thickness (Abaie et al., 1964). Overlying the halite-dominated evaporite unit in the Alborz and Sarajeh fields is a predominantly fine-grained sequence of Upper Red Formation, almost 4000 m thick. The clastics were divided into the units M1, M2, and M3 by Abaie et al. (1964). All these units are characterized by varying percentages of sandstones, gypsiferous shales, and siltstones. However, this stratigraphic scheme is only locally applicable, because basin center deposits, such as those penetrated in the Alborz and Sarajeh fields, are predominantly fine grained, while extensive coarse clastic sequences are present toward the basin margins. For example, in the Khu-e-Zangavar syncline west of Saveh dam (Fig. 2), the Upper Red Formation has been mapped as three units; from base to top, these are: Mm—red marl, sandy marl, sandstones and conglomerates; Ms—dark red-brown conglomerates and sandstones; and Mc—gray coarse pebbly conglomerate (Geological Survey of Iran, Geological Map of Iran, Saveh).

Amini (1997) demonstrated different entry points of sediment into the Upper Red Formation basin, particularly from the north and the south, using paleocurrent indicators and sediment provenance. Volcanic detritus dominates the clastic content of the Upper Red Formation. In general, volcanics derived from the southern margin are predominantly aphanitic volcanic lithics, of more basic composition than the comparatively acidic, vitric volcanic lithics and individual (igneous) mineral grains derived from the north (Amini, 1997). Lithic clasts derived from the Qom Formation are also abundant in the Upper Red Formation. Amini (1997) noted that within the ~1250-m-thick conglomeratic section at the Yazdan anticline section, there is an upward change from Qom Formation–dominated lithics, to volcanic dominated, then to mixed Qom Formation and volcanic contributions.

The Upper Red Formation is predominantly composed of continental deposits, and consequently is very poorly dated. The top of the Qom Formation is dated as near the end of the Burdigalian, ca. 17 Ma ago (Schuster and Wielandt, 1999; Daneshian and Ramezani Dana, 2007), so the Upper Red Formation has traditionally been dated as in the remainder of the Miocene. Recent magnetostratigraphy data from Ballato et al. (2008) suggest that the Upper Red Formation adjacent to the southern Alborz Mountains ranges in age between 17.5 and 7.5 Ma. The top of the Upper Red Formation in this area is marked by the Hezardarreh and Kahrizak Formations, which are coarse clastic, alluvial fan–system deposits (Ballato et al., 2008). Given the localized depositional trend of such deposits, and the time-transgressive nature of the similar coarse-grained Batkhyari Formation in the Zagros Mountains (Fakhari et al., 2008), there is every reason to suspect that the Hezardarreh and Kahrizak Formations pass basinward into fine-grained Upper Red Formation–type facies. Consequently, in this paper it is assumed that the age range of the fine-grained Upper Red Formation section imaged in seismic data in the Saveh-Qom area is ca. 17 Ma old to Pliocene age. This is simply based on the assumption that the depositional and structural processes that occurred during the late Miocene are similar to those today, and so it is difficult to confine the Upper Red Formation to an arbitrary time limit within the Miocene.

BASIN DEVELOPMENT

Onset of Subsidence in the Central Basin

Around Tafresh (Fig. 2A) the Qom Formation and Lower Red Formations unconformably overlie early Eocene units; to the north toward Saveh, they overlie late Eocene units. From outcrop mapping and seismic reflection data, the Qom Formation and Lower Red Formation generally overlie the eroded Eocene surface with a low-angle contact, and there is no indication of local onlap onto rugged topography. A 30-km-long cliff exposure of Lower Red Formation and Qom Formation shows this low-angle surface clearly (Fig. 2A). Consequently, there must have been considerable erosion of the volcanic arc topography preceding the regional subsidence that formed the Central Basin. However, there are some indications of remnant topography. Huber (1952) noted that younging of the base of the Qom Formation from Oligocene to Miocene occurs over 75 km in the eastern Qom-Saveh area, but within 10 km west of Saveh, and that in places, reefal Qom Formation overlies directly remnant Eocene topography. The widespread Oligocene-age erosion is of considerable tectonic significance for the Saveh area because it coincides approximately with the end of subduction and onset of Arabia-Eurasia collision. The unconformity is not just marked by regional uplift; Huber (1952) and Gansser (1955b) recorded evidence from outcrops in central Iran for late Eocene–early Oligocene deformation, where the Eocene section was strongly folded, then eroded prior to the Lower Red Formation deposition.

Basin Development during the Oligocene–Early Miocene

A problem with understanding the early basin development from the Oligocene to the early Miocene is that the overprint of late Miocene–Pliocene transpressional deformation is very strong. Older fault trends are commonly masked or inverted because the basin margins have been uplifted, eroded, and deformed by folds and thrusts. In addition, the uplifted areas are mostly devoid of 2D seismic surveys, so coverage of areas that may contain basin-bounding faults is far from comprehensive. Nevertheless, sufficient detail is present in outcrops and seismic data to determine the structural style during the early stage of basin development.

Sediment thicknesses and subsidence rates indicate that basin deposition changed considerably from the Lower Red Formation–Qom Formation time to the Upper Red Formation time. In the Qom-Saveh area the Lower Red Formation and Qom Formation are each typically ~1 km thick. The two formations together represent the time span of ca. 30 to17 Ma ago. Deposition rates are much less than the Upper Red Formation, where as much as 8 km thickness of section was deposited between the Burdigalian and the Pliocene (a time span of ~12–14 my). The

Downloaded from http://pubs.geoscienceworld.org/gsa/geosphere/article-pdf/5/4/325/3337666/i1553-040X-5-4-325.pdf
by guest

geographic distribution of the Lower Red Formation is also different from that of the Upper Red Formation. The Lower Red Formation is focused in the Saveh-Qom-Shurab area, where the Qom Formation is of late Oligocene to early Miocene age. To the north the Lower Red Formation and lower part of the Qom Formation is absent, and early Miocene age Qom Formation directly overlies Eocene volcanics (Yort-e-Shah area, Fig. 2; Gansser, 1955a). Seismic data also indicate that there is little or no erosion of the upper surface of the Qom Formation, and that northward within the Saveh area the Qom Formation thins stratigraphically, not by erosion. However, northeast to the Great Kavir, the description of 1–2-km-thick Eocene–Oligocene evaporites (Jackson et al., 1990) indicates the existence during Lower Red Formation time of a very large depocenter on the northwest margin of the Central Iran block. The Yort-I-Shah area (Fig. 2) may have been a significant Oligocene paleohigh that separated the Great Kavir and Saveh-Qom Lower Red Formation basins. Conversely, the Upper Red Formation is present extensively in central Iran and outcrops are present northward from the south of the Qom Saveh area to the Alborz Mountains (e.g., Jackson et al., 1990; Ballato et al., 2008).

Isopach maps of the Qom Formation show gradual thickness changes around the basin, the Qom Formation depobelt wrapping around the western side of the Central Iran microplate (Fig. 5; Gansser, 1955a). The thickest Qom Formation section trends northwest-southeast in a series of subbasins and is southwest of the Saveh-Qom area (Fig. 5). The basin location is indicated by the dominance of marls in the section (70% marl, 15%–20% sandstone, and 10% limestone; Furrer and Sonder, 1955). The two thickest occurrences of the Qom Formation are (1) near the northern edge of the Eocene volcanics-dominated massif at Kahak, where ~1500 m of Qom Formation is present (Fig. 5, location a), and (2) ~60 km west of Saveh, where ~2300 m thickness of Qom Formation is present (Fig. 5, location b; Furrer and Sonder, 1955). The isopach of the Qom Formation indicates that the main depocenter was inverted to form the Eocene volcanic massifs that extend southwest of the Saveh-Qom area (Fig. 5).

In outcrop and seismic data, there is little clear-cut indication of extensive syndepositional normal faulting affecting the Lower Red and Qom Formations. Generally gradual changes in Qom Formation thickness and facies are the widespread characteristic of the formation. Deposition appears to have occurred in a broad sag-type basin with no clear regional control by faulting. However, as is discussed below, locally some normal faults appear to have affected sediment thickness and facies in the Lower Red and Qom Formations.

Evidence for Localized Normal Faulting Affecting the Lower Red and Qom Formations

Around the Alborz and Sarajeh anticlines seismic reflection data and satellite images show a number of normal faults within the Lower Red and Qom Formations (Figs. 6 and 7). The seismic lines in Figures 6 and 7 show expansion of the Qom Formation toward the north-northeast into normal faults that were subsequently subjected to inversion. Inversion on the fault shown

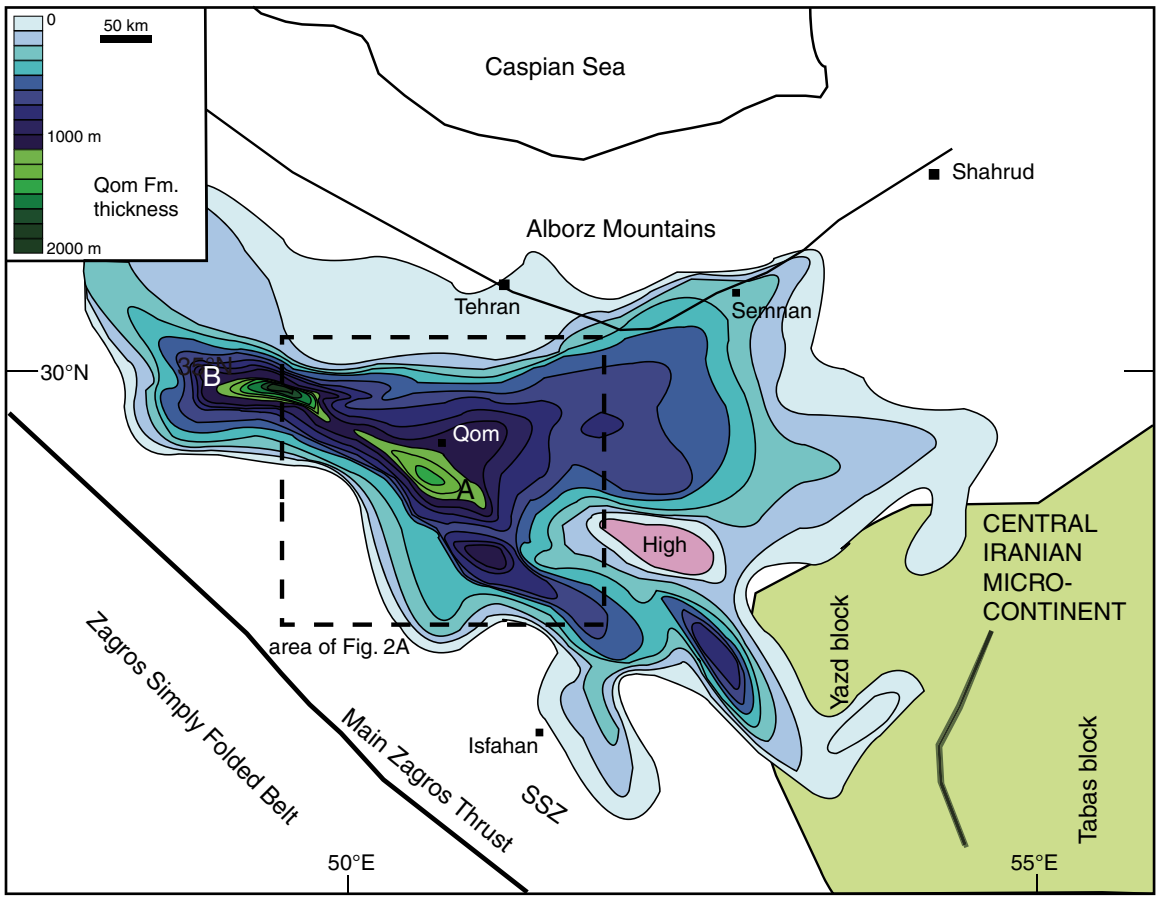

Figure 5. Isopach map of the Qom Formation (based on Gansser, 1955a). SSZ—Sanadaj-Sirjan zone.

Downloaded from http://pubs.geoscienceworld.org/gsa/geosphere/article-pdf/5/4/325/3337666/i1553-040X-5-4-325.pdf
by guest

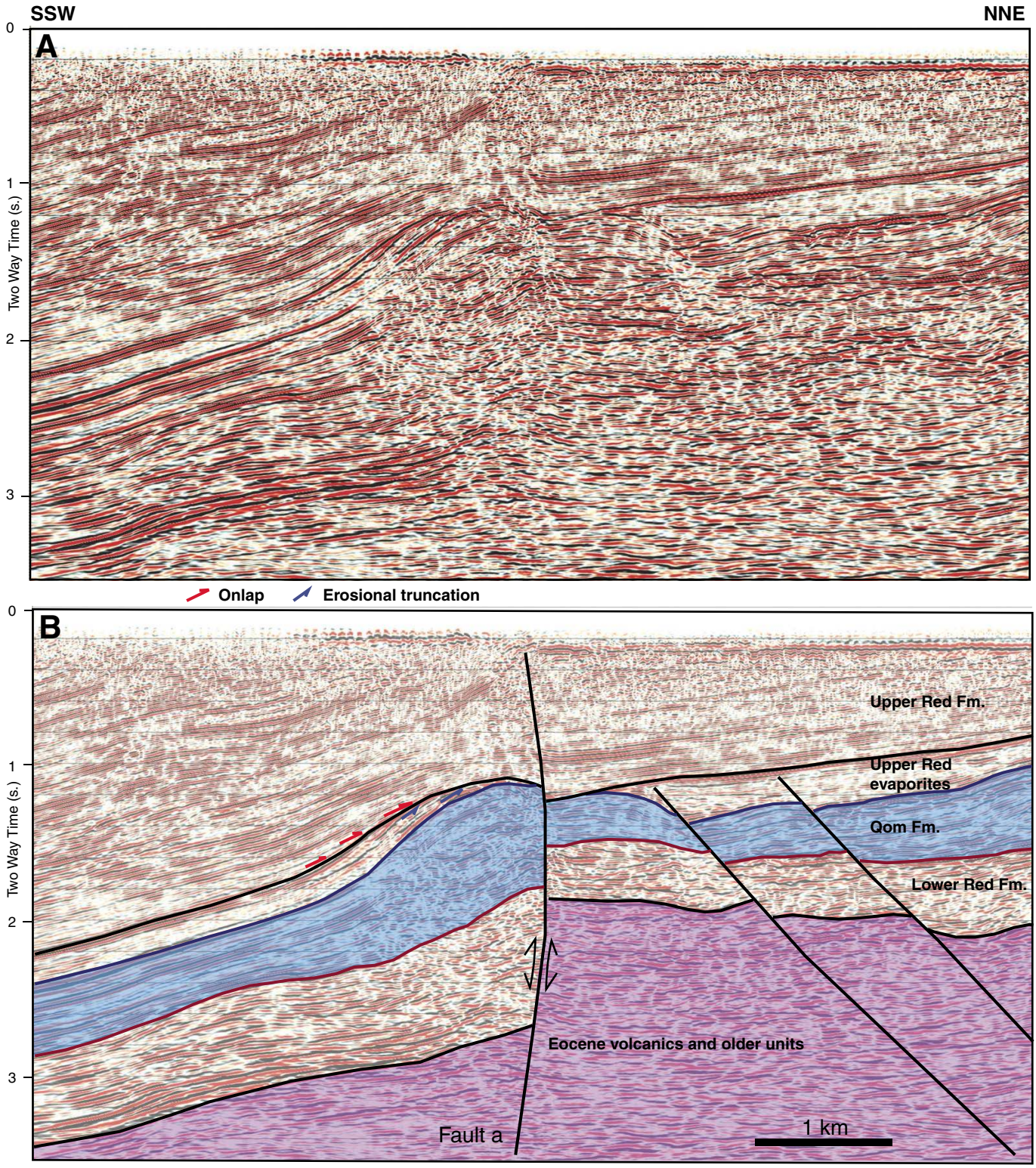

Figure 6. Seismic line with an example of an inverted northwest-southeast–striking normal and/or transtensional fault. (A) Uninterpreted line. (B) Interpreted line. The Lower Red and Qom Formations clearly show expansion toward the north-northeast, and the fault has the characteristics of a normal fault. Early Upper Red Formation inversion resulted in the Upper Red Formation thinning by onlap and erosion onto the inverted footwall high. Inversion during the later Upper Red Formation also reactivated the fault. Tilting both by fault movement to the south-southeast of the seismic line, and by inversion to the north, rotated fault a to a high angle late in its history. See Figure 2B for location.

Downloaded from http://pubs.geoscienceworld.org/gsa/geosphere/article-pdf/5/4/325/3337666/i1553-040X-5-4-325.pdf
by guest

in Figure 6 occurred during early Upper Red Formation time and resulted in the absence of Upper Red Formation evaporites at the crest of the structure. This is basement-involved inversion that occurred in a location where the Lower Red Formation evaporites thinned considerably from the major depocenter to the southwest. Figure 7 shows larger-scale inversion during the upper part of the Upper Red Formation. A satellite image of the Mill anticline (Fig. 8) shows slightly overturned, north-younging Qom Formation affected by a number of minor faults within the Qom Formation that tend to stop at the top of the formation (Fig. 8). The prominent horizon of the d member anhydrite is much closer to the top of the Qom Formation in the vicinity of location 2 than to the west and east. This difference is at least partly caused by a small horst block formed by syndepositional normal faults.

The largest inferred normal or transtensional fault in the Saveh-Qom area is between the Alborz and Sarajeh anticlines and a line of outcrops to the south (Khurabad area), where the full Central Basin stratigraphy is exposed at the surface (Fig. 2). We refer to this as the Khurabad fault. The presence of as much as 3 km thickness of Lower Red Formation evaporites in the cores of the Alborz and Sarajeh anticlines, and the extensive evaporites extruded along the margin of the basin adjacent to the anticlines (Khurabad-Shurab area; Fig. 2), suggest that a very large volume of halite was locally deposited during Lower Red Formation time. To explain this local halite depocenter, together with strata patterns within the Upper Red Formation, the Khurabad fault is inferred to have controlled syndepositional expansion of the section (Fig. 9). Loading of the salt in the hanging wall of the normal fault by Upper Red Formation deposition either drove the salt along the normal and/or transtensional fault as diapirs or laterally into a salt roller that later evolved into the Sarajeh anticline. The southern limb of the anticline displays much greater thickness of Upper Red Formation than the northern limb, a characteristic interpreted to be the result of both normal fault activity and downbuilding caused by salt withdrawal. The seismic line in Figure 9 and other nearby lines do not image clearly the Khurabad fault in the vicinity of the Alborz and Sarajeh anticlines. Just to the southeast, however, where the fault trends north-northwest–south-southeast to north-south and is known as the Ab-Shirin-Shurab fault, the fault zone is imaged as a high-angle fault that dips steeply to the northeast to east (Fig. 10). The oblique-slip fault shows a large normal component of offset; however, in this location the main displacement occurred during the Upper Red Formation.

Basin Evolution of the Upper Red Formation

The onset of Upper Red Formation deposition is commonly marked by the presence of an ~400-m-thick sequence of evaporites and interbedded clastics. The Upper Red Formation evaporites are not present everywhere: in places their absence is simply the result of salt dissolution, or salt withdrawal, and residual

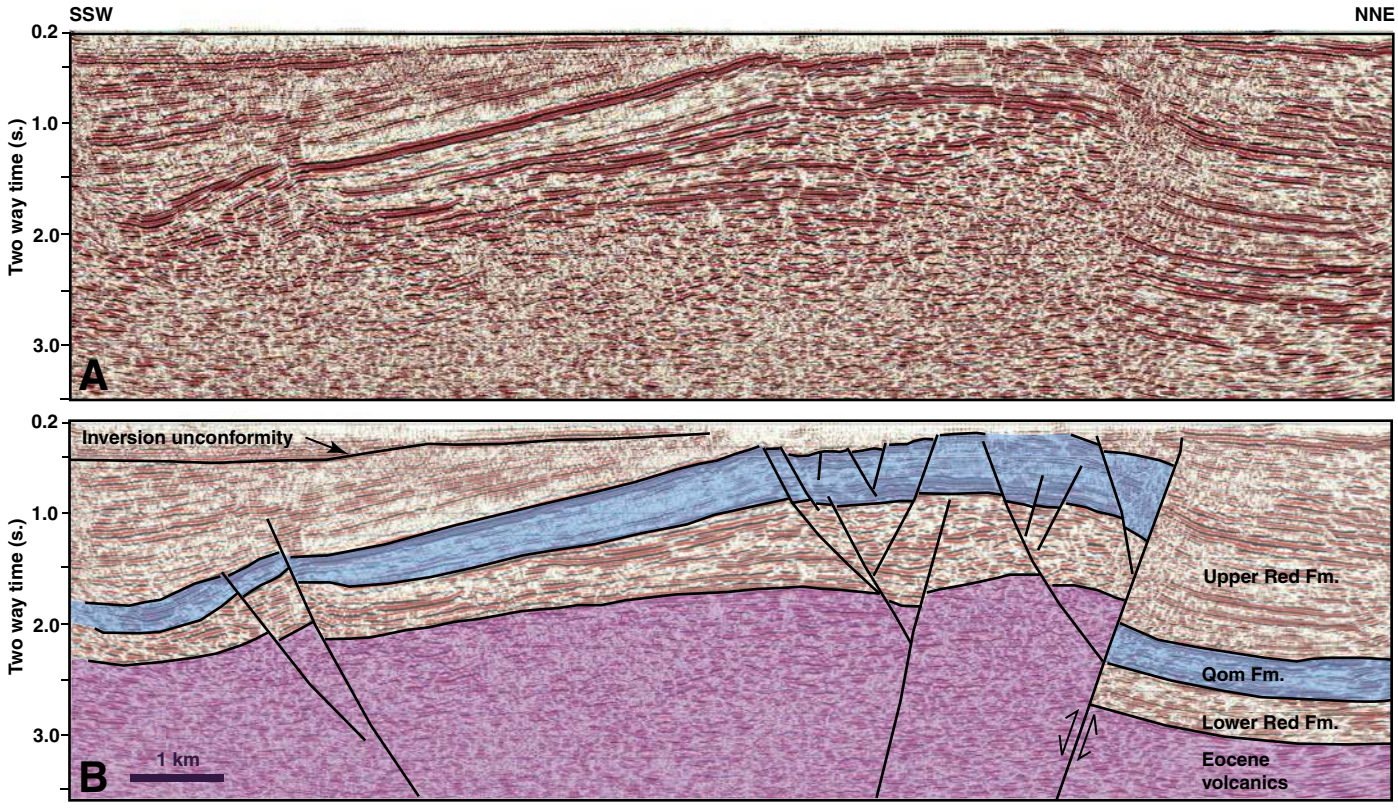

Figure 7. Two-dimensional seismic section across an inverted west-northwest–east-southeast–striking normal or transtensional fault. (A) Uninterpreted seismic line. (B) Interpreted line. Normal fault activity during the Lower Red and Qom Formations is indicated by expansion of the section toward the north-northeast, into a south-southwest–dipping fault near the north end of line. Numerous secondary normal faults are also present. Inversion during the Upper Red Formation is clearly marked by a shallow angular unconformity present in the southern half of the seismic line. See Figure 2B for location.

Downloaded from http://pubs.geoscienceworld.org/gsa/geosphere/article-pdf/5/4/325/3337666/i1553-040X-5-4-325.pdf
by guest

anhydrite beds mark the zones where salt was once present. In other areas the salt was simply not deposited; particularly notable is the absence of demonstrable Upper Red Formation evaporites and/or residual anhydrites in surface outcrops in the Saveh to Saveh Dam area (Fig. 2). Seismic reflection data from the southeast part of the study area (Shurab-Kassan area) reveal an example of a small synformal minibasin in the lower Upper Red Formation section (Fig. 11). The localized synformal basin is not fault controlled and is directly above the Upper Red Formation evaporites. Local sediment loading of a thick salt sequence seems the best explanation for the restricted geometry, location, and occurrence of the basin.

The onset of Upper Red Formation deposition heralded a considerable change in structural style. Examples of geohistory plots at the crest of the Alborz anticline and the depocenter between Saveh and Kuh-e-Namak (Fig. 12) illustrate that the change in structural style is associated with much more rapid subsidence during the time of deposition of the Upper Red Formation than that of the Lower Red and Qom Formations (Fig. 12). The geohistory plots show that changing salt thickness during the life of the basin, erosion at the crests of anticlines, and uplift of the land surface have to be taken into account when considering the subsidence history of the basin. For software-based basin modeling (including creating the geohistory plots in Fig. 12), absolute ages must be assigned to sedimentary units, even if they are not precisely known. Hence the 3 Ma age for the end of Upper Red Formation deposition in Figure 12 is an estimate only, not a precise age.

Determining the origin of the early Upper Red Formation subsidence is difficult because the Saveh area has undergone extensive, late, complex deformation that is the dominant structural imprint on the area. The Yort-e-Shah area provides the best evidence for the nature of the early Upper Red Formation subsidence. Seismic and drilling gas storage well data have established that a shallow, tilted fault block with Upper Red Formation and Qom Formation is offset by a fault from a deep depocenter (Fig. 13). The simplest and most obvious interpretation, based on the location of Qom Formation reflection terminations and expansion of the lower Upper Red Formation section toward the fault, is of a normal or oblique normal fault that was subsequently inverted (Fig. 14A). Alternatively, it is possible to interpret the fault as a steeply dipping strike-slip fault, or thrust fault (Figs. 14B, 14C), but the interpretation requires explanation as to why reflections on the south side of the fault

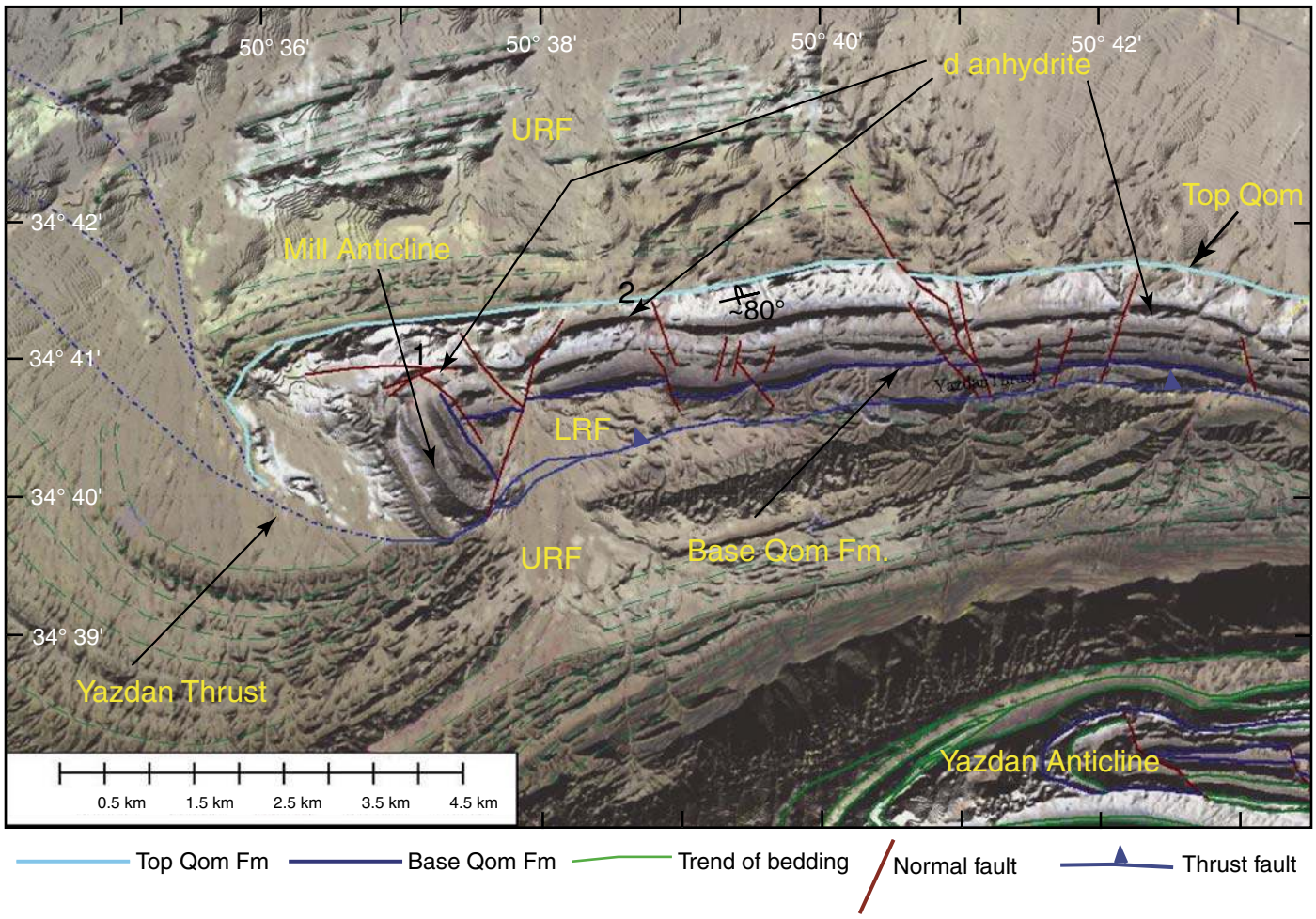

Figure 8. Partially transparent 15 m Aster satellite image, overlaid on 30-m-slope shaded digital elevation model for the Mill anticline showing normal faulting, folding, and thrusting of the Qom Formation. 1—location of Mill oil seep, 2—syndepositional horst block. See Figure 2B for location. URF—Upper Red Formation; LRF—Lower Red Formation.

Downloaded from http://pubs.geoscienceworld.org/gsa/geosphere/article-pdf/5/4/325/3337666/i1553-040X-5-4-325.pdf
by guest

terminations do not extend up to the inferred vertical or north-dipping fault.

Large thrusts overriding a foredeep basin can give rise to a deep depocenter in the footwall of the thrust, as proposed for the Upper Red Formation adjacent to the Alborz Mountains (Ballato et al., 2008). However, such geometries are not appropriate for the Lower Red Formation in the Saveh-Qom area for several reasons. (1) The massifs that were uplifted by the thrusts have a covering of Lower Red Formation, Qom Formation, and Upper Red Formation, i.e., they were uplifted late, not early in the history of the Upper Red Formation, and for a time were actually part of the Upper Red Formation depositional basin. (2) While the massifs are large, they are not part of a classic fold-and-thrust belt; the mass of the blocks is not large enough to drive development of a major foredeep basin, particularly not one with Upper Red Formation sediment thicknesses of 8 or more km. (3) There is no typical thrust-associated deformation of the footwall area such as overturned footwall synclines. This style is very different from the lack of deformation,

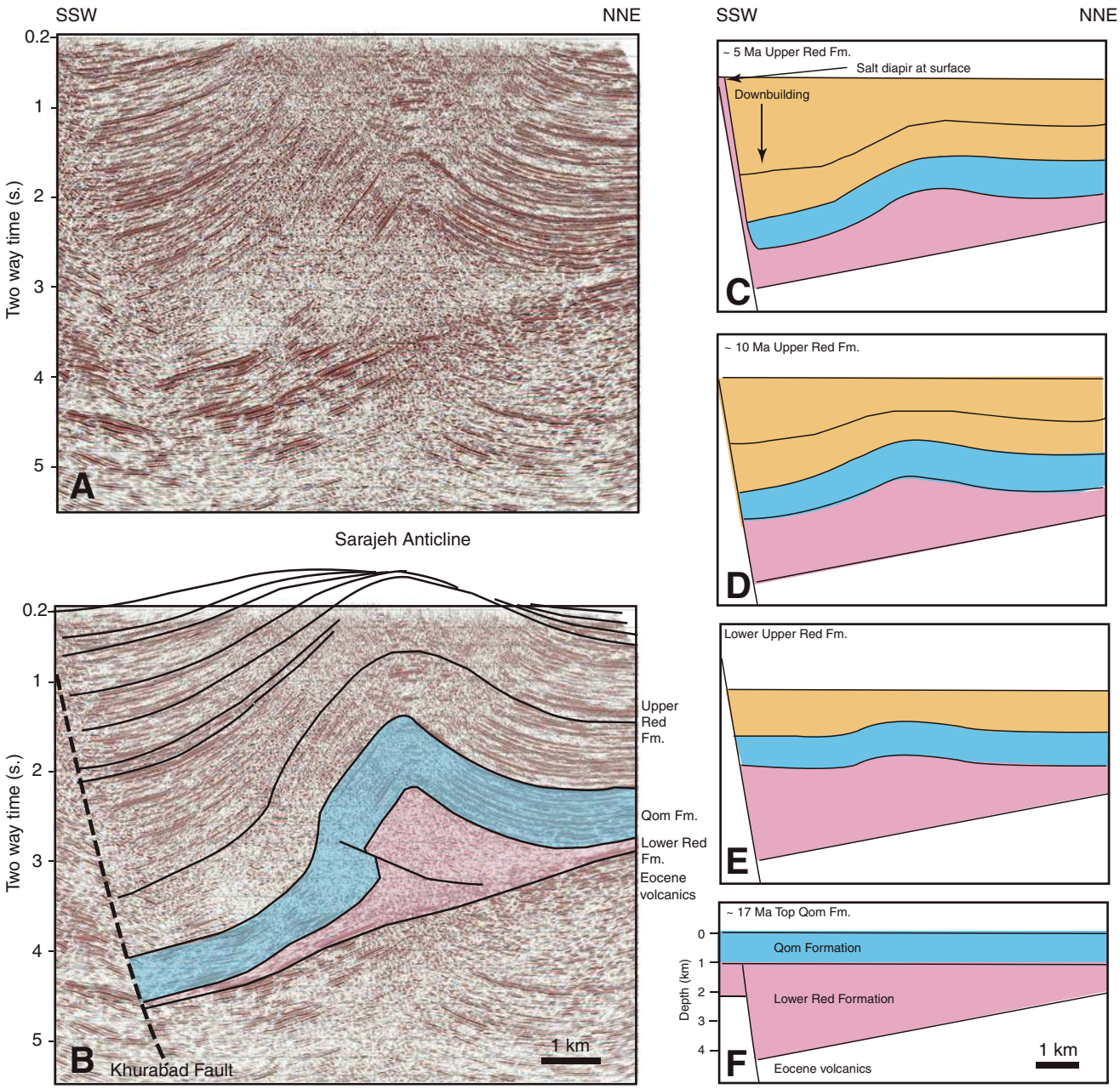

Figure 9. Example of a detachment fold on a two-dimensional seismic line across the Sarajeh anticline. (A) Uninterpreted line. (B) Interpreted line. Line drawings based on B show the sequential evolution of the section from Qom Formation time to Upper Red Formation time in sections C, D, E, and F. Note that the Upper Red Formation section on the south-southwest side of the fold displays a stronger pattern of growth toward the Khurabad fault and thinning onto the Sarajeh anticline than the north-northeast side. This suggests that fold growth, and downbuilding due to salt withdrawal, not just fold growth, affected strata patterns during Upper Red Formation time. See Figure 2B for location.

Downloaded from http://pubs.geoscienceworld.org/gsa/geosphere/article-pdf/5/4/325/3337666/i1553-040X-5-4-325.pdf
by guest

or expansion of section, followed by late folding of the depocenter observed on the seismic lines in Figures 7, 9, 10, and 13.

The general style of seismic geometry seen in Figure 13 is present on six seismic lines in the area. There are several other areas where inverted normal fault geometries are present (Figs. 2, 6, 7, and 9), suggesting that the extensional or oblique-extensional fault interpretation is the most likely. Figure 15 illustrates the range of stress permutations that could have affected the Saveh area during the Oligocene–Pliocene. Assuming uniform regional stresses and basic strike-slip fault geometries (i.e., the location of releasing and restraining bends with respect to extension direction in Fig. 15), the likely stress regime during the evolution of the basin can be predicted. Figure 15B shows pure extension on northwest-southeast–trending faults, and may be appropriate for the Lower Red Formation and Qom Formation, which display depocenter development on northwest-southeast–trending faults. In Figure 15A, the early Upper Red Formation depocenters are distributed across both north-south and northwest-southeast faults. This distribution indicates that the scenario in Figure 15C (approximately east-northeast–west-southwest extension, with minor components of oblique motion), is most appropriate for the early Upper Red Formation. Under the dextral

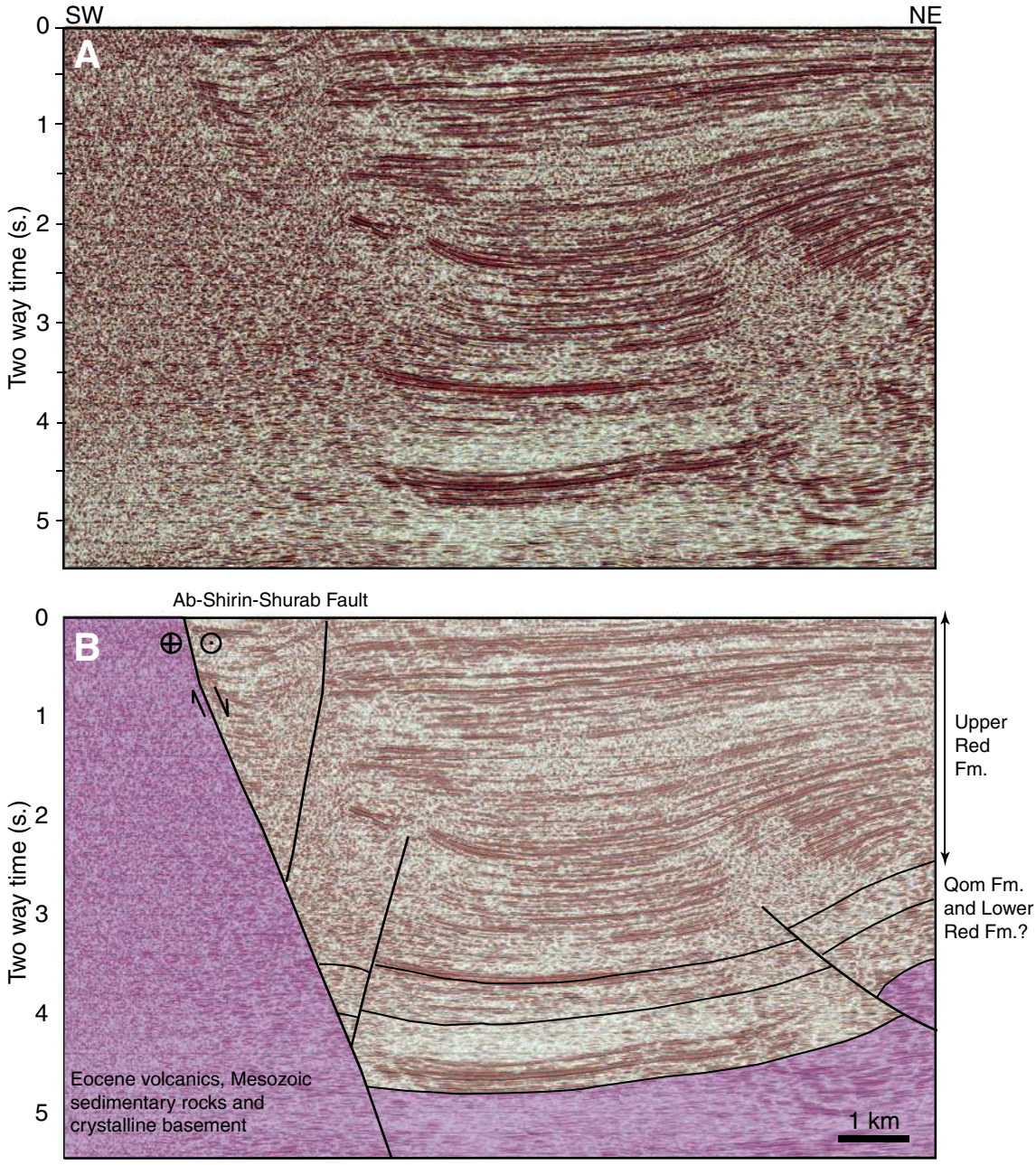

Figure 10. Seismic line across the high-angled boundary fault zone along the Ab-Shirin-Shurab fault zone. (A) Uninterpreted line. (B) Interpreted line. See Figure 2B for location.

Downloaded from http://pubs.geoscienceworld.org/gsa/geosphere/article-pdf/5/4/325/3337666/i1553-040X-5-4-325.pdf
by guest

transtension model in Figure 15D, the faults at location X should show little extension. The presence of large depocenters, however, indicates a considerable extensional component to these faults (Fig. 15A), suggesting that the oblique extension shown in Figure 15C is more appropriate for the lower Upper Red Formation setting than that shown in Figure 15D. Possibly stresses fluctuated between the northeast-southwest and east-west extension and/or transtension (Figs. 15C, 15D) during the time of the early Upper Red Formation; this could explain some of the early minor inversion seen on some northwest-southeast–striking normal faults (e.g., Fig. 6). Figure 15E illustrates the best defined of the deformation phases: late compression and/or dextral transpression.

The upper part of the Upper Red Formation section shows a clear change in reflection geometries marked by thinning onto folds. Figure 16 includes a partially restored cross section based on 2D seismic and outcrop data. The section marks a stage during Upper Red Formation deposition when the fold relief was much lower and Upper Red Formation deposition occurred all the way across the folds, with thinning onto the fold crests. During the later stages of fold development the fold crests were eroded. Synfolding geometries can also be seen in outcrops: in the Tafresh Massif, for example, a distinctive conglomerate composed predominantly of Qom Formation pebbles (attributed to the Pliocene on the 1:100,000-scale Tafresh geological map (Geological Survey of Iran, Geological Map of Iran, Tafresh) overlies conglomerates composed largely of volcanic clasts of the Upper Red Formation. The "Pliocene" conglomerate has been folded into a syncline beneath the Tafresh fault (thrust) and clearly shows progressively steeper dips downsection indicative of growth folding (Fig. 17).

During the later stages of folding, when basin subsidence failed to exceed fold growth and positive surface relief was attained at the fold crests, erosion began to affect the fold

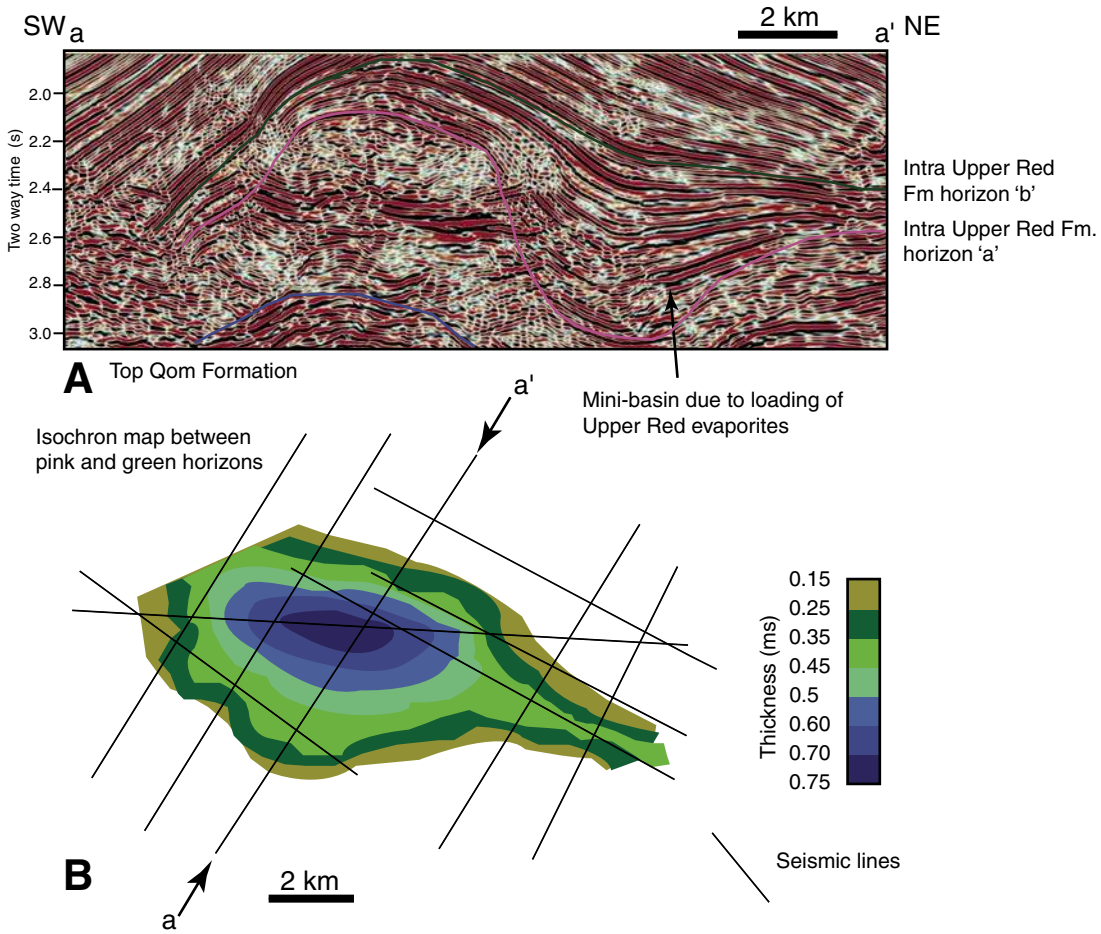

Figure 11. (A) Seismic line across a mini-basin in Upper Red Formation sedimentary rocks on the north-northeast side of a large anticline. The synclinal mini-basin is developed between the pink and green horizons, which are locally mapped seismic horizons within the lower part of the Upper Red Formation. In this locality the chaotic and/or transparent zone between the Upper Red Formation reflective section and the Qom Formation comprises both clastic units, and toward the base (above the blue horizon) ~400 m of evaporites. (B) Isochron map showing changes in vertical thickness in time (ms) between the pink and green horizons. Seismic line A crosses the center of a locally developed, depositional thick. This synformal thick is interpreted as a mini-basin created by loading of Upper Red Formation salt by early Upper Red Formation clastics. See Figure 2B for location.

Downloaded from http://pubs.geoscienceworld.org/gsa/geosphere/article-pdf/5/4/325/3337666/i1553-040X-5-4-325.pdf
by guest

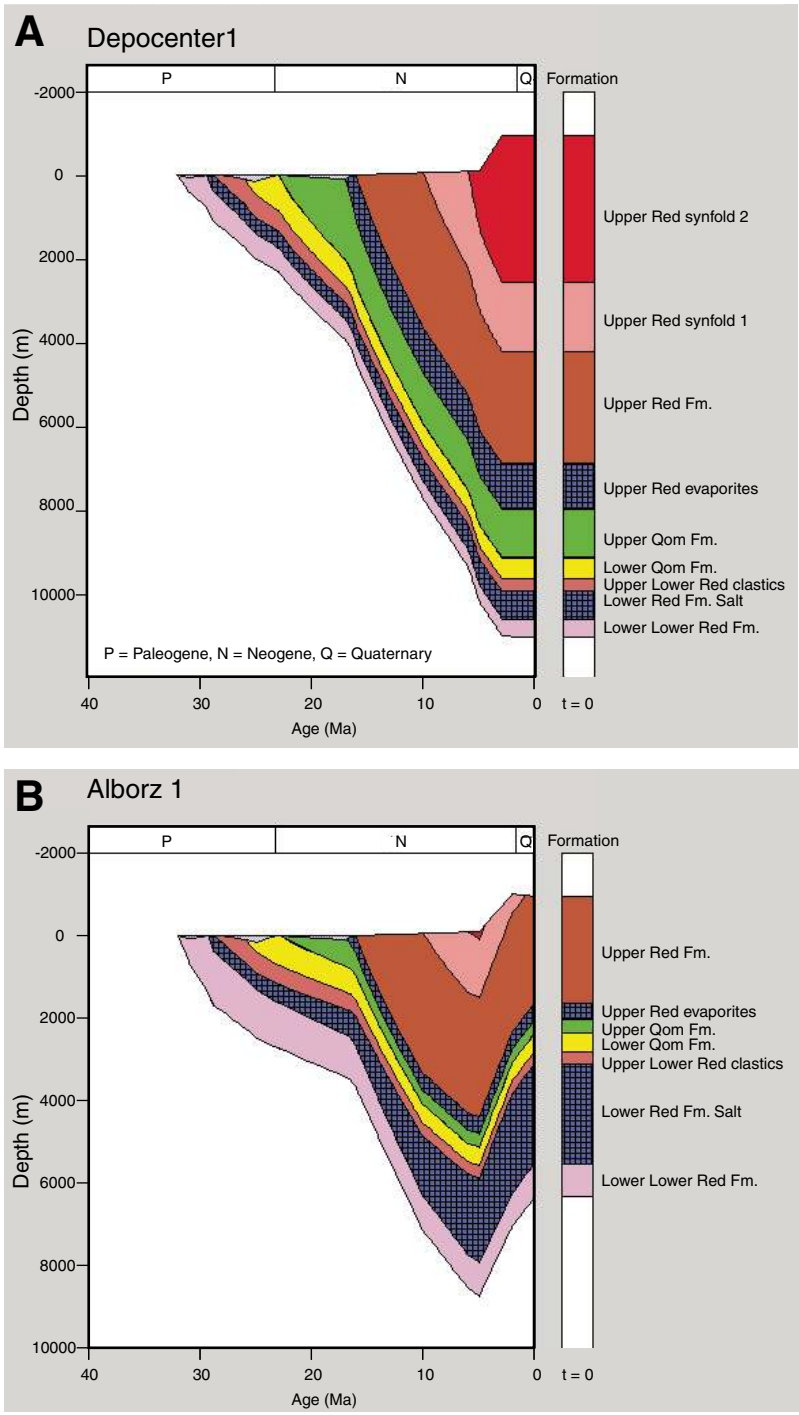

Figure 12. Geohistory plots. (A) The Saveh depocenter (based on seismic horizons). (B) The Alborz anticline (based on well data). Depths are in meters below present-day sea level.

crests. Restoration of seismic reflection geometries across the fold crests of two well-defined anticlines, coupled with vitrinite reflectance data and basin modeling by PTTEP, indicates that by the end of folding the Sarajeh anticline had lost ~900 m of section (Fig. 9), while the Alborz anticline had ~1600 m of section removed (Fig. 12). In the main depocenter southeast of Saveh, the section estimated to correspond with the period of strongest folding appears to be locally thick (~2500 m). This section thins onto the Alborz anticline to the southeast, and is removed by erosion to the northwest. The thickness of this upper section suggests that a significant time span (millions of years) needs to be allotted to this latest episode of deformation.

TRANSPRESSIONAL STRUCTURAL ELEMENTS

The Saveh-Qom area contains a number of distinct structural styles that reflect: (1) changing deformation styles through time, (2) different structural position (particularly within a transpressional system), and (3) facies changes within the sedimentary section that affect the mechanical stratigraphy, especially the type and thickness of evaporites. In this section we describe examples of the different structural elements. Deformation styles can be broadly divided into basement-involved structures and thin-skinned or detached structures. The terms "thick-skinned" and "basement-involved" are used for faults that cut through the Central Basin sedimentary section into the underlying Eocene volcanics section and Mesozoic section; i.e., the basement of the Central Basin. "Thin-skinned" or "detached" refer to movement on one or more of the evaporite units within the sedimentary section overlying the Eocene volcanics. Some evaporite deformation may be a consequence of sediment loading and independent of regional tectonics. However, much of the thin-skinned deformation is linked with basement-involved deformation, and hence is a manifestation of regional deformation. The transpressional belt developed in an area that had already been deformed during the Cenozoic. Consequently a number of fabrics were available for reactivation, in particular the early Upper Red Formation extensional-transtensional fault patterns (Fig. 15A) and early-formed salt diapirs.

The topography of the Saveh exploration block shown in Figure 18 illustrates the regional structural trends: a broad flat area in the east and central part of the block marks a region where the original Upper Red Formation fault-bounded basin is best preserved. Within this area the Alborz and Sarajeh anticlines

Downloaded from http://pubs.geoscienceworld.org/gsa/geosphere/article-pdf/5/4/325/3337666/i1553-040X-5-4-325.pdf
by guest

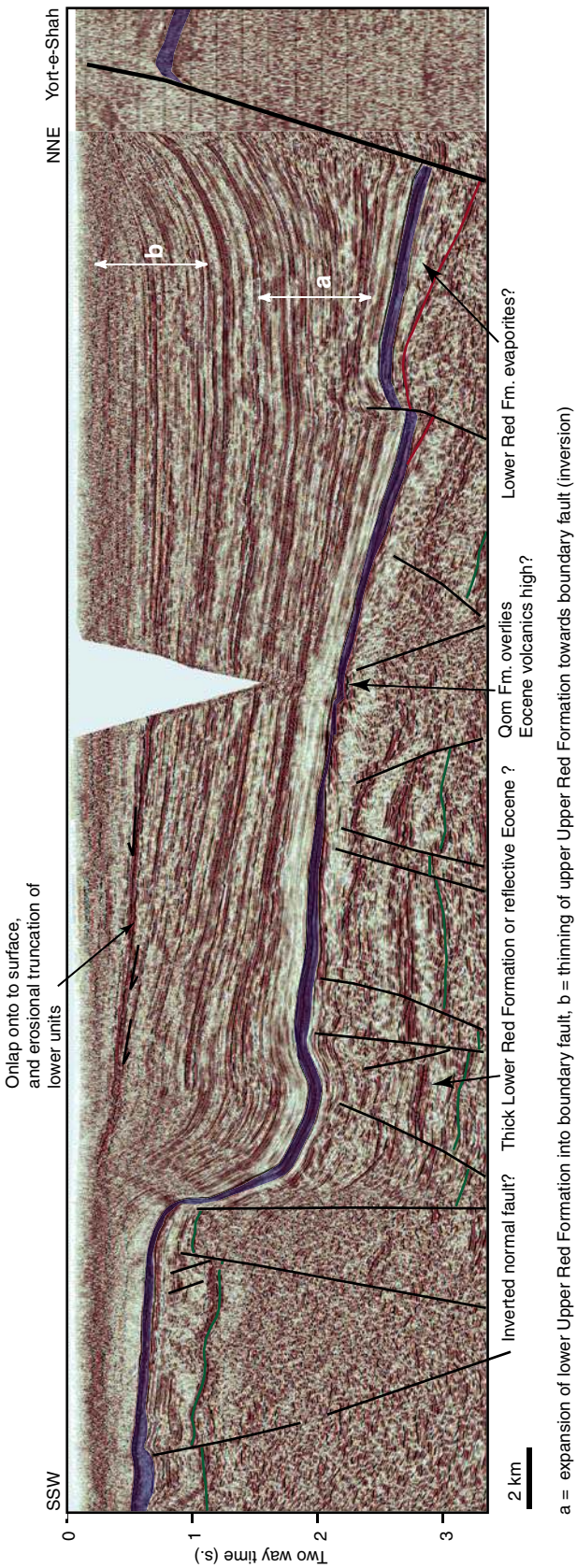

Figure 13. Two-dimensional seismic section across the northeast basin in the study area (see Fig. 2B for location). The age of the section underlying the Qom Formation is uncertain. However, the regional onlap of the Qom Formation onto the Eocene rocks occurs in the vicinity of this line, and hence suggests that the deep section is mostly or entirely of Eocene age, not Lower Red Formation. The line shows evidence for Eocene extension that reactivated in places during deposition of the Qom and Upper Red Formations.

form very low relief hills, while the salt diapir at Kuh-e-Namak is the most prominent topographic feature. Massifs bound the basin to the north and south. Westward, toward Saveh, the basin becomes increasingly narrow until the northern and southern uplifted areas bounding the basin meet at a narrow, strike-slip-fault–controlled valley.

Basement-Involved Transpression Deformation

Three main types of basement-involved faults are present in the area. The first type involves older high-angle extensional or transtensional faults that were active during or before deposition of the early Upper Red Formation. The second and third types of basement-involved faults include thrusts and strike-slip faults and/or transpressional faults that formed during deposition of the late Upper Red Formation and resulted in considerable uplift and erosion of the massifs that compose the Urumieh-Dokhtar volcanic belt. The characteristics of these faults are described in the following.

Inverted Normal and/or Transtensional Faults

Typically inverted normal or transtensional faults show a large component of normal offset and expansion of the early Upper Red Formation section, and occasionally of the Lower Red and Qom Formations (see preceding discussions of evidence for localized normal faulting affecting the Qom Formation, and basin evolution of the Upper Red Formation). In contrast, the upper section is strongly folded and detached from the lower part of the section (Fig. 19). Three large, west-northwest–east-southeast– to east-west–trending normal faults in the study area show such characteristic (Figs. 2 and 19). Some of the early normal faults also appear to have been reactivated as strike-slip faults during the later stage of folding and thrusting.

Some of the major massif-bounding thrusts may be late Oligocene–middle Miocene normal or transtensional faults that were subsequently inverted (Fig. 7). For example, the Talkhab thrust fault (Fig. 2) is shown on the geological map as dipping to the north-northeast, emplacing Eocene volcanics and Qom Formation in the hanging wall over Jurassic rocks in the footwall. If this relationship is correct, then the southern boundary fault to the massif is an inverted normal fault.

Thrust Faults

The clearest examples of basement-involved thrusting occur on the basin margins, where Eocene volcanics are thrust over the Central Basin stratigraphy, in particular the Indes fault

Downloaded from http://pubs.geoscienceworld.org/gsa/geosphere/article-pdf/5/4/325/3337666/i1553-040X-5-4-325.pdf
by guest

(Figs. 2 and 20) and the Saveh fault (Figs. 2 and 19). The Indes fault forms a very clear feature on the southwest margin of the basin, where the Lower Red Formation and Qom Formation were overturned in the footwall of the thrust (Fig. 20). The overturned beds at the surface are part of a major syncline with ~5 km vertical relief in the footwall of the Indes fault (Fig. 21). In the Saveh area a thrust sheet composed predominantly of Eocene volcanics was transported to the southwest onto the northeast margin of the basin during late Upper Red Formation time, and is associated with asymmetric folding of the Upper Red Formation (Fig. 21).

In general, the basin-margin thrusts trend west-northwest–east-southeast to northwest-southeast. Fault zone striations tend to plunge steeply, and indicate a small component of dextral strike-slip motion (Fig. 22). Measured surface dips of the thrust planes are typically 30°–40°. It is uncertain how the fault dips change with depth. Interpretations include (in order of diminishing influence of strike-slip deformation) upward-steepening faults into large-scale flower structures; maintaining the same dip with depth; or faults becoming become lower angle with depth, as is more typical for detached thrusts. These different interpretation possibilities cannot be definitively resolved with the available data.

In the Saveh area, the Saveh and Koushk Nousrat faults in map view (Fig. 2) form outcrop geometries that are straight to gently curvilinear, and are little deflected by topography, indicating that they are steeply dipping. Along the Koushk Nousrat fault a large fold in Eocene volcanics is repeated on both sides of the fault by a dextral offset of ~7–11 km (Fig. 2); this is not a true piercing point-derived offset, but probably is a reasonable indicator of the offset magnitude. The offset is seen in distinctive light colored volcanics on satellite images within the lower Eocene volcanics. One extensive outcrop near the old Tehran-Saveh road shows Qom Formation carbonates dipping south to south-southwest at 70°–80°, younging to the south and overthrust along the Koushk Nousrat fault to the north by Eocene volcanics. Striations dips are high, ~70°–75°E, but less so than minor faults that dip 80°–90°S; consequently, reverse motion with a minor dextral component is indicated. On seismic data the eastern end of the fault trend terminates in a large antiformal high (Fig. 23). At the plunging nose of the massif are outcrops of Qom Formation that show pervasive bedding-parallel (burial) and tectonic stylolites, which indicate that the Qom Formation was deeply buried before exhumation. Estimates from seismic data suggest at least 4 km burial along a south-dipping normal fault, which was inverted during time of deposition of the late Upper Red Formation (Fig. 9).

The Lower Red, Qom, and Upper Red Formations are commonly overturned in large synclines in the footwalls of the major thrusts, a phenomenon that is exemplified by the Indes fault (Figs. 21 and 24). The Qom Formation tends to be highly fractured and strongly affected by tectonic pressure-solution cleavage in such locations (with pressure-solution seams striking between ~080° and 110°). Consistent with the transpressional style of deformation, the orientations of the most important folds in the region are parallel or subparallel to the northwest-southeast– to west-northwest–east-southeast–striking faults (Fig. 22). The Alborz and Sarajeh anticlines, Khurabad folds and thrusts, Khu-e-Zangavar syncline, and Samar Dasht folds are some large-scale examples.

The west-northwest–east-southeast to northwest-southeast strikes of major faults and folds

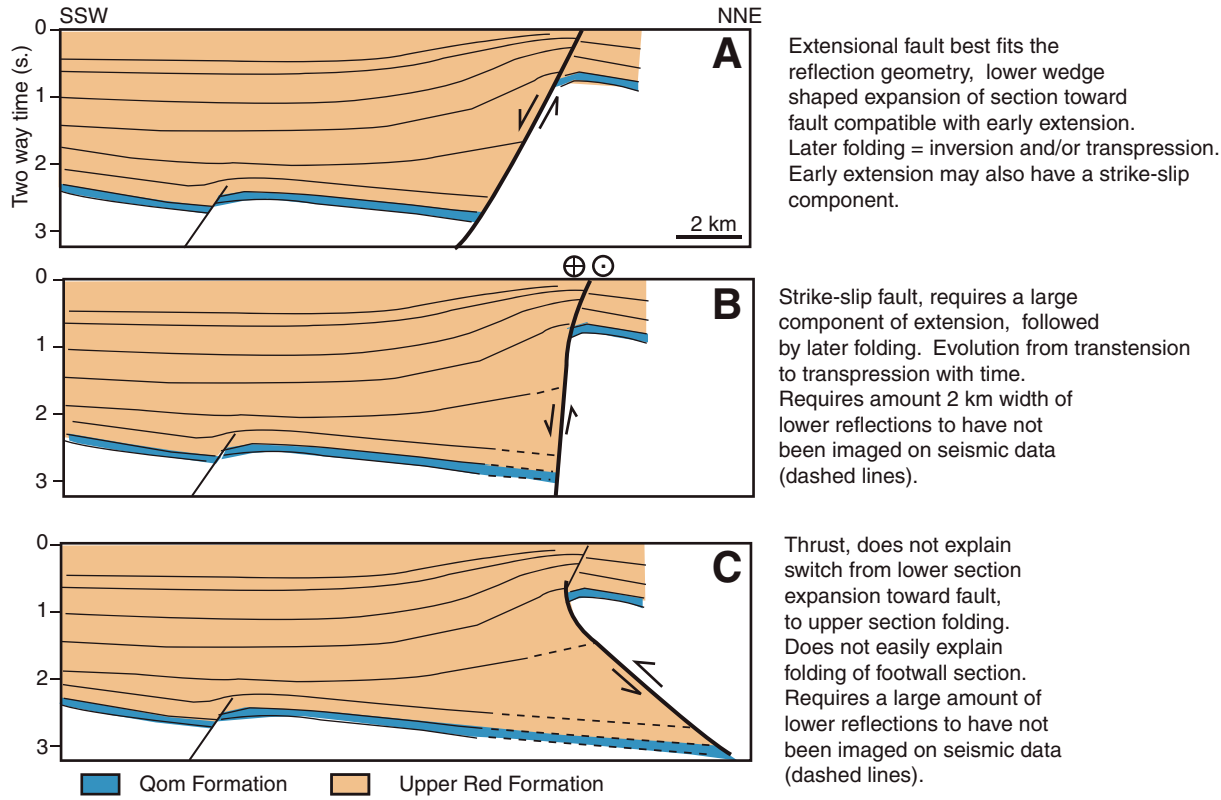

Figure 14. Line drawings based on the seismic line in Figure 13, showing the different ways in which the main bounding fault can be interpreted. (A) Normal or transtensional fault. (B) Strike-slip fault. (C) Thrust fault or transpressional fault.

Downloaded from http://pubs.geoscienceworld.org/gsa/geosphere/article-pdf/5/4/325/3337666/i1553-040X-5-4-325.pdf
by guest

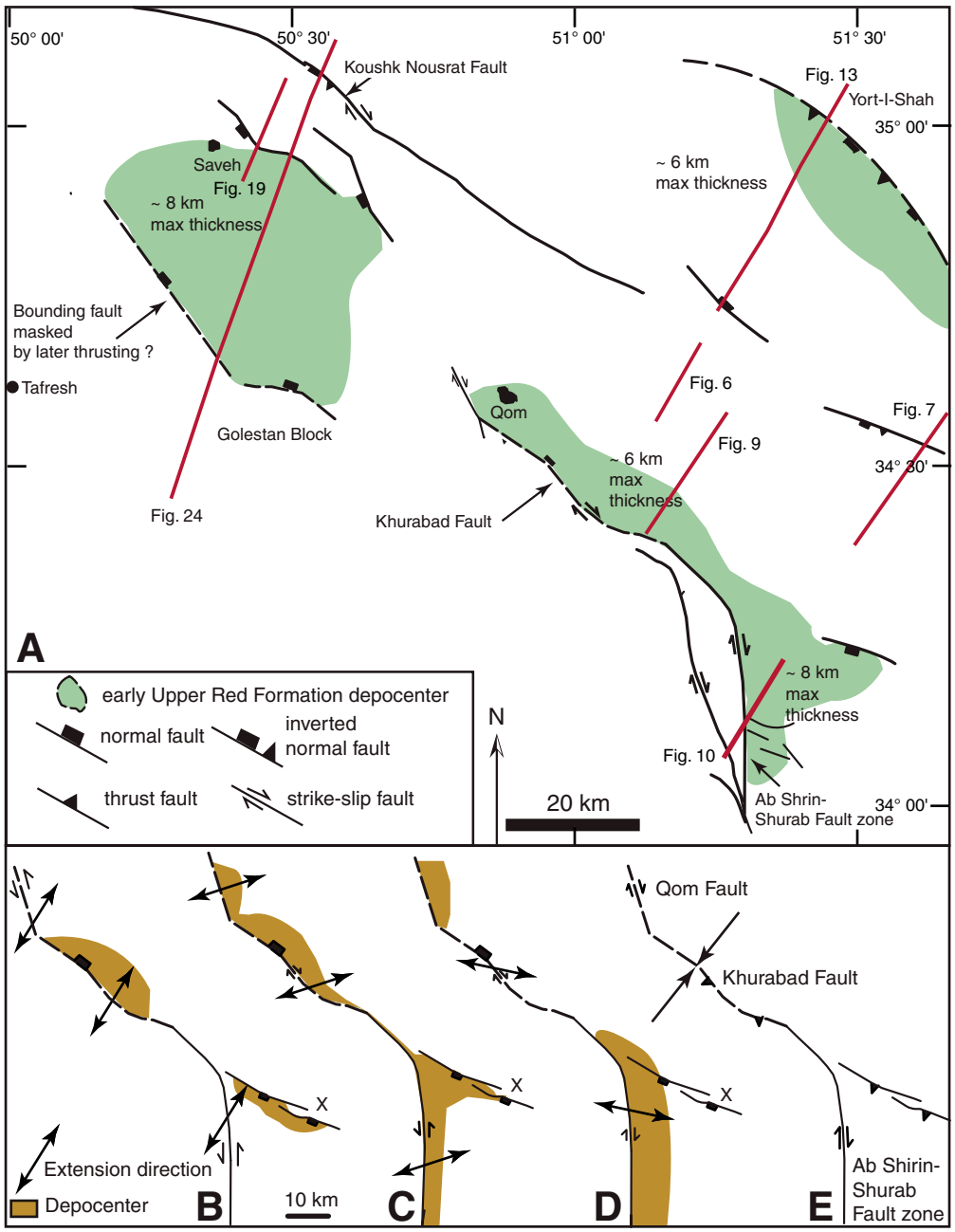

Figure 15. Top (A): Structure map showing the known active faults and depocenter locations during the early stage (early-middle Miocene) of Upper Red Formation deposition in the Saveh-Qom area, based on two-dimensional seismic reflection and outcrop data. Seismic lines that show support for the presence of Lower Red, Qom, and early Upper Red Formation normal or transtensional faults are shown in red lines. See Figure 2 for locations. Lower panel: illustration of the key fault geometries in the Saveh area (north-south–, northwest-southeast–, north-northeast–south-southwest–, west-northwest–east-southeast–trending faults) and the implications for location of basin depocenters with changing stress regimes. B—Northeast-southwest extension. C—East-northeast–west-southwest oblique extension. D—West-northwest–east-southeast extension and/or dextral transtension. E—Northeast-southwest compression and/or dextral transpression.

Downloaded from http://pubs.geoscienceworld.org/gsa/geosphere/article-pdf/5/4/325/3337666/i1553-040X-5-4-325.pdf
by guest

Downloaded from http://pubs.geoscienceworld.org/gsa/geosphere/article-pdf/5/4/325/3337666/i1553-040X-5-4-325.pdf
by guest

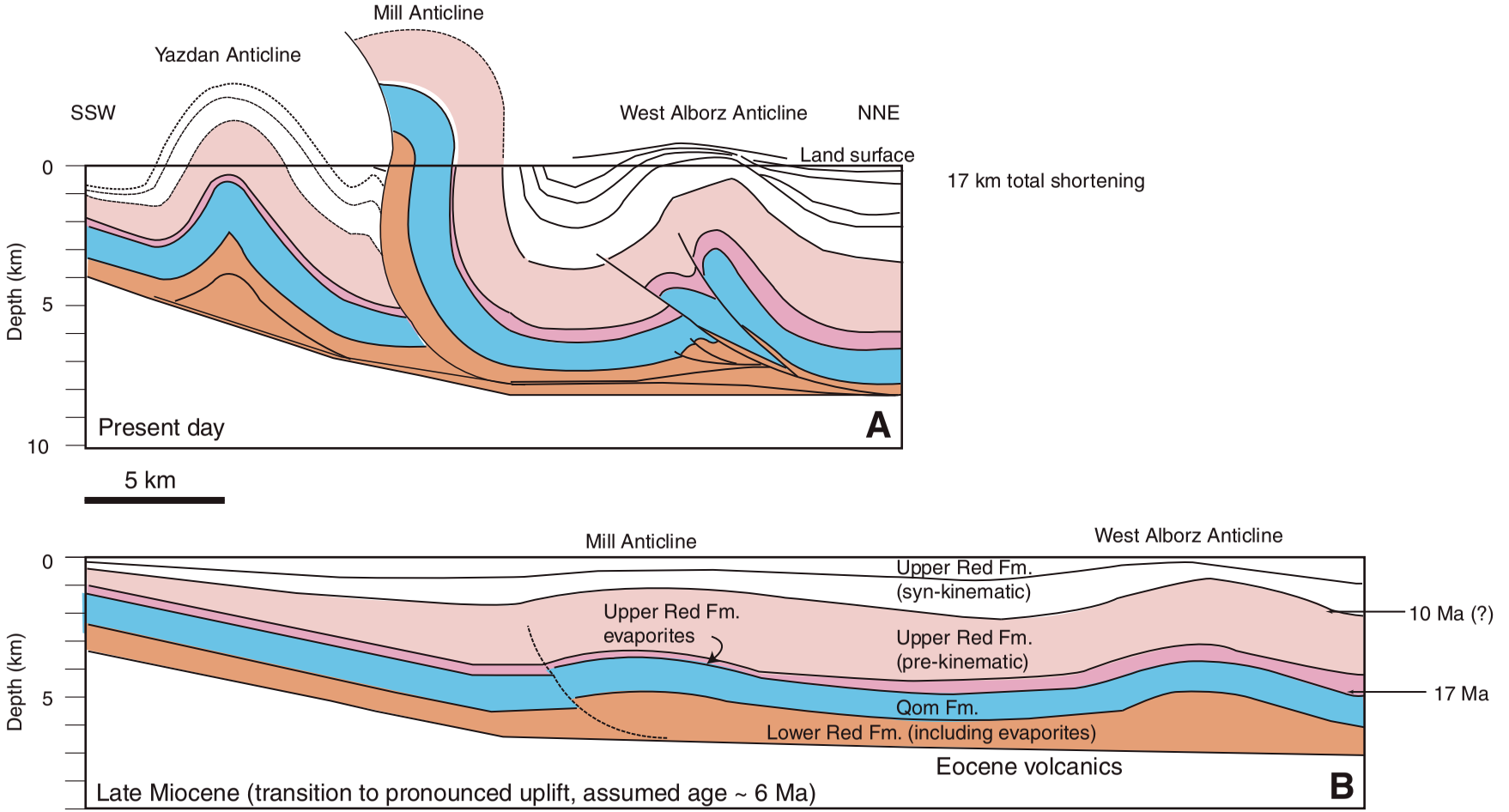

Figure 16. (A) Present-day section. (B) Partially restored section. Sections are across the detached fold-and-thrust area of the Central Basin (see Fig. 2B for location). Based on seismic reflection data (northern part of section) and outcrop data (Mill and Yazdan anticlines).

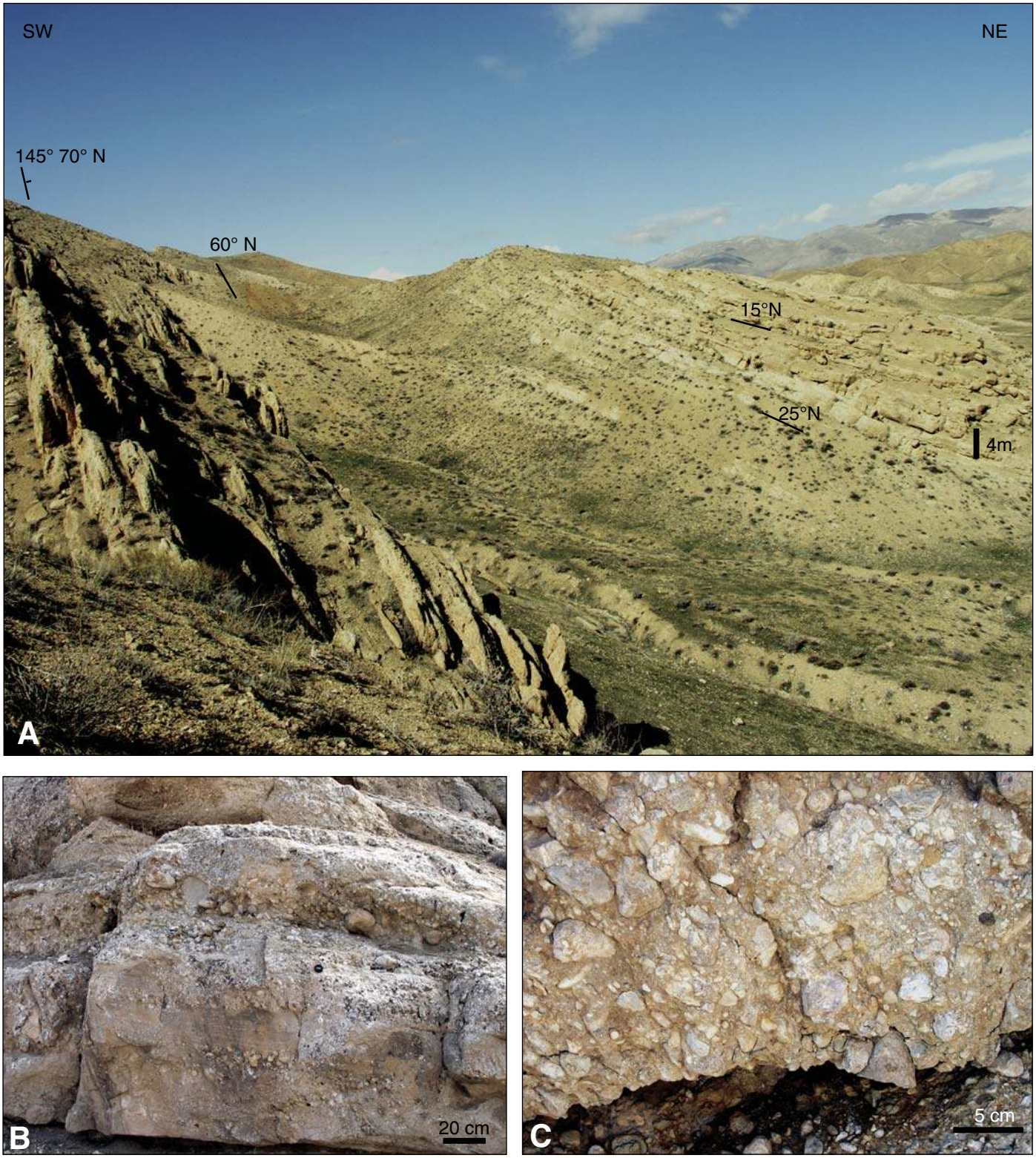

Figure 17. Photograph of the Pliocene conglomerates. (A) View of hillside showing progressive decrease in rotation of bedding upsection due to folding occurring during deposition. The conglomerates are composed predominantly of Qom Formation clasts (B and C). See Figure 2A for location.

Downloaded from http://pubs.geoscienceworld.org/gsa/geosphere/article-pdf/5/4/325/3337666/i1553-040X-5-4-325.pdf
by guest

in the area form the dominant structural trend. Other important orientations are east-west to east-northeast–west-southwest, and north-northwest-south-southeast (Figs. 2 and 22). Different structural styles are associated with these two trends. The east-west to east-northeast–west-southwest trends are restraining-bend geometries with respect to the general northwest-southeast to north-northwest–south-southeast fault trends, and hence they are zones of purer thrust motion (Fig. 15E). The Golestan block, Yazdan-Zandar anticline trend is the best-developed example of a restraining bend in the Saveh-Qom area (Fig. 2).

The Golestan block is a small uplifted block of Eocene volcanics, thrust to the north over the Upper Red Formation (Fig. 25). To the east the northward-vergent, thick-skinned thrust passes laterally into the southward-vergent, thin-skinned thrusts of the west Alborz-Mill-Yazdan anticline trends. It is a relatively small scale example of the lateral passage between thick-skinned and thin-skinned structures. The eastward-plunging edge of the Golestan block displays Lower Red Formation and Qom Formation overlying the Eocene volcanics. The Golestan block is interpreted here as an uplifted footwall area to a large, north- to northeast-dipping normal fault, with a structural geometry similar to the Yort-e-Shah area, at the north end of the seismic line in Figure 13. The Upper Red Formation in the hanging wall is very thick (>6 km), and it is unlikely that the immediately adjacent Golestan block was once covered by a similar thickness of Upper Red Formation. It is much more likely that the Upper Red Formation thickness was controlled by a north-dipping normal or subvertical transtensional fault. Then during the late Upper Red Formation time the block was thrust to the north and acted as a buttress, with folding concentrated in the thick Upper Red Formation section (Fig. 23). Seismic data show the folding to be detached within the Upper Red Formation.

Strike-Slip Faults

North-northwest–south-southeast–trending faults are best seen along the southern margin of the Saveh-Qom area in three main places: where the Indes fault bends east of the village of Indes, and extends down to the Golestan block (Fig. 19); the Qom fault, southwest of Qom (Fig. 23); and the Ab-Shirin-Shurab fault zone (Fig. 26). These fault zones all show important dextral offsets, but less associated thrusting and folding. They appear to be fault zones of greater strike-slip offset than the west-northwest–east-southeast to northwest-southeast faults. Examples in Figure 2 are the Qom fault zone, which accommodates the change in trend from the east-west Yazdan anticline to the north-west-southeast–striking Khurabad folds and thrusts, and the Ab-Shirin-Shurab fault zone (Fig. 26). None of these north-northwest–south-southeast–striking fault zones traverses the basin; they either die out within the basin, or they pass into northwest-southeast–striking fault systems. The strike-slip faults appear to act at least in part as transfer zones, and may well have reactivated preexisting fabrics and accommodated strain partitioning of oblique plate convergence, since they are present as important regional features elsewhere in Iran (e.g., Authemayou et al., 2006).

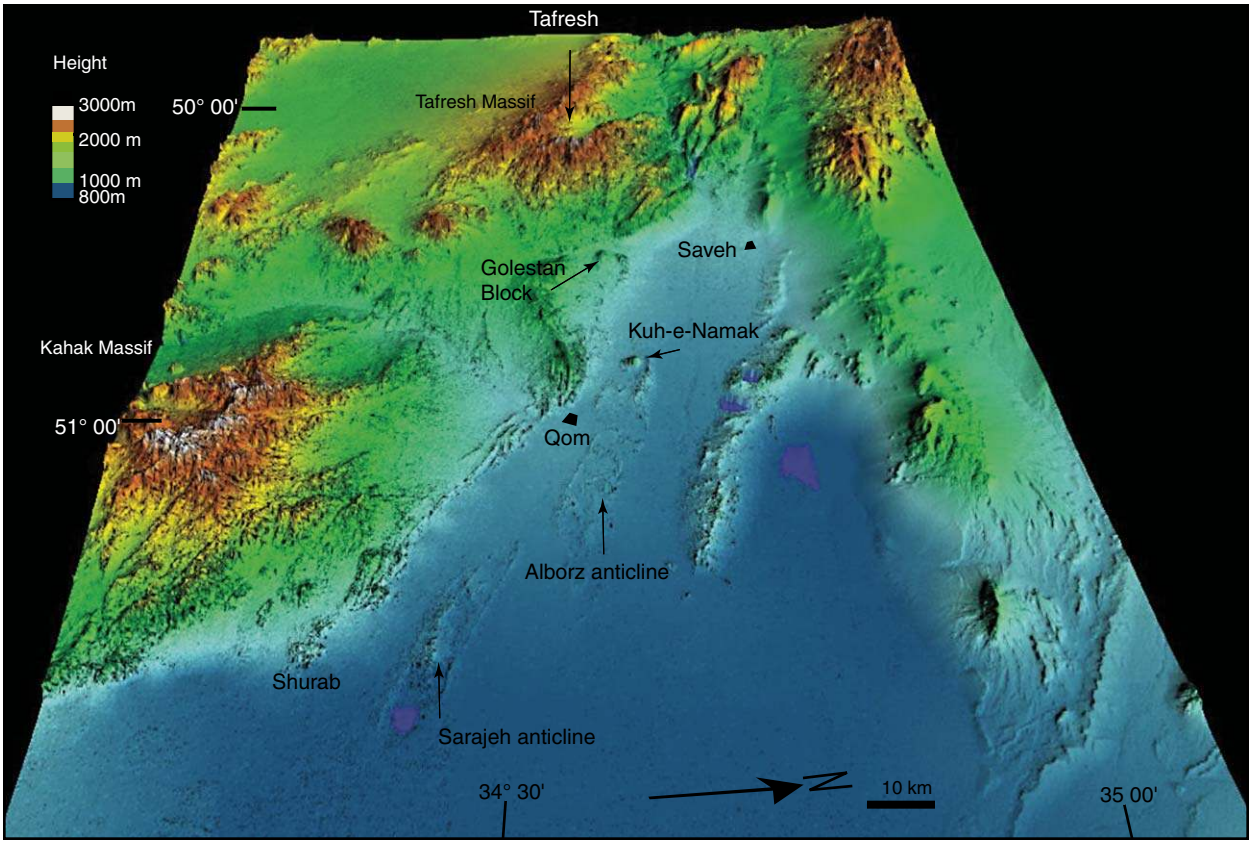

Figure 18. Three-dimensional perspective of a digital elevation model for the Qom-Saveh area, showing the large massifs south of the Central Basin region flanking the flat-lying remnant of the Central Basin. View is to the west. During the early to middle Miocene the Central Basin extended across the Tafresh and Kahak massifs.

Downloaded from http://pubs.geoscienceworld.org/gsa/geosphere/article-pdf/5/4/325/3337666/i1553-040X-5-4-325.pdf
by guest

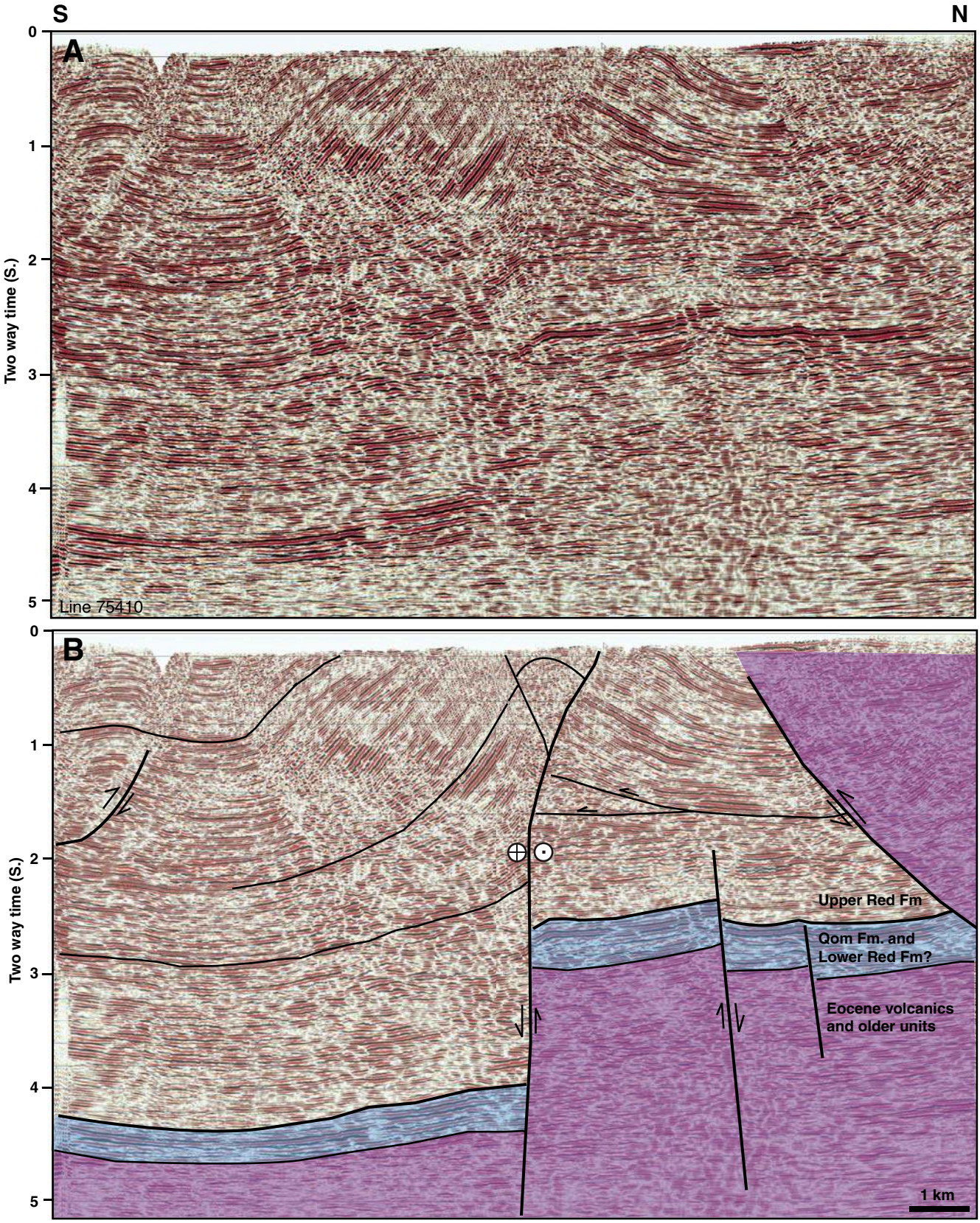

Figure 19. (A) Uninterpreted seismic line. (B) Interpreted seismic line. Lines are across the Saveh area showing older high-angle faulting, and younger thrusting and folding affecting the Upper Red Formation. There appears to be considerable strain partitioning, with strike-slip deformation concentrated on the vertical fault in the basin center, and compression accommodated by the lower-angle thrust on the eastern margin of the basin that emplaces Eocene volcanics over sedimentary rocks of the Central Basin. See Figure 2B for location.

Downloaded from http://pubs.geoscienceworld.org/gsa/geosphere/article-pdf/5/4/325/3337666/i1553-040X-5-4-325.pdf
by guest

The Ab-Shirin-Shurab fault zone is seen in Figure 10 as a steeply dipping fault, with a large normal component of offset that developed during Upper Red Formation time. On the northeast side of the fault is the thick Upper Red Formation depocenter, with >8 km of section. On the southwest side is the footwall area seen in Figure 26. The satellite image draped over a 30 m digital elevation model shown in Figure 26 illustrates the major surface features of the area: the Eocene volcanic massif is thrust to the northeast over Upper Red Formation outcrops. The Lower Red, Qom, and Upper Red Formations are offset ~4 km by a prominent dextral strike-slip fault, and a number of salt diapirs are present on the northeast margin of the outcrops. These diapirs appear to have come up the Ab-Shirin-Shurab fault zone. The area is a good example of the broad range of structural styles present in the basin.

Basement-Involved, Fault-Related Folds

The Eocene massifs form prominent, isolated high areas (Fig. 18) that are strongly folded on a large scale. Whereas some folding occurred prior to the formation of the central basin, the large-scale folds, and uplift of the massifs is clearly of late Miocene–Pliocene age, and involved deformation, uplift, and erosion of the Lower Red, Qom, and Upper Red Formations. The large-scale folding of the massifs is well illustrated on geological maps and satellite images (Figs. 2 and 25) and in the field (Fig. 4A). Figure 25 shows large-scale folds in the predominantly brown and black units of Eocene volcanics in the Tafresh massif. These units form a broad anticlinal dome that plunges to the southeast, accompanied by large secondary folds. Folding is a response to the thrusts that bound the massifs as well as thrusts within the massifs (Figs. 20 and 21).

Uplift of the Massifs

The crests of the massifs along the southern margin of the Central Basin are almost 2 km higher than the land surface of the Central Basin (Fig. 18). Assuming that the ~3 km thickness of Lower Red Formation to Upper Red Formation section present on the lower parts of the massifs once extended to the crests, then thrusting and folding has uplifted the massifs by ~5 km compared with the adjacent basins.

Figure 21 is a section based on outcrop data and a seismic reflection line that extends across the Central Basin west of Saveh. The section shows basement-involved shortening where Eocene rocks are thrust over the southwest and northeast margins of the basin. The calculated total shortening is ~28 km. Figure 27 expands the section shown in Figure 21 across the Central Basin west of Saveh and the Tafresh massif. The section shows basement-involved shortening

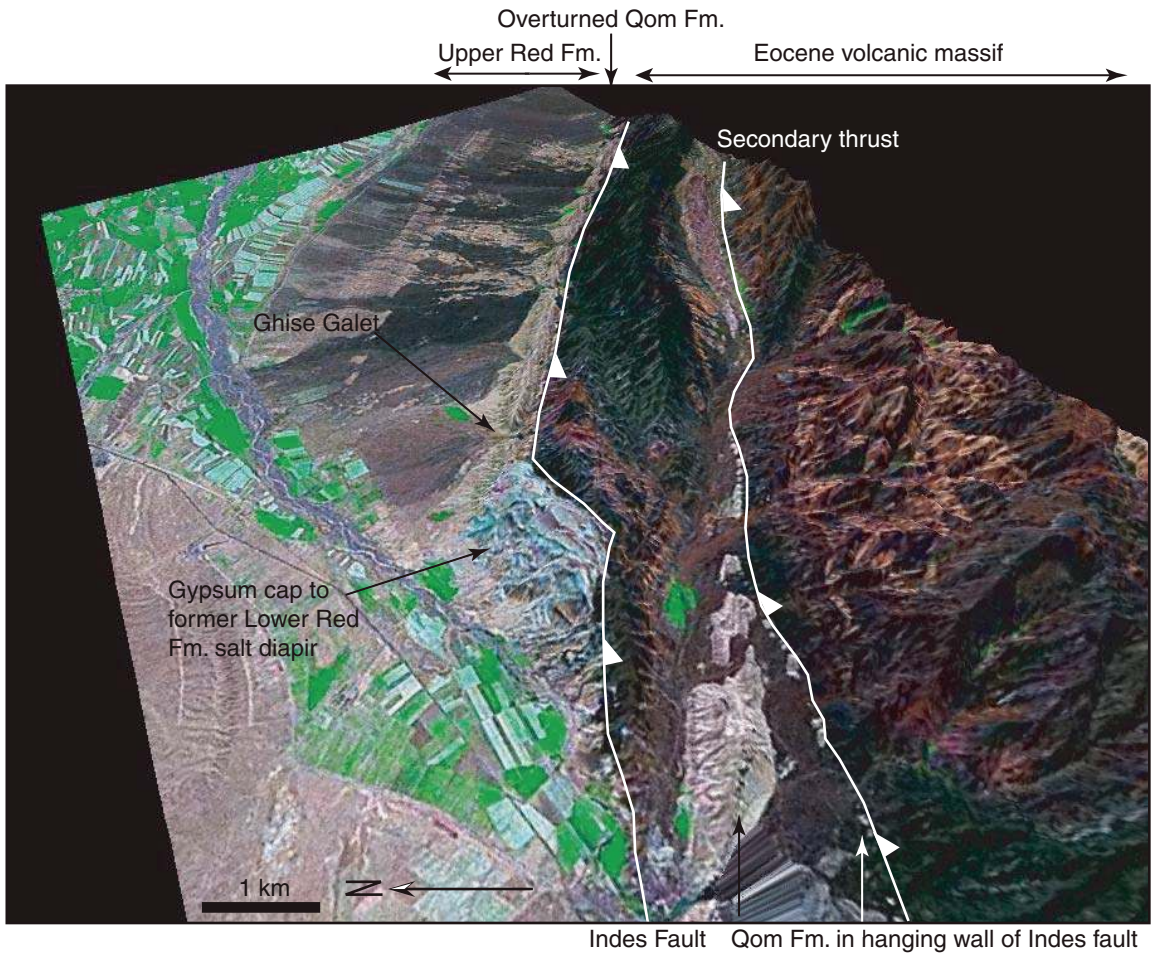

Figure 20. Three-dimensional perspective satellite image of the Gise Ghalet area, where the Indes fault has thrust Eocene volcanics over overturned Central Basin sedimentary rocks. A salt diapir has been intruded at an apparent left-stepping geometry in the Indes fault. See Figure 2B for location.

Downloaded from http://pubs.geoscienceworld.org/gsa/geosphere/article-pdf/5/4/325/3337666/i1553-040X-5-4-325.pdf
by guest

where Eocene rocks are thrust over the southwest and northeast margins of the basin. Total shortening is ~38 km, based on simple line-length measurement of the top Eocene volcanics–base Central Basin horizon (between locations a and a′ in Fig. 27). The present-day distance between a and a′ is 91 km and the original line length is 129 km, which indicates ~29% shortening.

Thin-Skinned Deformation

Evaporites are present at several levels in the Central Basin: at one or more stratigraphic levels in the Lower Red Formation; as thin primary anhydrites, particularly the widespread D member level of the Qom Formation, and at the base of the Upper Red Formation. Evaporites are known in the Central Basin from both outcrops and wells in the Alborz and Sarajeh anticlines. In places evaporites are present in outcrops in stratigraphic continuity (e.g., Zandar and Yazdan anticlines), while in other places they form diapirs (Marg, Gise Ghalet, Kuh-e-Namak, Shurab) (Gansser, 1955a; Chazan, 1970; Talbot and Aftabi, 2004; Fig. 2). Some of the diapirs are still active, particularly Kuh-e-Namak, while others have collapsed and most of the salt in the diapirs has been leached out (e.g., Shurab area, Fig. 26). The evaporites are important structurally as detachment horizons, diapers, and as seals to overpressured fluids (including the hydrocarbons in the Alborz field; Mostofi and Gansser, 1957; Abaie et al., 1964; Gretener, 1982).

In many parts of the Central Basin it appears that the most significant deformation is associated with Lower Red Formation evaporites. In particular, diapirs in the Shurab area, west of the Gise Ghalet, and at Marg (Fig. 2) are all located within the Qom and Lower Red Formations, and hence are sourced from the Lower Red Formation. The Lower Red Formation evaporite diapirs are most evident along the southwestern parts of the basin, suggesting that the evaporite source layer was originally thickest here, and that the evaporites thin depositionally northeastward. Upper Red Formation evaporites are best seen in the central part of the Saveh-Qom area; evidence for their presence includes (1) the salt diapir outcrops of Kuh-e-Namak in the west (Talbot and Aftabi, 2004), (2) well penetrations of Upper Red Formation evaporites in the Alborz and Sarajeh anticline in the east (Abaie et al., 1964), and (3) outcrops around the Yazdan and Zandar anticlines, where residual gypsum and anhydrites after halite are

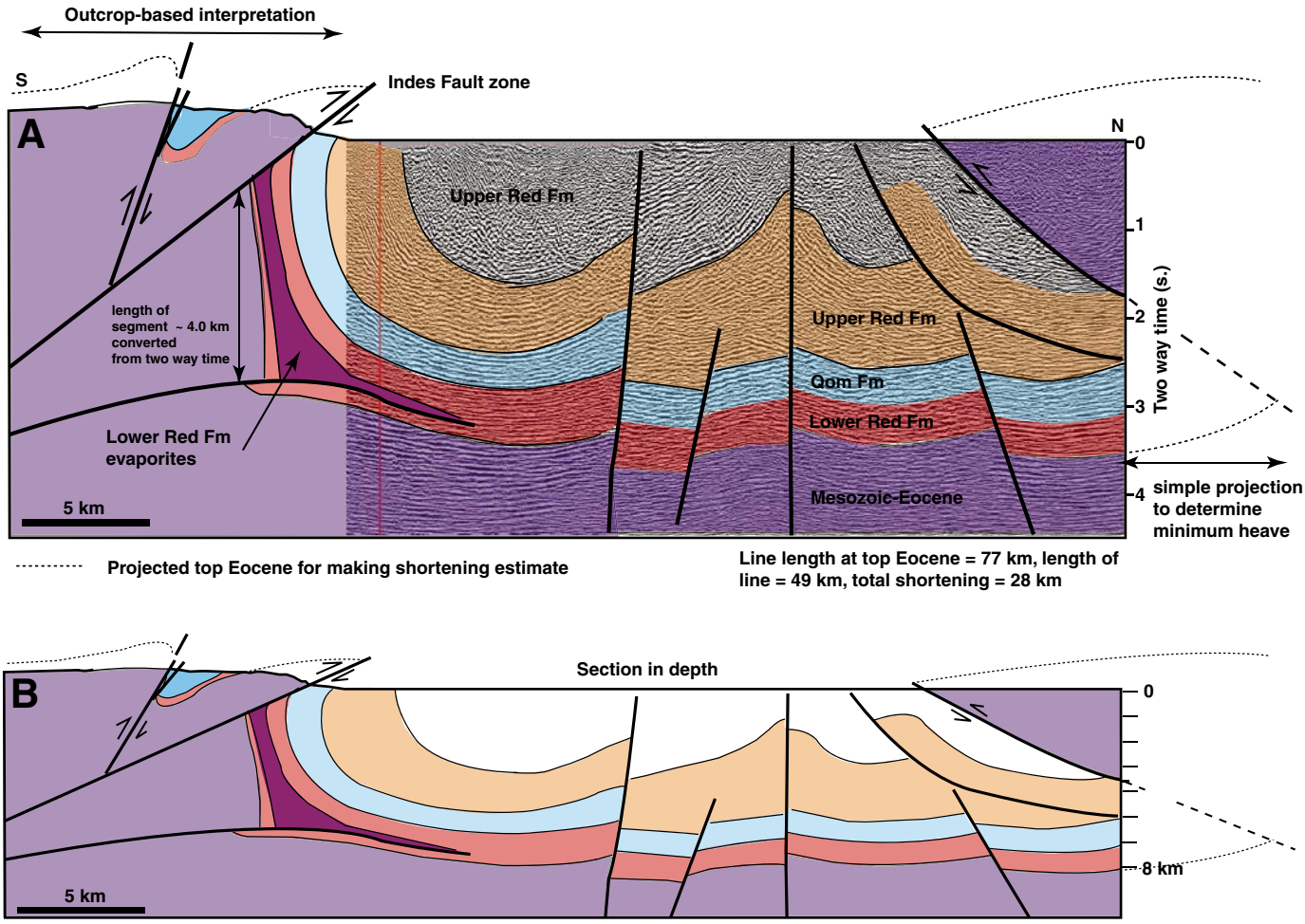

Figure 21. (A) Time-depth seismic section across the northwest part of the Central Basin based on seismic reflection data and outcrop data. (B) Line drawing depth section of A; vertical = horizontal scale. Shortening across the section is only an approximate calculation, because the transpressional nature of deformation in the area is non-plane strain. Most of the shortening is accommodated by the large thrusts on the margins of the basin. See Figure 2B for location.

Downloaded from http://pubs.geoscienceworld.org/gsa/geosphere/article-pdf/5/4/325/3337666/i1553-040X-5-4-325.pdf
by guest

present. Farther west in the Saveh area there is less evidence for the presence of Upper Red Formation evaporites, particularly around the Indes fault area, where there is no residual gypsum-anhydrite present in the lower part of the Upper Red Formation.

Structural Styles of the Evaporites

The Marg and Gise Ghalet diapirs (Fig. 20) are located at apparent restraining-bend geometries in oblique thrusts. However, at least in the case of Gise Ghalet, diapirism may have been initiated prior to thrusting. Diapir growth during deposition of the Qom Formation is suggested by the thin section, only ~250 m thick (compared with more typical thicknesses of 900—1000 m), the local presence of conglomeratic units, and several internal angular unconformities. Consequently, the diapir geometry may well have imposed a pseudo-restraining-bend geometry on the later thrust.

The diapirs in the Shurab area (Fig. 26) are adjacent to the Khurabad fault (Fig. 2). As discussed herein (see the section Evidence for Localized Normal Faulting Affecting the Lower Red and Qom Formations), the Khurabad fault initially controlled the basin depocenter and permitted accumulation of thick Lower Red Formation salt. During Upper Red Formation deposition the salt became loaded, unstable, and began to move. Once the transpressional stage of deformation occurred, the salt moved diapirically up the bounding transtensional fault, and in particular the Ab-Shirin-Shurab strike-slip fault zone (Fig. 8). The diapirs around Shurab are no longer active; the area comprises residual caps of Lower Red Formation sedimentary rocks, and volcanics with residual pods of salt.

The Kuh-e-Namak diapir contains two different types of halite, a clean, white halite, and a red banded halite, inferred by Talbot and Aftabi

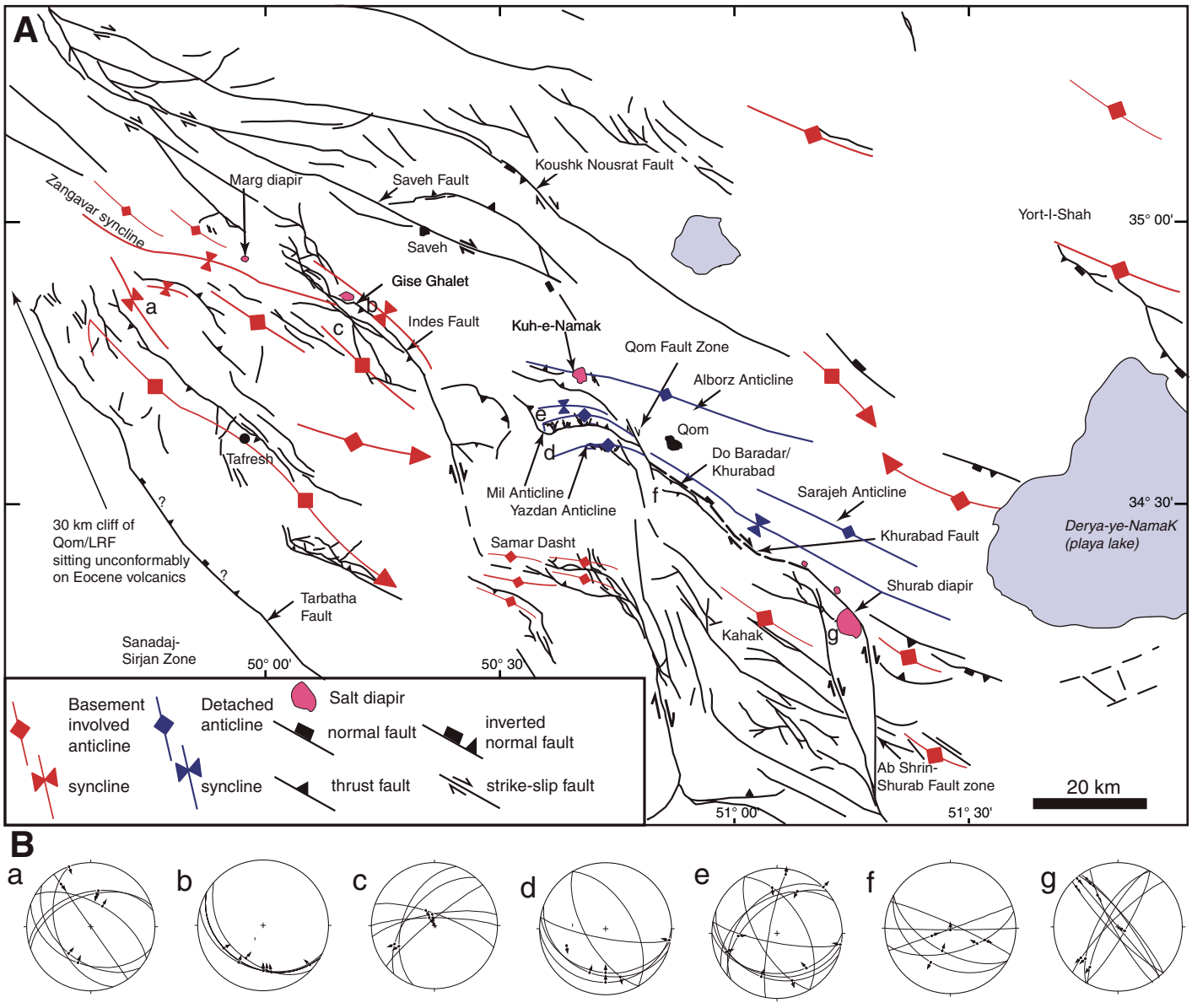

Figure 22. (A) Map showing the key Oligocene–Holocene structural features of the Qom-Saveh area (approximately the same area as Fig. 2A). (B) The stereonet plots of fault orientations and slickenside orientations for locations a–g shown in A. LRF—Lower Red Formation.

Downloaded from http://pubs.geoscienceworld.org/gsa/geosphere/article-pdf/5/4/325/3337666/i1553-040X-5-4-325.pdf
by guest

(2004) to be derived from the Lower Red Formation and Upper Red Formation, respectively. Unlike the Shurab diapirs the Kuh-e-Namak diapir is still active, with the salt hill rising ~300 m above the surrounding plains. Kuh-e-Namak does not occur at a single major fault zone, but rather at the intersection of the Qom fault zone, a west-northwest–east-southeast–striking thrust, and a pair of north-south–striking normal faults (Fig. 22). The normal faults are probably a response to depletion of one or both of the salt source layers during diapirism when, during compression, the salt diapir grew to the surface after tapping both the Lower Red Formation and Upper Red Formation evaporites.

In places salt diapirs moved during the Miocene, and were then squeezed and formed welds as a result of folding during Upper Red Formation time. Such deformation resembles that described from the Prebetics by Roca et al. (2006). The presence of welds and salt withdrawal can be seen in outcrops as residual gypsum, and in the subsurface by discordant structural geometries and synformal growth geometries within reflections that are not easily explained by bounding faults or simple folding (Figs. 8 and 10). The best examples of these features in outcrops and in seismic data are from the Saveh area (Fig. 2). East of the Saveh dam section are a number of small gypsum outcrops, characterized by nodular gypsum formed as a residual product of salt dissolution.

Salt Detachments

A key aspect of evaporite units is their ability to act as a detachment horizon for thrusts. The most important detachment level for the Saveh-Qom area is in the Lower Red Formation. This detachment is seen in seismic data across the Sarajeh, Alborz, West Alborz, and Mill anticlines (Figs. 8 and 28), and the trend appears to continue to the Yazdan anticline (Figs. 2 and 16). This detachment level locally displays classic thin-skinned structural geometries, in particular detachment folds and fault-propagation

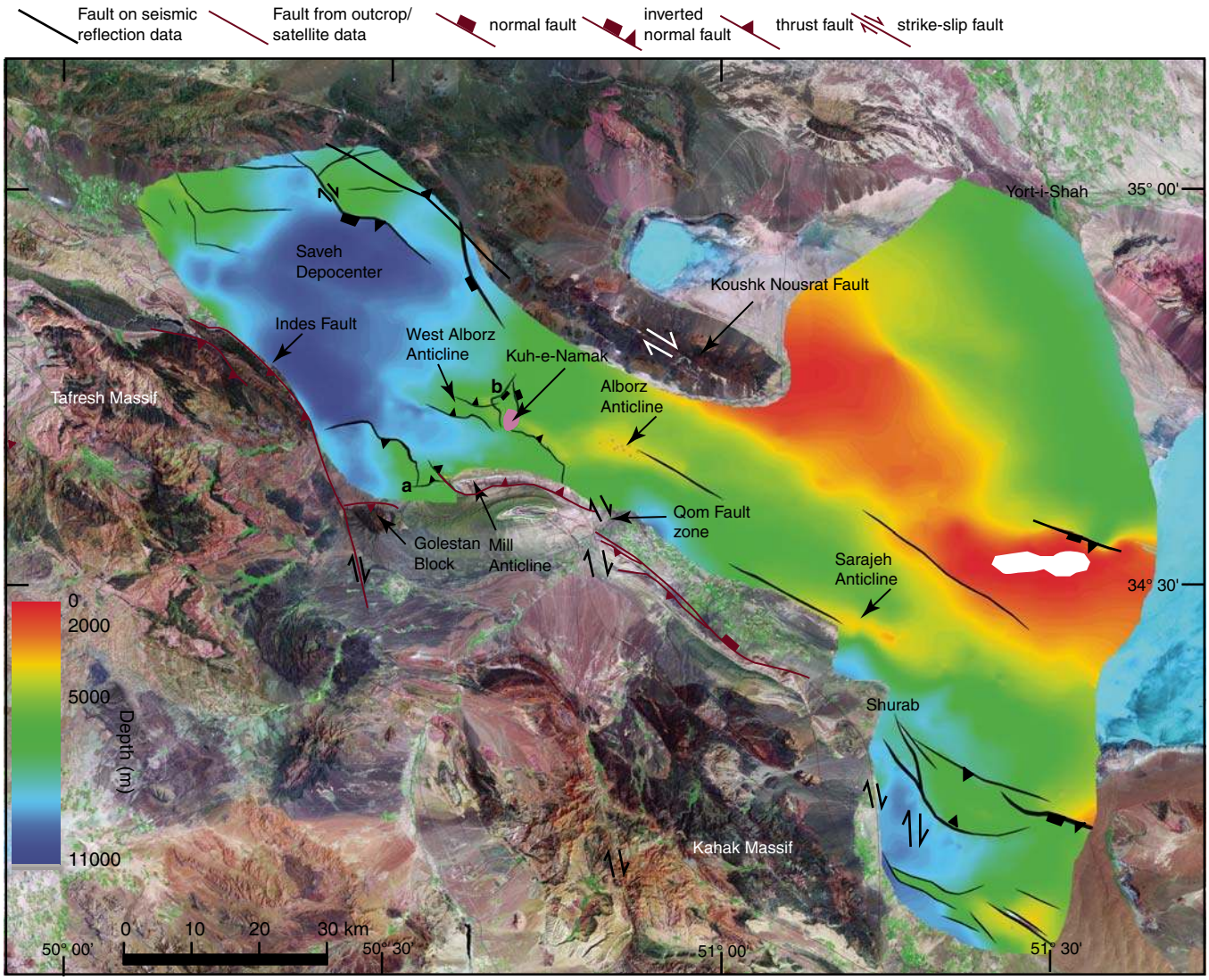

Figure 23. Depth map for the top Qom Formation based on seismic reflection data for the Central Basin imposed on satellite image of the Qom-Saveh area. a—location of transfer zone between north-dipping thin-skinned fault and south-dipping thick-skinned fault; b—location of growth faults associated with salt movement.

Downloaded from http://pubs.geoscienceworld.org/gsa/geosphere/article-pdf/5/4/325/3337666/i1553-040X-5-4-325.pdf
by guest

Downloaded from http://pubs.geoscienceworld.org/gsa/geosphere/article-pdf/5/4/325/3337666/i1553-040X-5-4-325.pdf
by guest

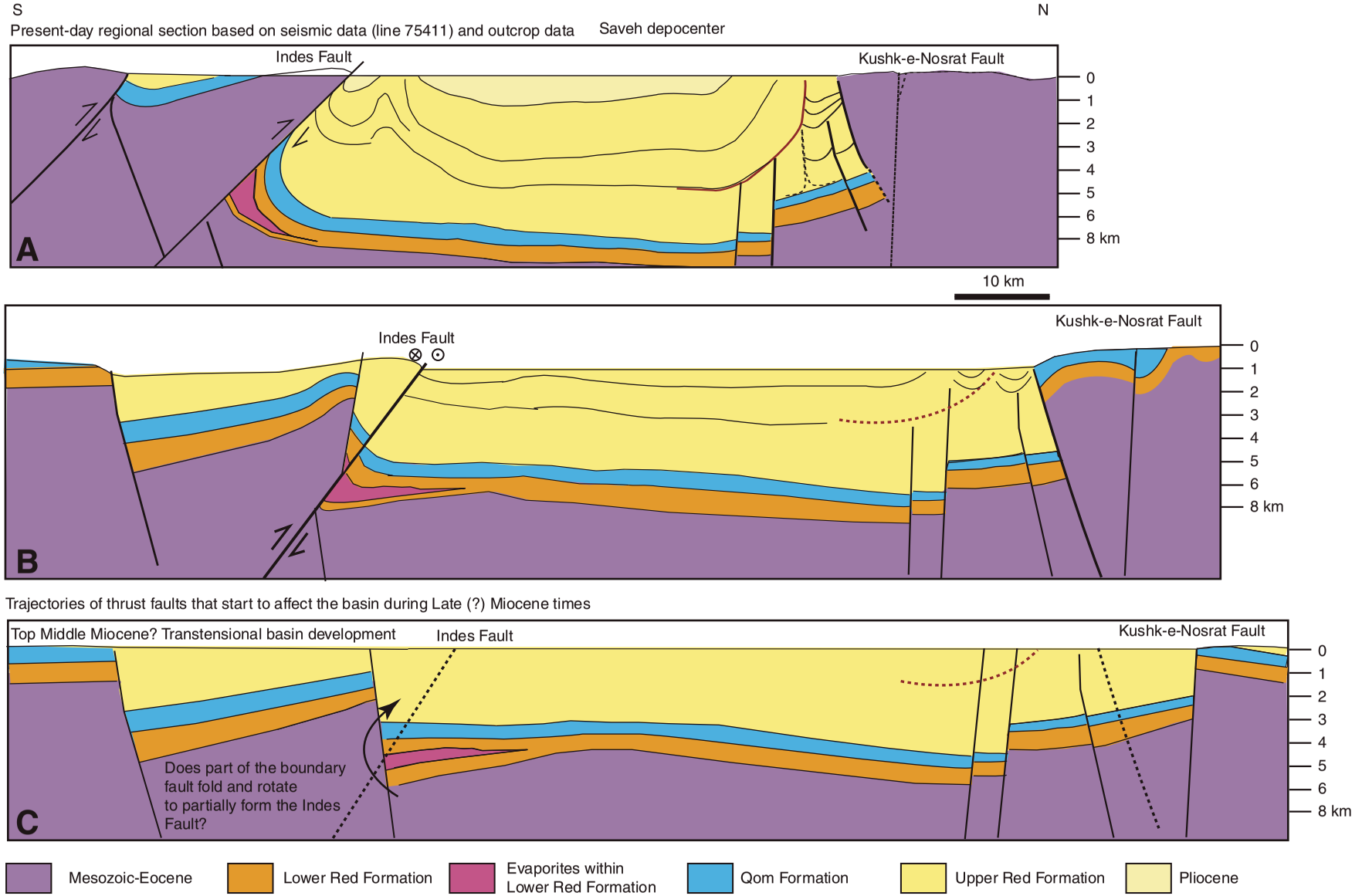

Figure 24. Series of restorations showing the evolution of the Central Basin during the Miocene–Holocene based on seismic reflection and outcrop data. (A) Present-day section. (B) Start of basin inversion due to dextral transpression during the late Upper Red Formation (ca. 10 Ma ago?). Deposition in the basin center occurred in a mini-foredeep basin setting. (C) End of transtensional phase (middle to late Miocene), when the Central Basin reached its greatest extent during the early Upper Red Formation. See Figure 2B for location.

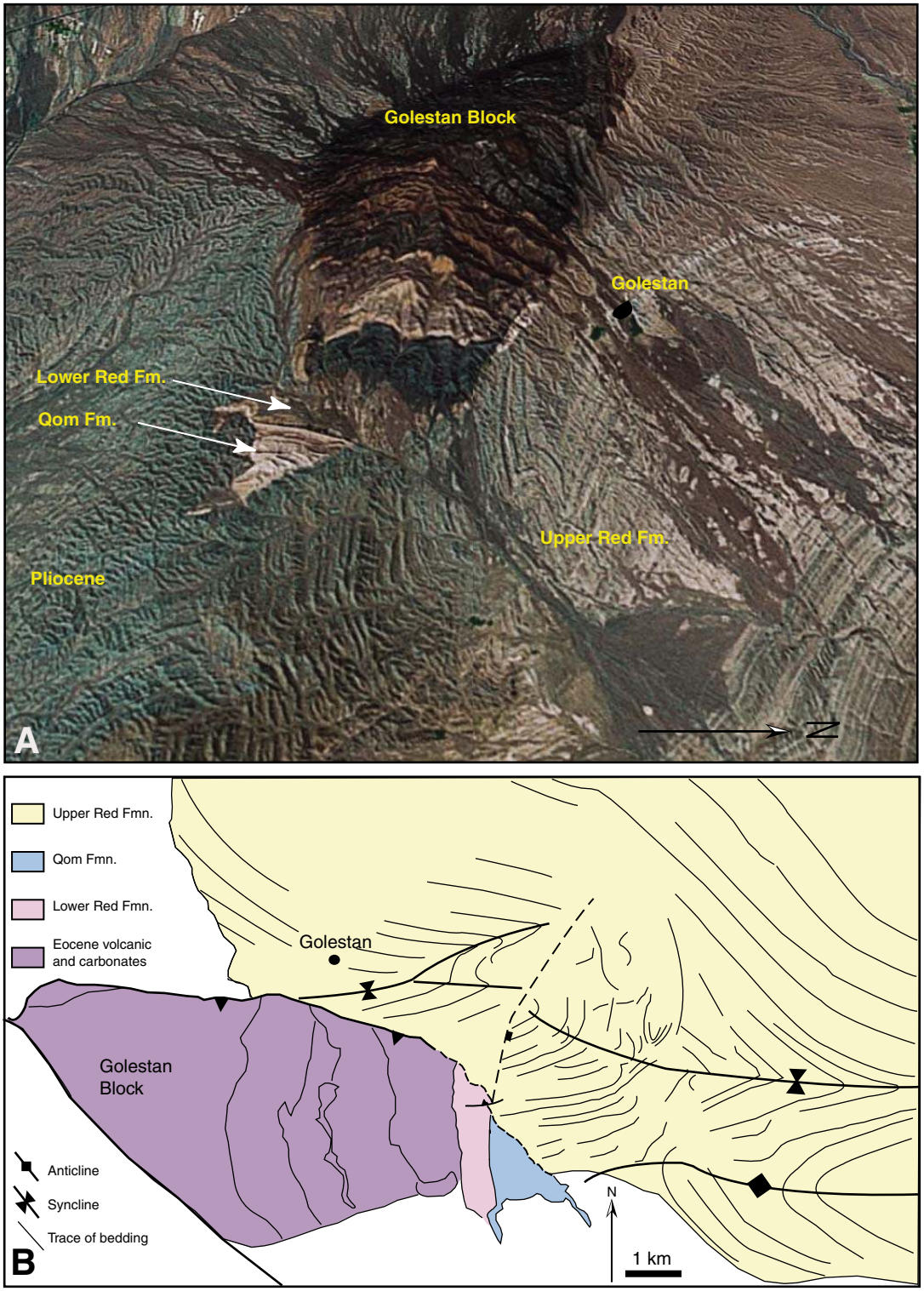

Figure 25. (A) Three-dimensional perspective image of the Golestan block showing the juxtaposition of the Eocene volcanics with folded Upper Red Formation. See Figure 2B for location. (B) Geological map of the same area. The Golestan block is a relatively small example of the interaction between thick-skinned thrusting and Central Basin sedimentary rocks.

Downloaded from http://pubs.geoscienceworld.org/gsa/geosphere/article-pdf/5/4/325/3337666/i1553-040X-5-4-325.pdf
by guest

folds (Figs. 8 and 16). The Upper Red Formation is generally not strongly detached from the Qom Formation along the Upper Red Formation evaporites, although examples of small thrusts and folds that detach in the evaporates can be seen in seismic reflection data.

Figure 28 shows the distribution of Lower Red Formation salt thickness in two-way traveltime as mapped from seismic reflection data. Two prominent salt accumulations (as thick as 3 km) occur in the cores of the Alborz and Sarajeh anticlines. As discussed earlier, this salt depocenter appears to be controlled by the transtensional Khurabad fault (Fig. 9). The Alborz and Sarajeh folds resemble Zagros-type detachment folds in size and geometry. However, the folds differ from the Zagros type in being isolated features, not an extensive chain. The isolation is caused by the limited area of the evaporites resulting from fault control, depositional distribution, or postdepositional salt removal. An additional effect of fault control is to locally rotate the detachment to a relatively high angle, for example the ~6° dip of the detachment to the south-southwest into the Khurabad fault (Fig. 9).

The thinning patterns of Qom Formation reflections around the Sarajeh anticline suggest that the anticline was a local high during Qom Formation deposition, probably due to an underlying salt pillow. This preexisting high later acted as the perturbation that localized transpressional folding. The crestal area of the Alborz anticline is also a simple detachment fold. However, the fold structure becomes more complex to the west (West Alborz anticline), where blind imbricate thrusts affect the core of the structure (Fig. 29). Salt withdrawal to feed the adjacent Kuh-e-Namak diapir probably depleted the salt detachment layer relatively early during folding. Consequently, the classic problem of balancing line length progressing from the outer arc of the fold to the fold core resulted in thrusting within the anticline core, rather than the flow of salt, as seen farther east (cf. Figs. 9 and 29).

The Khurabad fault dies out westward, so that in the vicinity of the West Alborz anticline a broader detachment surface developed where three thin-skinned structures are present (the West Alborz, Mill, and Yazdan anticlines; Fig. 2; Gansser, 1955a, 1957; Furrer and Sonder, 1955). The Mill anticline is a particularly striking structure imaged both in seismic data and by almost 100% surface exposure (Figs. 8 and 29). In outcrop the Qom Formation forms a west-northwest–east-southeast–trending ridge of slightly overturned Qom Formation that dips ~80° to the south-southwest and youngs to the north-northeast (Fig. 8). South of the Qom Formation a narrow strip of Lower Red Formation is separated by the Dochah-Yazdan thrust from Upper Red Formation to Pliocene rocks farther to the south. At the north-northwest end of the Qom Formation ridge, bedding turns to the south-southwest to form the Mill anticline, which is terminated at the Yazdan thrust (Fig. 8). When outcrop data are combined with adjacent seismic data, the Dochah-Yazdan thrust is seen to be strongly folded, dipping ~80° to the south-southwest at the surface and curving around to dip to the north-northeast in the subsurface before flattening out into the Lower Red Formation evaporite detachment at ~5 km depth (Fig. 29). The Dochah-Yazdan thrust has accommodated a considerable amount of thin-skinned shortening (~10 km, Fig. 16).

The area of thin-skinned structures around the Mill anticline is terminated laterally to the

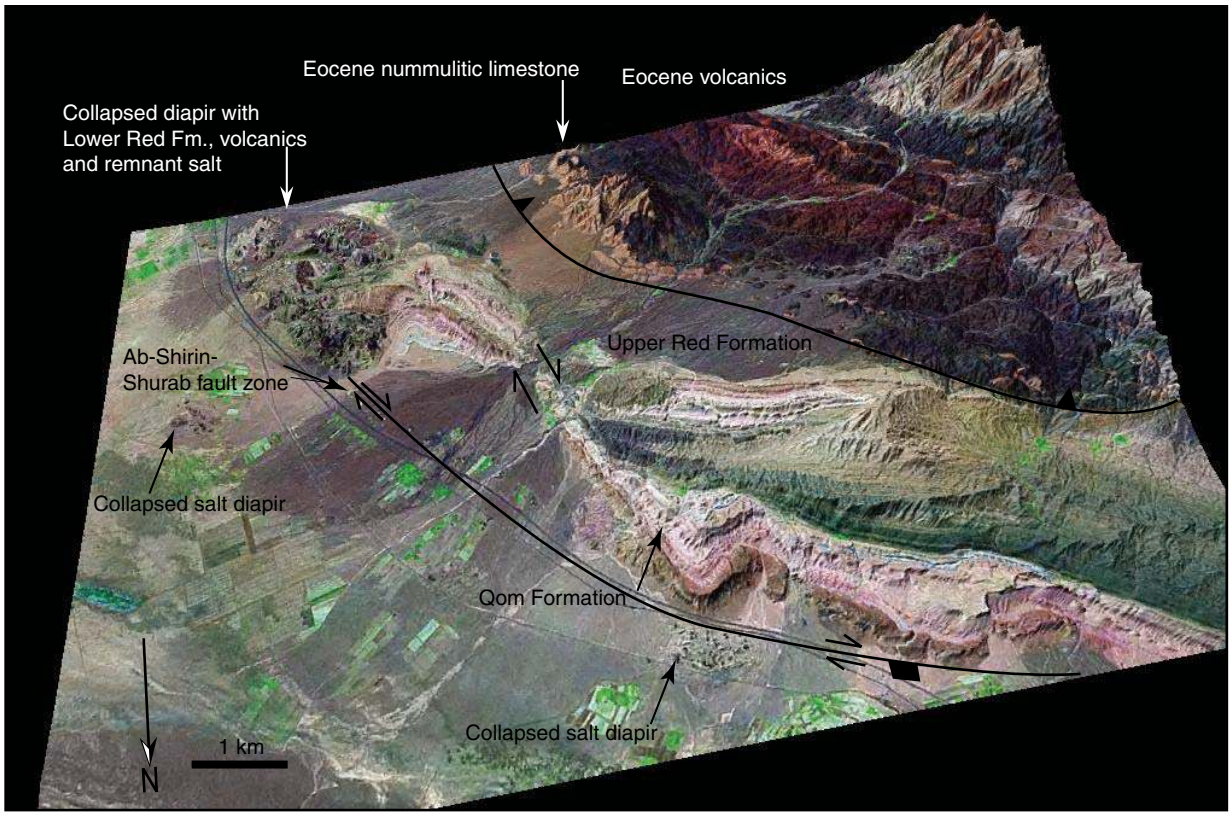

Figure 26. Three-dimensional perspective image; view is to the southeast of the Ab-Shirin-Shurab fault zone and Shurab salt diapir. See Figure 2B for location.

Downloaded from http://pubs.geoscienceworld.org/gsa/geosphere/article-pdf/5/4/325/3337666/i1553-040X-5-4-325.pdf
by guest

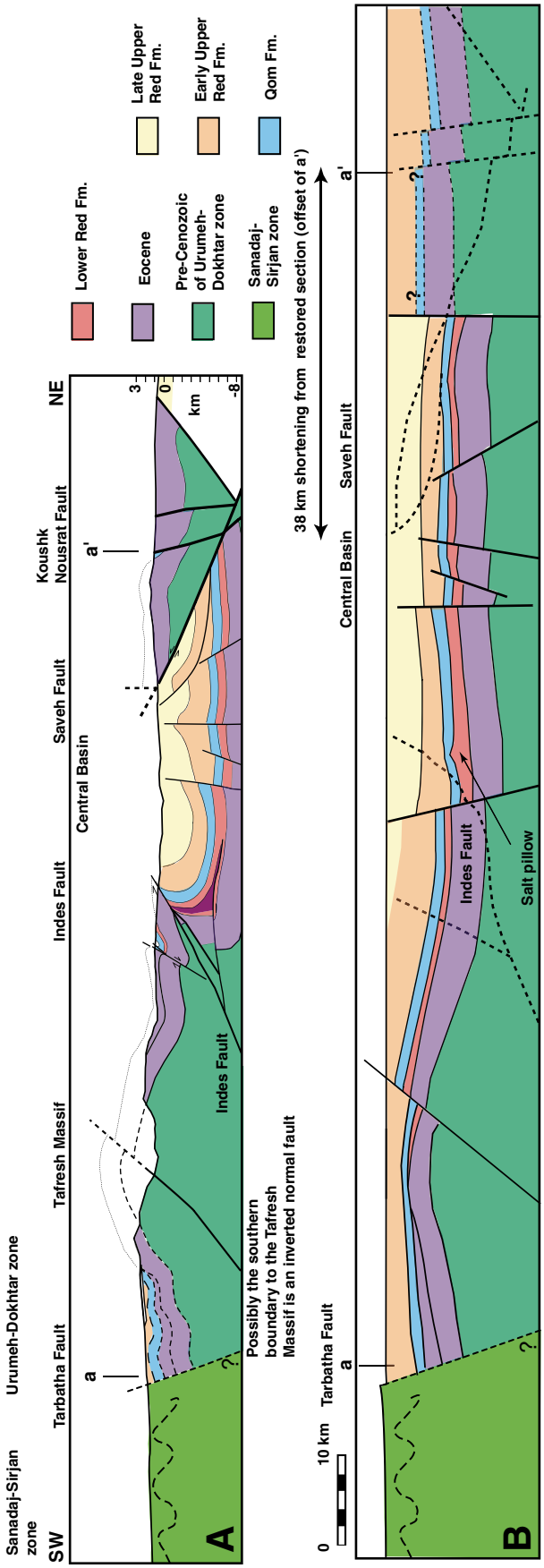

Figures 27. (A) Depth converted line drawing of the seismic line shown in Figure 19, coupled with a more regional cross section based on outcrop data. (B) One possible restoration scenario. Note: across the massifs the Central Basin stratigraphy is simplified from the main Central Basin area, the Qom Formation and Lower Red Formation are amalgamated into one unit, and the subdivision of the Upper Red Formation is not made. See Figure 2A for location.

east and west by oblique-trending structures. The outcrop trace of the Dochah-Yazdan fault displays an oblique ramp geometry at the western end of the Mill anticline, where it cuts across the Qom Formation and Upper Red Formation in the hanging wall to the northwest. The fault dies out along the oblique segment and displacement is transferred to a north-verging basement-involved thrust (Fig. 23). To the east the Mill anticline is abruptly terminated by a number of closely spaced northwest-southeast–striking, dextral strike-slip faults (the Shad Gholi, Idaghoh, Khed faults), collectively referred to as the Qom fault zone (Fig. 2).

The transition to thick-skinned structures at the northwest end of the Mill anticline occurs at the southern end of the Saveh depocenter. The main Saveh depocenter (Fig. 24) does not contain folded Qom Formation, suggesting that the Lower Red Formation salt was not present in the main depocenter during the Upper Red Formation folding event. Possible explanations for the absence of salt include (1) nondeposition, (2) early dissolution during burial by the Upper Red Formation, or (3) early salt movement during early Upper Red Formation time that left a primary weld by the time thrusting began. Evidence for explanation 3 as a contributing factor is provided by the diapir at Gise Ghalet (Fig. 20) that illustrates that in some parts of the Saveh area the Lower Red Formation salt was once mobile.

Urumieh-Dokhtar Zone: A Major Belt of Transpressional Deformation

The massifs in the south of the Saveh area have large, plunging folds at their northwest and southeast terminations. For example, the pronounced valley south of Qom (Fig. 18) is formed between the southeast-plunging Tafresh massif and the northwest-plunging Kahak massif. Satellite images of the Kahak massif clearly show basement-involved east-west–striking folds and thrusts linked by northwest-southeast–trending strike-slip faults. Reports on outcrop geology by Huber (1951), Frei (1951), and Stocklin (1954) show that strongly folded and faulted Central Basin stratigraphy is present in the massifs south of the Qom-Saveh area. The map pattern geometry of folds and faults seen in these basement-involved structures closely resembles that seen farther north in detached structures (Fig. 2B), emphasizing the commonality of origin. The structural patterns described for the Qom-Saveh area also appear to be applicable over much of the Urumieh-Dokhtar zone. Satellite images and geological maps show that the main Eocene volcanic massifs are strongly deformed by an anastamosing network of faults (Fig. 1B). On

Downloaded from http://pubs.geoscienceworld.org/gsa/geosphere/article-pdf/5/4/325/3337666/i1553-040X-5-4-325.pdf
by guest

most published maps of the region several large, isolated northwest-southeast–trending dextral strike-slip faults are shown offsetting geological units in the northern Sanadaj-Sirjan and southern Urumieh-Dokhtar zones. Interpretation of satellite images, together with geological maps, strongly indicates that many of these fault zones are not isolated, but instead are linked by west-northwest–east-southeast– and east-west–trending faults to form large-scale rhomboid geometries, or strike-slip duplex geometries. These rhomboid lenses tend to display much better developed fold-and-thrust geometries than the areas outside of the lenses. The chain of massifs along the southern border of the Central Basin displays present-day maximum elevations of ~3 km (Fig. 1A). There is a commonality of deformation style and elevation in the entire southern margin of the Urumieh-Dokhtar zone, with the massifs lying at large-scale restraining bends within this system. Rather than simply representing an Eocene volcanic trend, the Urumieh-Dokhtar zone is interpreted here as a well-organized transpressional belt that accommodated a significant amount (~38 km) of late Miocene–Holocene shortening.

The deformation in the Urumieh-Dokhtar zone shows a very strong basement-involved component that passes in places into thin-skinned deformation where sedimentary basins are present. The thick-skinned deformation seen in this area may well provide a good analogue for the inferred role of thick-skinned deformation in the Zagros Mountains (e.g., Talebian and Jackson, 2004; Sepehr and Cosgrove, 2005). However in the Zagros Mountains the cover of sedimentary rocks is much greater than in the Iran Plateau area, and so masks the thick-skinned deformation style.

DISCUSSION: INTERPRETATION OF BASIN DEVELOPMENT

Although forearc and backarc locations have been used to describe the Central Basin (e.g., Schuster and Wielandt, 1999; Hassanzadeh et al., 2002), this terminology is misleading. The basin overlies volcanic arc–related units, but the arc had died at the end of the Eocene, and was subsequently deformed, uplifted, and eroded prior to deposition of the Central Basin sediments. Central Basin deposition during the Oligocene and Miocene was accompanied by episodic calc-alkaline volcanism, including inferred post-collision, subduction-related adakites and shoshonites (Jahangiri, 2007). These volcanics are relatively low volume compared with those erupted during the Eocene.

The late Eocene–early Oligocene collision of Arabia with Eurasia can explain the cessation of major arc volcanism, deformation, uplift, and erosion of the arc. The broad sag-like basin geometry and minor or localized late Oligocene–early Miocene extensional faulting indicate that early basin subsidence was a response to a broad regional load (Figs. 30A, 30B, 30E, and 31C). The types of load include mechanical loads, such as a flexural response to crustal thickness variations, and thermal loads in response to cooling, in particular post-rift subsidence.

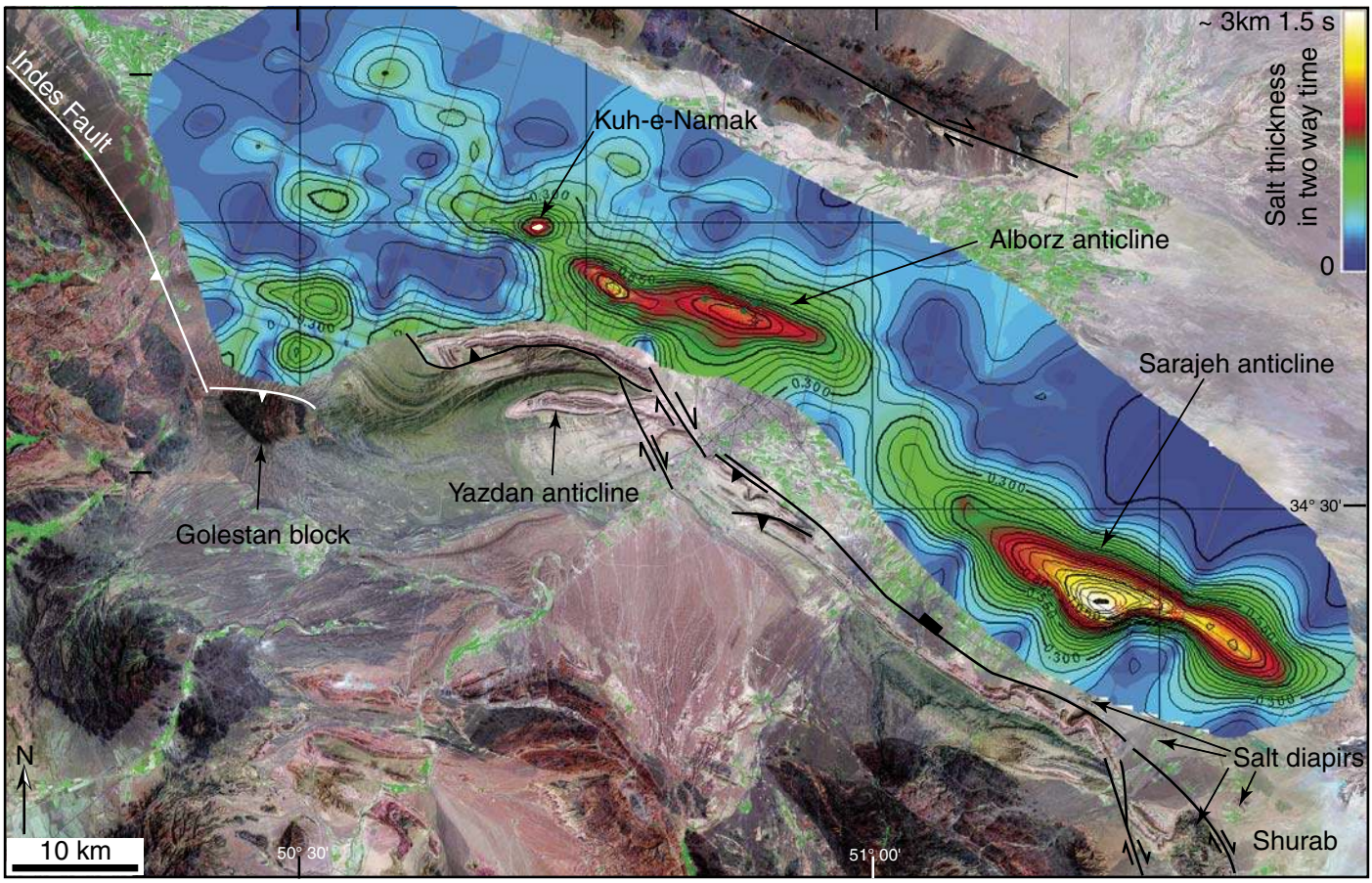

Figure 28. Isochron map of Lower Red Formation evaporites thickness (in two-way traveltime) based on two-dimensional seismic data, overlaid on 30 m resolution satellite image. Alborz-Sarajeh anticline area.

Downloaded from http://pubs.geoscienceworld.org/gsa/geosphere/article-pdf/5/4/325/3337666/i1553-040X-5-4-325.pdf
by guest

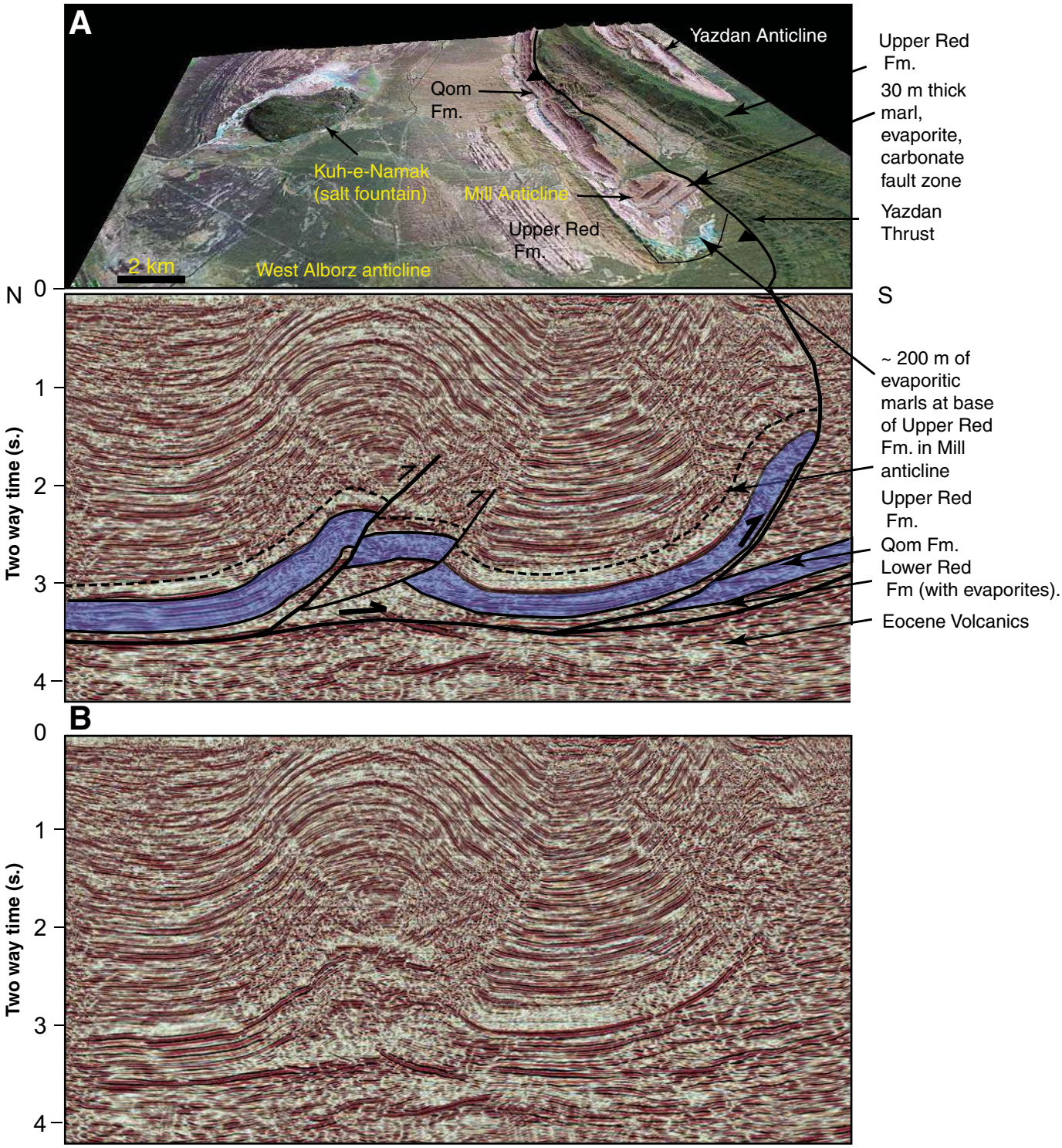

Figure 29. (A) Interpreted two-dimensional seismic line showing the thin-skinned deformation style (detached on Lower Red evaporites) of the Qom area; surface geology is illustrated on a three-dimensional perspective satellite image. (B) Uninterpreted version of seismic line in A. See Figure 2B for location.

Downloaded from http://pubs.geoscienceworld.org/gsa/geosphere/article-pdf/5/4/325/3337666/i1553-040X-5-4-325.pdf
by guest

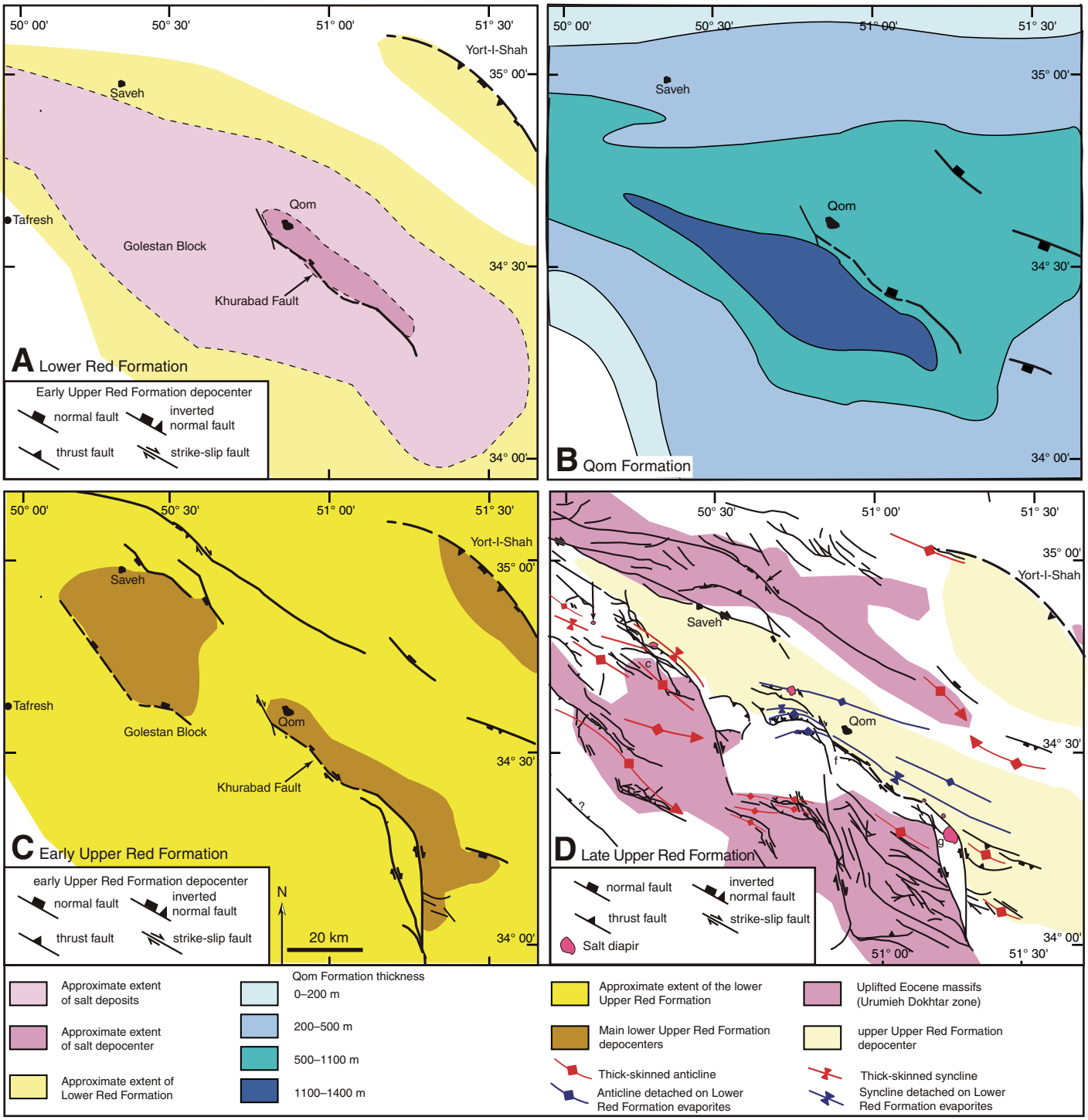

Figure 30. Evolution of the Central Basin in the Saveh-Qom area during the Oligocene–Pliocene. (A) Lower Red Formation deposition in a broad sag basin; only indication of fault control is along the Khurabad fault. (B) Qom Formation broad sag basin, with some local fault control. (C) Early Upper Red Formation, extensional and/or transtensional fault control on depocenter location with high subsidence rates. (D) Late Upper Red Formation; major uplift of basin margins is due to regional transpression. Deposition in remnant basins depocenters between the uplifted Eocene massifs.

Downloaded from http://pubs.geoscienceworld.org/gsa/geosphere/article-pdf/5/4/325/3337666/i1553-040X-5-4-325.pdf
by guest

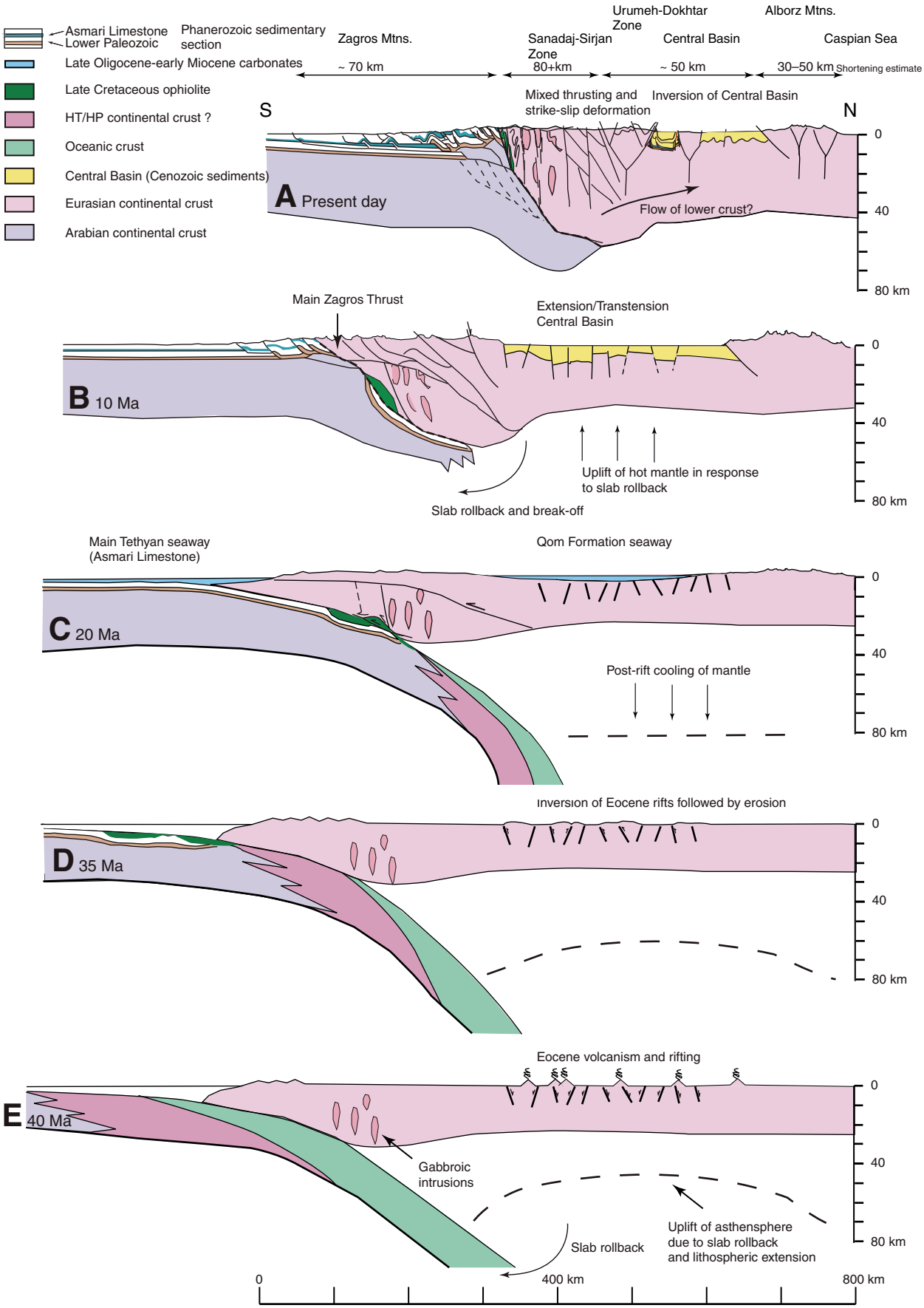

Downloaded from http://pubs.geoscienceworld.org/gsa/geosphere/article-pdf/5/4/325/3337666/i1553-040X-5-4-325.pdf
by guest

Figure 31. Sequential evolution of Iran during the Cenozoic based on data described in this paper for the Central Basin, Guest et al. (2006b) and Ballato et al. (2008) for the Alborz Mountains, McQuarrie (2004) for the Zagros Mountains (note that this interpretation minimizes the extent of basement-involved deformation beneath the Zagros Mountains), and Agard et al. (2005) for the Sanadaj-Sirjan zone and general tectonic evolution. Although the section is semi-schematic and does not fit a single profile across Iran, it is largely based on actual cross sections and is in proportion. Crustal profile modified from Kaviani et al. (2007). (A) Present day, transpressional stage, with extensive dextral strike-slip motion. (B) Compression and/or transpression in internal Zagros Mountains, Sanadaj-Sirjan zone, and Alborz Mountains. Extension or transtension deformation affected the Central Basin, possibly as a result of subduction rollback. (C) Shortening confined to Sanadaj-Sirjan zone area. Subsidence and deposition in the foredeep region of the Main Tethyan seaway (Asmari Limestone); the Qom Formation is interpreted as being deposited in a thermal subsidence basin. Ophiolite partially scraped off and incorporated into overlying plate. (D) Initial continental collision caused inversion of the Eocene rift system. Convergence between Arabia and Eurasia was largely accommodated by subduction, not crustal shortening. (E) Stage just prior to collision; subduction of oceanic crust (Semail Ocean), with intrusion of gabbros into the Sandaj-Sirjan zone (Agard et al., 2005), and mixed subduction and rift-related volcanism in the overriding plate. Rifting occurred during the Eocene, possibly as a result of subduction rollback. Shortening estimates are from McQuarrie (2004; Zagros Mountains); data for Sanadaj-Sirjan zone are from Agard et al. (2005); Central Basin data are from this paper; Alborz Mountains data are from Allen et al. (2004) and Guest et al. (2006b). High temperature–low pressure (HT/LP) crust indicates the area of the crust that may partly contain high-density crustal rocks resulting from subduction and exhumation (e.g., eclogites); this area of crust was possibly more prone to breakoff and subduction than normal crust.

A number of studies have noted that the ~20 Ma duration of Eocene volcanic activity in central Iran marks an anomalous flareup of volcanic activity along the margin (e.g., Berberian and Berberian, 1981; Amidi et al., 1984; Kazmin et al., 1986). One explanation is that extensive rifting of the Eocene volcanic arc was important for attaining the high volume of Eocene volcanics (Amidi et al., 1984; Kazmin et al., 1986), and that slab rollback was the main driving mechanism for extension (e.g., Vincent et al., 2005; Fig. 31E). Recently several Eocene-age metamorphic core complexes have been discovered within the Eocene volcanic belts, indicating that considerable extension accompanied volcanism (e.g., Verdel et al., 2007; Kargaranbafghi et al., 2008).

Figure 13 shows a seismic line in the Saveh-Qom area where, unusually, the sub-Qom Formation section is well imaged: in outcrops in this area, only the Miocene part of the Qom Formation is present directly overlying the Eocene section. Therefore, although the presence of Lower Red Formation cannot be excluded, the most likely interpretation is that the extensive normal fault system underlying the Qom Formation is clear evidence for Eocene extension. Some of the extensional faults were subsequently reactivated during Qom Formation and Upper Red Formation time.

The discussion above indicates that the Eocene tectonic setting in central Iran is appropriate for thermal subsidence to have acted as the main driving mechanism of basin development during Lower Red Formation and Qom Formation deposition (Fig. 31C). The three-armed geometry of the Central Basin seen in the Qom Formation isopach map (Fig. 5) could represent a post-rift basin following an earlier (Eocene) rift that avoided the stronger crust of the Central Iran microplate, and wrapped around its western margin. Central Basin subsidence was probably also enhanced by other mechanisms, including loading by thrust sheets (particularly along the southern border with the Sanadaj-Sirjan zone), and local extension. Provided extension is relatively minor and does not cause net heating of the mantle (to offset post-rift cooling), normal faulting can accompany thermal subsidence.

During deposition of the Upper Red Formation the structural styles affecting the Saveh-Qom area are interpreted here to have evolved from oblique extension (Fig. 15, scenario B to C) to dextral transpression (Figs. 30C, 30D). There are occasional indications of minor inversion during the early Upper Red Formation, but in general the early Upper Red Formation marks a time of widespread deposition in oblique extensional to transtensional fault-controlled depocenters (Fig. 29). The later Upper Red Formation marks a period of widespread basin inversion and destruction. This resulted in more geographically restricted depocenters, bounded by uplifted massifs, which loaded the basin remnants so that they subsided as miniforedeep basins.

The two basin types interpreted for the Upper Red Formation in the Qom-Saveh area contrast with an Upper Red Formation depocenter on the southern margin of the Alborz Mountains that Ballato et al. (2008) proposed formed in a foreland basin setting throughout deposition of the Upper Red Formation. The different interpretations in the two areas are not necessarily incompatible. The change from carbonate deposition during the Qom Formation to clastic-dominated red bed deposition during the Upper Red Formation clearly marks a regional change in sediment supply and uplift that eliminated the seaway ca. 17 Ma ago. Uplift in the Crush zone and Sanadaj-Sirjan zone to the south of the Central Basin, and the Alborz Mountains to the north, would have provided the necessary uplift and supply of clastic material to the Central Basin (Fig. 31B). Consequently, compressional to transpressional deformation may well have occurred during deposition of the entire Upper Red Formation for the Alborz Mountains (Ballato et al., 2008) and the Sanadaj-Sirjan zone (Agard et al., 2005). However, transpression occurred later in the intervening area of the Central Basin, after ~5 km or more of sediment was deposited in the main Upper Red Formation (transtensional) depocenters.

The origin of the extension that affected the Lower Red Formation, Qom Formation to a lesser extent, and the early Upper Red Formation to a greater extent, within a post-collisional setting is uncertain. Extension appears to have occurred prior to region uplift, and hence prior to any mantle-driven process responsible for plateau uplift (such as mantle delamination; e.g., Maggi and Priestley, 2005). Seismic wave velocities in the upper mantle also indicate it is unlikely that mantle delamination occurred (Kaviani et al., 2007). The shallow mantle underlying the Iran Plateau and Alborz Mountains is relatively low velocity, due to either higher mantle temperatures and/or higher fluid content than the mantle under the Zagros Mountains (Kaviani et al., 2007). Post-collision extension in the hinterland of a fold-and-thrust belt and hot shallow mantle could arise from slab rollback of oceanic crust and the leading edge of the continental margin, such as that seen in the Carpathians–Pannonian system and Rif-Betic Cordillera–Alboran Sea (Fig. 31B; e.g., Royden, 1993; Morley, 1993; and see review in Morley, 2002). In the case of the Iran Plateau the amount of extension seen in the Central Basin

Downloaded from http://pubs.geoscienceworld.org/gsa/geosphere/article-pdf/5/4/325/3337666/i1553-040X-5-4-325.pdf
by guest

does not appear to be as large as in the two examples above, but may be of similar origin.

In the Saveh-Qom area there is no precise dating of the onset transpression, marked by folding and thrusting within depocenters, uplift of the Urumieh-Dokhtar zone to elevations of ~3 km, and uplift of the Central Basin from near sea level to 900–1000 m. It should also be noted that these two uplifts may both be linked to compression, but arose by different mechanisms and have somewhat different timing (within the middle Miocene–Holocene). The more geographically limited, larger magnitude uplift of the Urumieh-Dokhtar zone appears to be directly related to transpressional deformation. The more regional uplift marked by the 900–1000 m uplift of the basin surface suggests a broader, tectonically controlled feature, for example, uplift in response to hot mantle, or flow of ductile lower crust from the areas with a greater upper crustal load (i.e., more mountainous regions) into the basinal areas (the latter interpretation is preferred; Fig. 31B). Within the Central Basin the switch from no thinning to thinning onto folds near the midpoint (in terms of thickness) of the Upper Red Formation section suggests an approximate coincidence between the increase in deformation proposed for the Zagros and Alborz Mountains (7 Ma ago in Allen et al., 2004; 12 Ma ago in Guest et al., 2006a, 2006b), and the switch in deformation style during Upper Red Formation time. For ease of reference (and for basin modeling purposes; Fig. 12), we refer to 10 Ma ago as the onset of widespread folding in the Qom-Saveh area and 3 Ma ago as marking the end of major deformation. However, neither date is precise. Undeformed volcanics loosely dated as late Miocene–Pliocene overlie deformed Upper Red Formation sediments, which indicates that there is an unconformable relationship that can be used to mark the termination of the major phase of transpressional deformation. Earthquake and GPS data show that the Central Basin is a low-strain region today relative to the simple folded zone and high Zagros and Alborz Mountains (Hessami et al., 2003; Vernant et al., 2004). Although deformation rate is considerably reduced from Upper Red Formation time, there is evidence to indicate that the region is not completely inactive. Deformation younger than the Upper Red Formation is seen in numerous outcrops of tilted, poorly consolidated conglomerates and sandstones. In addition, south of Qom, a 5.5 Mw earthquake (Global Centroid Moment Tensor catalog number 200706181429A; http://www.globalcmt.org/CMTsearch.html) with an 18.5-km-deep hypocenter and oblique strike-slip plane solution for a northwest-southeast–striking fault (northeast-southwest maximum horizontal stress direction) occurred on 18 June 2007. The modern north-south to northeast-southwest maximum horizontal stress orientation (Heidbach et al., 2007) in central Iran is similar to that required for dextral transpression during the Upper Red Formation.

The late Upper Red Formation transpressional deformation caused shortening of at least 38 km in the Qom-Saveh-Tafresh area (17 km thin-skinned shortening in the basin; Fig. 14; 38 km for Fig. 27; see Fig. 31A). Although this is a relatively modest amount of shortening in comparison with many mountain belts, in the context of late Miocene–Holocene collision 38 km is significant. The shortening estimate represents ~4 mm/a, or 20% of the regional 2 cm/a convergences rate for the Arabian plate-Eurasian plate collision zone for the past 10–12 Ma (e.g., McQuarrie et al., 2003; Allen et al., 2004). Over the same time period the simple and high Zagros Mountains have shortened by 70 ± 20 km, based on regional balanced cross sections (McQuarrie, 2004), while shortening estimates for the Alborz Mountains range between 30 km (Allen et al., 2004) and 53 ± 3 km (Guest et al., 2006b). The width of the Central Basin region discussed here is ~80 km, compared with ~150 km for the Zagros Mountains and 100 km for the Alborz Mountains. Hence in terms of shortening per kilometer, the Central Basin is comparable with the Alborz and Zagros Mountains.

There is a pronounced time gap in the identification of large-scale regional deformation between the onset of collision in the late Eocene–early Oligocene (ca. 40 Ma ago) and the initiation of major deformation in the Central Basin, Zagros, and Alborz in the middle or late Miocene (e.g., Allen et al., 2004). This intervening period of ~19-25 Ma is equivalent to ~380–500 km of post-collisional convergence, assuming convergence rates of ~2 cm/a (McQuarrie et al., 2003). This convergence must be accommodated either by underthrusting or subduction of continental crust and/or by crustal shortening. Only the Sanadaj-Sirjan zone and Crush zone show evidence for significant Oligocene–early Miocene shortening (~100 km; Agard et al., 2005), and hence account for only a fraction of the total convergence. Deformation in the Central Basin cannot add to the Oligocene–early Miocene shortening total, but strengthens the view that late Miocene–Holocene crustal shortening is the most prominent tectonic phase (Allen et al., 2004; Guest et al., 2006a, 2006b). The data suggest that subduction or underthrusting of continental crust was important during the Oligocene–early Miocene, and that during the middle Miocene–Holocene crustal shortening accommodated much more of the convergence. Crustal shortening became particularly well developed from the late Miocene onward.

CONCLUSIONS

The Central Basin records important information about the early stages of development of a continental plateau area in the upper plate of a continent-continent collision zone. A summary of the basin evolution in the Saveh-Qom area is shown in Figures 30 and 31. Collision of Arabia and Eurasia resulted in folding, uplift, and erosion of the Eocene arc volcanics belt. Possibly the folding seen in the Eocene section adjacent to the Central Basin described by Huber (1952) and Gansser (1955b) is related to inversion of normal faults, since the development of folds appears to be local rather than regional (Fig. 31D). Rather than compression and plateau-building continuing to affect central Iran during the Oligocene, continent convergence became accommodated elsewhere (probably predominantly by subduction or underthrusting of continental crust), and central Iran underwent broad subsidence, permitting the deposition of the Lower Red Formation and Qom Formation at or near sea level (Fig. 31C). The subsidence is interpreted to have resulted from thermal subsidence following Eocene rifting, combined with local loading by thrust sheets and local extension.

The Qom Formation marks a period of tectonic quiescence, with little coarse clastic material entering the Central Basin. This picture changed during the Burdigalian, when coarse clastics entered the basin as a consequence of contraction-related uplift in the Sanadaj-Sirjan zone and Alborz Mountains (e.g., Agard et al., 2005; Ballato et al., 2008). However, during the time of deposition of the early Upper Red Formation, oblique extension or transtensional deformation dominated the Central Basin, which enabled the deposition of thick clastic sequences over a wide area, including the future Urumieh-Dokhtar zone (Fig. 30C). Only later during the Upper Red Formation (probably late Miocene–Pliocene) did transpressional deformation enter the basin and invert >50% of the original basin area (Figs. 30, 31B, and 31A).

Development of the plateau phase in the Saveh-Qom area is of middle Miocene–late Miocene age (probably commencing ca. 10 Ma ago), and uplift occurred as a result of at least 38 km shortening (probably 50 km or more shortening for the entire Central Basin). Dextral transpression and possibly heating of the mantle lithosphere lifted the basin surface from near sea level to 900–1000 m, while the Urumieh-Dokhtar zone became the main focus of deformation and was lifted to maximum elevations of

Downloaded from http://pubs.geoscienceworld.org/gsa/geosphere/article-pdf/5/4/325/3337666/i1553-040X-5-4-325.pdf
by guest

~3 km, in addition to undergoing erosion of as much as 5 km thickness of Central Basin sedimentary rocks.

The dextral transpressional system is interpreted to form a linked system of anastamosing faults along a northwest-southeast trend >400 km long. Transpressional deformation formed thrusts and folds along east-west to west-northwest–east-southeast orientations, and stronger dextral offsets on faults oriented northwest-southeast to north-northwest–south-southeast. Significant thin-skinned folding and thrusting occur where thick evaporites are present. The deformation fits with approximately north-south to north-northeast–south-southwest–oriented maximum horizontal stress direction, similar to the modern stress orientation (Heidbach et al., 2007). Basement-involved deformation is juxtaposed with detached structural styles. The largest basement-involved folds are those affecting entire massifs, and have wavelengths of tens of kilometers, while the detached folds have wavelengths as large as ~10 km. There are abrupt lateral changes in the Central Basin between basement-involved folds and detached folds.

The Zagros Mountains are world famous for their exposures of large folds with accompanying salt piercement features. Exposures in the Central Basin are of equal quality and display a similar mix of Cenozoic rock types, but the rocks are deformed in a more complex manner. The suspected interaction of basement-involved and thin-skinned deformation in the Zagros Mountains is much more clearly expressed in the Central Basin.

ACKNOWLEDGMENTS

We thank the NIOC (National Iranian Oil Company) and PTTEP (PTT Exploration and Production) for permission to publish the paper. Detailed and constructive reviews by Mark Allen, Paolo Ballato, and Manfred Strecker helped improve the manuscript considerably and are gratefully acknowledged.

REFERENCES CITED

Abaie, I., Ansari, J.J., Badakhshan, A., and Jaafari, A., 1964, History and development of the Alborz and Sarajeh fields of central Iran: World Petroleum Congress Proceedings, Section II, Paper 13, PD3, p. 697–713.

Agard, P., Omrani, J., Jolivet, L., and Mouthereau, F., 2005, Convergence history across Zagros (Iran): Constraints from collisional and earlier deformation: International Journal of Earth Sciences, v. 94, p. 401–419, doi: 10.1007/s00531-005-0481-4.

Allen, M.B., and Armstrong, H.A., 2008, Arabia-Eurasia collision and the forcing of mid-Cenozoic global cooling: Palaeogeography, Palaeoclimatology, Palaeoecology, v. 265, p. 52–58, doi: 10.1016/j.palaeo.2008.04.021.

Allen, M., Jackson, J., and Walker, R., 2004, Late Cenozoic reorganization of the Arabian-Eurasian collision and the comparison of short-term and long-term deformation rates: Tectonics, v. 23, doi: 10.1029/2003TC001530.

Amidi, S.M., Emami, M.H., and Michel, R., 1984, Alkaline character of Eocene volcanism in the middle part of central Iran and its geodynamic situation: Geologische Rundschau, v. 73, p. 917–932, doi: 10.1007/BF01820882.

Amini, A., 1997, Provenance and depositional environment of the Upper Red Formation, Central Zone, Iran [Ph.D. thesis]: Manchester, UK, University of Manchester, 320 p.

Authemayou, C., Chardon, D., Bellier, O., Malekzadeh, Z., Shabanian, E., and Abbassi, M.R., 2006, Late Cenozoic partitioning of oblique plate convergence in the Zagros fold-and-thrust belt (Iran): Tectonics, v. 25, doi: 10.1029/2005TC001860.

Axen, G.J., Lam, P.S., Grove, M., Stockli, D.F., and Hassanzadeh, J., 2001, Exhumation of the west-central Alborz Mountains, Iran, Caspian subsidence, and collision-related tectonics: Geology, v. 29, p. 559–562, doi: 10.1130/0091-7613(2001)029<0559:EOTWCA>2.0.CO;2.

Ballato, P., Nowaczyk, N.R., Landgraf, A., Strecker, M.R., Friedrich, A., and Tabatabaei, S.H., 2008, Tectonic control on sedimentary facies pattern and sediment accumulation rates in the Miocene foreland basin of the southern Alborz mountains, northern Iran: Tectonics, v. 27, doi: 10.1029/2008TC002278.

Berberian, F., and Berberian, M., 1981, Tectono-plutonic episodes in Iran, *in* Gupta, H.K., and Delany, F.M., eds., Zagros, Hindu Kush, Himalaya, geodynamic evolution: American Geophysical Union Geodynamics Series, v. 3, 323 p.

Berberian, M., and King, G.C.P., 1981, Towards a palaeogeography and tectonic evolution of Iran: Canadian Journal of Earth Sciences, v. 18, p. 210–265, doi: 10.1139/e81-163.

Bina, M.M., Bucur, I., Prevot, M., Meyerfeld, Y., Daly, L., Cantagrel, J.M., and Mergoil, J., 1986, Palaeomagnetism, petrology and geochronology of Tertiary magmatic and sedimentary units from Iran: Tectonophysics, v. 121, p. 303–329, doi: 10.1016/0040-1951(86)90050-8.

Chazan, W., 1970, Etude géologique preliminaire des depots potassifères d'Iran: Mineralium Deposita, v. 5, p. 280–299, doi: 10.1007/BF00201993.

Daneshian, J., and Ramezani Dana, L., 2007, Early Miocene benthic foraminifera and biostratigraphy of the Qom Formation, Deh Namak, central Iran: Journal of Asian Earth Sciences, v. 29, p. 844–858, doi: 10.1016/j.jseaes.2006.06.003.

Delaloye, M., and Desmons, J., 1980, Ophiolites and mélange terranes in Iran: A geochronological study and its paleotectonic implications: Tectonophysics, v. 68, p. 83–111, doi: 10.1016/0040-1951(80)90009-8.

Fakhari, M.D., Axen, G.J., Horton, B.K., Hassanzadeh, J., and Amini, A., 2008, Revised age of proximal deposits in the Zagros foreland basin and implications for Cenozoic evolution of the High Zagros: Tectonophysics, v. 451, p. 170–185, doi: 10.1016/j.tecto.2007.11.064.

Frei, E., 1951, Geological report on Qum-Kashan-Nananz-Soh-Saveh (south) Area: Iran Oil Company Geological Report no. 8, 163 p.

Furrer, M.A., and Sonder, P.A., 1955, The Oligo-Miocene marine formation in the Qum region (Central Iran): Proceedings, Fourth World Petroleum Congress, Section 1/A/5, Carlo Colombo, Rome, p. 270–277.

Gansser, A., 1955a, New aspects of the geology of Central Iran: Proceedings, Fourth World Petroleum Congress, Section 1/A/5, Carlo Colombo, Rome, p. 286–305.

Gansser, A., 1955b, Geological note on NW Iran: Iran Oil Company Geological Report No. 98, 76 p.

Gansser, A., 1957, Die geologische erforschung der Qum gegend, Iran: Bulletin der Verengung Schweizerisches Petroleum-Geologen und -Ingenieur, v. 23, p. 1–16.

Geological Survey of Iran, Geological Map of Iran, 1:100,000 Series, Aran, Sheet 6258.

Geological Survey of Iran, Geological Map of Iran, 1:100,000 Series, Farmahin, Sheet 5959.

Geological Survey of Iran, Geological Map of Iran, 1:100,000 Series, Qom, Sheet 6159.

Geological Survey of Iran, Geological Map of Iran, 1:100,000 Series, Saveh, Sheet 6060.

Geological Survey of Iran, Geological Map of Iran, 1:100,000 Series, Tafresh, Sheet 6059.

Ghazi, A.M., and Hassanipak, A.A., 1999, Geochemistry of subalkaline and alkaline extrusives from the Kermanshah ophiolite Zagros suture zone, western Iran: Implications for Tethyan plate tectonics: Journal of Asian Earth Sciences, v. 17, p. 319–332, doi: 10.1016/S0743-9547(98)00070-1.

Gretener, P.E., 1982, Another look at Alborz Nr. 5 in central Iran: Bulletin Vereinigung von Petroleum-Geologen und Ingenieuren, v. 48, p. 1–8.

Guest, B., Stockli, D.F., Grove, M., Axen, G.J., Lam, P.S., and Hassanzadeh, J., 2006a, Thermal histories from the central Alborz Mountains, northern Iran: Implications for the spatial and temporal distribution of deformation in northern Iran: Geological Society of America Bulletin, v. 118, p. 1507–1521, doi: 10.1130/B25819.1.

Guest, B., Axen, G.J., Lam, P.S., and Hassanzadeh, J., 2006b, Late Cenozoic shortening in the west-central Alborz Mountains, northern Iran, by combined conjugate strike-slip and thin-skinned deformation: Geosphere, v. 2, p. 35–52, doi: 10.1130/GES00019.1.

Harzhauser, M., and Piller, W.E., 2007, Benchmark data of a changing sea—Palaeogeography, palaeobiogeography and events in the Central Paratethys during the Miocene: Palaeogeography, Palaeoclimatology, Palaeoecology, v. 253, p. 8–31.

Hassanzadeh, J., Ghazi, A.V., Axen, G., and Guest, B., 2002, Oligo-Miocene mafic-alkaline magmatism in north and northwest of Iran: Evidence for the separation of the Alborz from the Urumieh-Dokhtar magmatic arc: Geological Society of America Abstracts with Programs, v. 34, no. 6, p. 331.

Hessami, K., Jamali, F., and Tabassi, H., 2003, Major active faults of Iran: Tehran, Ministry of Science, Research and Technology, International Institute of Earthquake Engineering and Seismology, scale 1:2,500,000.

Horton, B.K., Hassanzadeh, J., Stockli, D.F., Axen, G.J., Gillis, R.J., Guest, B., Amini, A., Fakhari, M.D., Zamanzadeh, S.M., and Grove, M., 2008, Detrital zircon provenance of Neoproterozoic to Cenozoic deposits in Iran: Implications for chronostratigraphy and collisional tectonics: Tectonophysics, v. 451, p. 97–122, doi: 10.1016/j.tecto.2007.11.063.

Huber, H., 1951, Geology of parts of the Western Kavir area and oil possibilities of Northern Region No. 2: National Iranian Oil Company Geological Report no. 19, 39 p.

Huber, H., 1952, Geological report on the Upper Qara-Chai area between Saveh and Hamadan: Iranian Oil Company Geological Report no. 99, 48 p.

Jackson, M.P.A., Cornelius, R.R., Craig, C.H., Gansser, A., Stocklin, J., and Talbot, C.J., 1990, Salt diapirs of the Great Kavir, central Iran: Geological Society of America Memoir 177, 136 p.

Jahangiri, A., 2007, Post-collisional Miocene adakitic volcanism in NW Iran: Geochemical implications: Journal of Asian Earth Sciences, v. 30, p. 433–447, doi: 10.1016/j.jseaes.2006.11.008.

Kargaranbafghi, F., Foeken, J.P.T., Neubauer, F., and Stuart, F.M., 2008, How Chapedony metamorphic core complex (Central Iran) became cool and how it was overprinted by Neogene asthenosphere uprise: Inferences from (U-Th)/He thermochronology: Geophysical Research Abstracts, v. 10, p. EGU2008–A-08889.

Kaviani, A., Paul, A., Bourova, E., Hatzfeld, D., Pedersen, H., and Mikhtari, M., 2007, A strong seismic velocity contrast in the shallow mantle across the Zagros collision zone (Iran): Geophysical Journal International, v. 171, p. 399–410, doi: 10.1111/j.1365-246X.2007.03535.x.

Kazmin, V.G., Sbortshikov, I.M., Ricou, L.-E., Zonenshian, L.P., Boulin, J., and Knipper, A.J., 1986, Volcanic belts and markers of the Mesozoic-Cenozoic active margin of Eurasia: Tectonophysics, v. 123, p. 123–152, doi: 10.1016/0040-1951(86)90195-2.

Lanphere, M.A., and Pamic, J., 1983, $^{40}Ar/^{39}Ar$ ages and tectonic setting of ophiolite from the Neyriz area

Downloaded from http://pubs.geoscienceworld.org/gsa/geosphere/article-pdf/5/4/325/3337666/i1553-040X-5-4-325.pdf
by guest

southeast Zagros range, Iran: Tectonophysics, v. 96, p. 245–256, doi: 10.1016/0040-1951(83)90220-2.

Letouzey, J., and Rudkiewicz, J.L., 2005, Structural geology in the Central Iranian Basin: Institut Français du Petrole report F0214001, 79 p.

Maggi, A., and Priestley, K., 2005, Surface waveform tomography of the Turkish-Iranian plateau: Geophysical Journal International, v. 160, p. 1068–1080, doi: 10.1111/j.1365-246X.2005.02505.x.

McQuarrie, N., 2004, Crustal scale geometry of the Zagros fold-thrust belt, Iran: Journal of Structural Geology, v. 26, p. 519–535, doi: 10.1016/j.jsg.2003.08.009.

McQuarrie, N., Stock, M., Verdel, C., and Wernicke, B.P., 2003, Cenozoic evolution of Neotethys and implications for the causes of plate motions: Geophysical Research Letters, v. 30, doi: 10.1029/2003GL017992

Morley, C.K., 1993, A possible delamination origin for hinterland basins to the Rif-Betic cordillera and Carpathians: Tectonophysics, v. 226, p. 359–376, doi: 10.1016/0040-1951(93)90127-6.

Morley, C.K., 2002, Tectonic settings of continental extensional provinces and their impact on sedimentation and hydrocarbon prospectivity, *in* Renaut, R.W., and Ashly, G.M., eds., Sedimentation in continental rifts: SEPM (Society for Sedimentary Geology) Special Publication 73, p. 25–56.

Mostofi, B., and Gansser, A., 1957, The story behind the 5 Alborz: Oil & Gas Journal, v. 55, p. 78–84.

Heidbach, O., Fuchs, K., Müller, B., Reinecker, J., Sperner, B., Tingay, M., and Wenzel, F., 2007, The World Stress Map—Release 2005: Paris, Commission of the Geological Map of the World, scale 1: 46,000,000, www.world-stress-map.org.

Reuter, M., Piller, W.E., Harzhauser, M., Mandic, O., Berning, B., Rogl, F., Kroh, A., Aubry, M.-P., Wielandt-Schuster, U., and Hamedani, A., 2007, The Oligo-Miocene Qom Formation (Iran): Evidence for an early Burdigalian restriction of the Tethyan Seaway and closure of its Iranian gateways: International Journal of Earth Sciences, doi: 10.1007/s00531 007-0269-9.

Roca, E., Maura, S., and Koyi, H.A., 2006, Polyphase deformation of diapiric areas in models and in the eastern Prebetics (Spain): American Association of Petroleum Geologists Bulletin, v. 90, p. 115–136.

Royden, L.H., 1993, The tectonic expression of slab pull at continental convergent boundaries: Tectonics, v. 12, p. 303–325, doi: 10.1029/92TC02248.

Schuster, F., and Wielandt, U., 1999, Oligocene and Early Miocene coral faunas from Iran: Palaeoecology and palaeobiogeography: International Journal of Earth Sciences, v. 88, p. 571–581, doi: 10.1007/s005310050285.

Searle, M.P., and Cox, J., 1999, Tectonic setting, origin, and obduction of the Oman Ophiolite: Geological Society of America Bulletin, v. 111, p. 104–122, doi: 10.1130/0016-7606(1999)111<0104:TSOAOO>2.3.CO;2.

Şengör, A.M.C., Cin, A., Rowley, D.B., and Nie, S.Y., 1993, Space-time patterns of magmatism along the Tethysides: A preliminary study: Journal of Geology, v. 101, p. 51–84.

Sepehr, M., and Cosgrove, J.W., 2005, Role of the Kazerun fault in the formation and deformation of the Zagros Fold-Thrust Belt, Iran: Tectonics, v. 24, doi: 10.1029/2004TC001725.

Sonder, P.A., 1951, Geological report on the region west of Qum: Iran Oil Company Geological Report no. 49a, 61 p.

Sonder, P.A., 1954, The Tertiary of the Qum-Shurab area: Iran Oil Company Geological Report no. 123, 74 p.

Sonder, P.A., 1956, Detailed investigations on the Marine Formation of Qum: Iran Oil Company Geological Report no. 154, 61 p.

Stampfli, G.M., and Borel, G.D., 2002, A plate tectonic model for the Paleozoic and Mesozoic constrained by dynamic plate boundaries and restored synthetic oceanic isochrones: Earth and Planetary Science Letters, v. 196, p. 17–33, doi: 10.1016/S0012-821X(01)00588-X.

Stocklin, J., 1954, Geology of Kuhestan-e-Qum and Rawand area: Iran Oil Company Geological report 126, 38 p.

Stocklin, J., 1968, Structural history and tectonics of Iran: A review: American Association of Petroleum Geologists Bulletin, v. 52, p. 1229–1258.

Talbot, C.J., and Aftabi, P., 2004, Geology and models of salt extrusion at Qum Kuh, central Iran: Geological Society of London Journal, v. 161, p. 321–334, doi: 10.1144/0016-764903-102.

Talebian, M., and Jackson, J., 2004, A reappraisal of earthquake focal mechanisms and active shortening in the Zagros Mountains of Iran: Geophysical Journal International, v. 156, p. 506–526, doi: 10.1111/j.1365-246X.2004.02092.x.

Verdel, C., Wernicke, B., Ramezani, P., Hassanzadeh, J., Renne, P.R., and Spell, T.L., 2007, Geology and thermochronology of Tertiary Cordilleran-style metamorphic core complexes in the Saghand region of central Iran: Geological Society of America Bulletin, v. 119, p. 961–977, doi: 10.1130/B26102.1.

Vernant, P., Nilforoushan, F., Hatzfeld, D., Abbassi, M.R., Vigny, C., Masson, F., Nankali, H., Martinod, J., Ashtiani, A., and Bayer, R., 2004, Present day crustal deformation and plate kinematics in the Middle East constrained by GPS measurements in Iran and northern Oman: Geophysical Journal International, v. 157, p. 381–389, doi: 10.1111/j.1365-246X.2004.02222.x.

Vincent, I., Allen, M.B., Ismail-Zadeh, A.D., Flecker, R., Foland, K.A., and Simmons, D., 2005, Insights from the Talysh of Azerbaijan into the Paleogene evolution of the South Caspian region: Geological Society of America Bulletin, v. 117, p. 1513–1533, doi: 10.1130/B25690.1.

Vincent, S.J., Morton, A.C., Carter, A., Gibbs, S., and Barabadze, T.G., 2007, Oligocene uplift of the Western Greater Caucasus: An effect of initial Arabia-Eurasia collision: Terra Nova, v. 19, p. 160–166, doi: 10.1111/j.1365-3121.2007.00731.x.

Walker, R., and Jackson, J., 2004, Active tectonics and late Cenozoic strain distribution in central and eastern Iran: Tectonics, v. 23, doi: 10.1029/2003TC001529.

Manuscript Received 01 January 2009
Revised Manuscript Received 14 March 2009
Manuscript Accepted 19 May 2009

Downloaded from http://pubs.geoscienceworld.org/gsa/geosphere/article-pdf/5/4/325/3337666/i1553-040X-5-4-325.pdf
by guest